



UNIVERSIDADE ESTADUAL DE CAMPINAS
FACULDADE DE ENGENHARIA DE ALIMENTOS

LAUANE NUNES

**WHEY PROTEIN STABILIZED EMULSIONS CONTAINING LUTEIN:
PROPERTIES, BIOACCESSIBILITY AND PUTATIVE APPLICATIONS**

**EMULSÕES ESTABILIZADAS COM PROTEÍNA DE SORO DE LEITE
CONTENDO LUTEÍNA: PROPRIEDADES, BIOACCESSIBILIDADE E POSSÍVEIS
APLICAÇÕES**

CAMPINAS

2023

LAUANE NUNES

**WHEY PROTEIN STABILIZED EMULSIONS CONTAINING LUTEIN:
PROPERTIES, BIOACCESSIBILITY AND PUTATIVE APPLICATIONS**

**EMULSÕES ESTABILIZADAS COM PROTEÍNA DE SORO DE LEITE
CONTENDO LUTEÍNA: PROPRIEDADES, BIOACESSIBILIDADE E POSSÍVEIS
APLICAÇÕES**

Thesis presented to the Faculty of Food Engineering of the University of Campinas in partial fulfillment of the requirements for the degree of Doctor in Food Science.

Tese apresentada à Faculdade de Engenharia de Alimentos da Universidade Estadual de Campinas como parte dos requisitos exigidos para a obtenção do título de Doutora em Ciência de Alimentos.

Orientador: Guilherme Miranda Tavares

ESTE TRABALHO CORRESPONDE À
VERSÃO FINAL DA TESE DEFENDIDA
PELA ALUNA LAUANE NUNES, E
ORIENTADA PELO PROF. DR.
GUILHERME MIRANDA TAVARES.

CAMPINAS

2023

Ficha catalográfica
Universidade Estadual de Campinas
Biblioteca da Faculdade de Engenharia de Alimentos
Claudia Aparecida Romano - CRB 8/5816

Nunes, Lauane, 1993-
N922w Whey protein stabilized emulsions containing lutein : properties,
bioaccessibility and putative applications / Lauane Nunes. – Campinas, SP :
[s.n.], 2023.

Orientador: Guilherme Miranda Tavares.
Tese (doutorado) – Universidade Estadual de Campinas, Faculdade de
Engenharia de Alimentos.

1. Carotenoides. 2. Emulsificação. 3. Sistemas de entrega. 4. Alimentos
funcionais. I. Tavares, Guilherme Miranda. II. Universidade Estadual de
Campinas. Faculdade de Engenharia de Alimentos. III. Título.

Informações Complementares

Título em outro idioma: Emulsões estabilizadas com proteína de soro de leite contendo luteína: propriedades, bioacessibilidade e possíveis aplicações

Palavras-chave em inglês:

Carotenoids
Emulsification
Delivery systems
Functional foods

Área de concentração: Ciência de Alimentos

Titulação: Doutora em Ciência de Alimentos

Banca examinadora:

Guilherme Miranda Tavares
Evandro Martins
Juliana Azevedo Lima Pallone
Samantha Cristina de Pinho
Paula Kiyomi Okuro

Data de defesa: 19-09-2023

Programa de Pós-Graduação: Ciência de Alimentos

Identificação e informações acadêmicas do(a) aluno(a)

- ORCID do autor: <https://orcid.org/0000-0003-2603-9766>

- Currículo Lattes do autor: <https://lattes.cnpq.br/7936367343441422>

COMISSÃO EXAMINADORA

Prof. Dr. Guilherme Miranda Tavares
Universidade Estadual de Campinas – FEA/DECAN
Presidente

Prof. Dr. Evandro Martins
Universidade Federal de Viçosa - DTA
Membro Titular

Profa. Dra. Samantha Cristina de Pinho
Universidade de São Paulo - FZEA
Membro Titular

Profa. Dra. Juliana Azevedo Lima Pallone
Universidade Estadual de Campinas – FEA/DECAN
Membro Titular

Dra. Paula Kiyomi Okuro
Universidade Estadual de Campinas – FEA
Membro Titular

A Ata de Defesa com as respectivas assinaturas dos membros encontra-se no SIGA/Sistema de Fluxo de Dissertações/Teses e na Secretaria do Programa de Pós-Graduação

AGRADECIMENTOS

Agradeço à UNICAMP, à Faculdade de Engenharia de Alimentos e as agências de fomento pela infraestrutura e oportunidade de desenvolver esse trabalho. Agradeço também ao professor Guilherme por toda dedicação, paciência, ensinamentos e apoio nesses anos. Você é um exemplo de pessoa e profissional para mim, sempre presente e com uma palavra de encorajamento para nos motivar, muito obrigada.

As técnicas do laboratório de Química de Alimentos da FEA, Rosemar, Regiane e Ana Augusta por toda ajuda durante a execução deste trabalho, foi um grande prazer trabalhar com vocês.

A todas as pessoas e laboratórios que foram essenciais para a realização de algumas partes do projeto. Obrigada Laboratório de Apoio Central (LAC), Instituto Nacional de Fotônica Aplicada à Biologia Celular (INFABIC) e professora Eneida de Paula do Instituto de Biologia da UNICAMP. Muito obrigada professor Rodrigo Stephani e equipe do laboratório de Química Tecnológica (QUIMTEC) da UFJF.

Agradeço imensamente à professora Milena Corredig, técnicas e colegas do Departamento de Ciência de Alimentos da Universidade de Aarhus e amigos da Dinamarca e Alemanha pela oportunidade de viver todas as experiências do intercâmbio e por aprender tanto.

Aos meus amigos do laboratório de Química de Alimentos da FEA, Láisa, Fabiane, Ernane, Alane, Mariana, Lívia, Danilo, Anne, Leandro e Álvaro. Aos meus amigos da república Rep-ense, Pedro, Ana Paula e Túlio. Muito obrigada pelo companheirismo, pela ajuda, diversão e por tornarem meus dias mais felizes. Obrigada por serem minha família em Campinas. Sou eternamente grata pela amizade e carinho de vocês.

Por fim, agradeço à minha família, em especial aos meus pais, por serem um exemplo de coragem e força. Obrigada por todo suporte, apoio e incentivo.

Este trabalho foi realizado com o apoio do Conselho Nacional de Desenvolvimento Científico e Tecnológico (CNPq), processo 141708/2018-2; Coordenação de Aperfeiçoamento de Pessoal de Nível Superior - Brasil (CAPES), processo 88887.573461/2020-00 e Código de financiamento 001; Fundação de Amparo à Pesquisa do Estado de São Paulo (FAPESP), processo 2017/09214-4.

RESUMO

Devido à alta demanda e interesse em ingredientes e alimentos saudáveis e nutritivos, leite e produtos lácteos têm sido usados como modelos preferenciais para explorar e validar o desenvolvimento de produtos/ingredientes inovadores em alinhamento com as demandas dos consumidores. As proteínas do leite também são apontadas como preferidas para a concepção de sistemas de entrega de compostos bioativos, como os carotenoides, uma vez que tais compostos não podem ser sintetizados pelo corpo humano e apresentam inúmeros benefícios, principalmente para crianças e idosos. Neste contexto, o objetivo desta tese foi avaliar a relação entre propriedades físico-químicas, bioacessibilidade e possíveis aplicações de emulsões estabilizadas por proteínas do soro contendo luteína. No geral, este estudo destaca a importância das etapas nas quais a luteína é incorporada em emulsões simples (O/W) e duplas (W/O/W). A emulsão simples O/W-L produzida através da dessolvatação (a solução etanólica de luteína foi adicionada na dispersão aquosa de proteínas do soro, depois o etanol foi eliminado por rotaevaporação e a etapa de emulsificação foi realizada) pode contribuir positivamente para estender a estabilidade química (cerca de 52 % da quantidade inicial de luteína resistiu contra fotodegradação durante 14 dias de exposição à luz) e física (os perfis de intensidade de retroespalhamento permaneceram inalterados durante 14 dias de armazenamento) de produtos contendo luteína. Enquanto a emulsão dupla W-L/O/W (produzida com luteína aprisionada por nanopartículas de proteínas do soro usando dessolvatação na fase aquosa interna de uma emulsão dupla) apresentou a menor estabilidade da luteína (43 % de perda de luteína) contra a exposição à luz durante 14 dias de armazenamento e a maior bioacessibilidade (28 %) da luteína após a digestão *in vitro* das amostras recém-produzidas. A incorporação de luteína na fase oleosa das emulsões duplas deve ser avaliada com cuidado, uma vez que a alta fração oleosa usada nessas emulsões contribuiu para a estabilidade química do carotenoide, apesar de ter afetado negativamente sua bioacessibilidade. No estudo de caso avaliado sobre fórmulas infantis (FI) contendo diferentes fontes proteicas, a temperatura crítica de armazenamento (50 °C) favoreceu o desenvolvimento mais rápido da reação de Maillard na FI de leite e de soja; prejudicou a capacidade de reidratação e favoreceu o aumento do teor de gordura livre da FI de arroz e de soja, podendo comprometer a integridade de compostos como os carotenoides. Uma vez que as interações entre os vários componentes podem se formar durante a produção, armazenamento e digestão das emulsões podem afetar a estabilidade e bioacessibilidade da luteína, é importante entender como formas otimizadas de incorporação de carotenoides em emulsões podem impactar esses parâmetros em produtos alimentícios formulados complexos,

como as fórmulas infantis, cuja demanda por carotenoides é alta e as concentrações são geralmente baixas. Este último ponto, aparece como perspectiva premente deste trabalho de doutorado.

Palavras-chave: carotenoides; emulsificação; sistemas de entrega; alimentos funcionais.

ABSTRACT

Due to the high demand and interest in healthy and nutritional ingredients and foods, milk and dairy products have been used as preferable models to explore and validate the development of innovative products/ingredients in alignment with consumers' demands. Milk proteins are also identified as preferred for the design of bioactive compound delivery systems, such as carotenoids, since such compounds cannot be synthesized by the human body and have numerous benefits, especially for children and the elderly. In this context, the aim of this thesis was to evaluate the relationship between physicochemical properties, bioaccessibility, and possible applications of emulsions stabilized by whey proteins containing lutein. Overall, this study highlights the importance of the steps in which lutein is incorporated in single (O/W) and double (W/O/W) emulsions. The O/W-L simple emulsion produced by desolvation (the ethanolic lutein solution was incorporated into the aqueous dispersion of whey proteins, then the ethanol was eliminated by rotary evaporation and the emulsification step was performed) may positively contribute to extending the chemical (about 52 % of the initial amount of lutein resisted photodegradation during 14 days of exposure to light) and physical (backscattering intensity profiles remained unchanged during 14 days of storage) stability of products containing lutein. While the W-L/O/W double emulsion (produced with lutein entrapped by whey proteins nanoparticles using desolvation within the inner water phase of a double emulsion) showed the lowest lutein stability (43 % of lutein loss) against light exposure during 14 days of storage, and the highest lutein bioaccessibility (28 %) after *in vitro* digestion of fresh-produced samples. The incorporation of lutein into the oil phase of the double emulsions must be carefully evaluated, since the high oil fraction used in these emulsions contributed to the chemical stability of the carotenoid, despite having negatively affected its bioaccessibility. In the study regarding infant formulas (IF) containing different protein sources, critical storage temperature (50 °C) favored the faster development of the Maillard reaction in milk-IF and soy-IF, impaired their rehydration ability, and favored the increase in the free fat content of rice-IF and soy-IF and may compromise the integrity of compounds such as carotenoids. Since the interactions between the various components may form during the production, storage, and digestion of the emulsions may affect the lutein stability and bioaccessibility, it is important to understand how optimized forms of incorporation of carotenoids in emulsions can impact these parameters in complexly formulated food products, such as infant formulas, whose demand for carotenoids is high and concentrations are generally low. This topic rises as a promising perspective of work from this thesis.

Keywords: carotenoids; emulsification; delivery systems; functional foods.

LIST OF FIGURES

CHAPTER 2 - LITERATURE REVIEW

Figure 2.1- Production of high-protein dairy ingredients.....	23
Figure 2.2- Changes in milk appearance after heat and high-pressure treatments. (A) and (C) untreated skim milk; (B) heated skim milk (100 °C/3 min); (D) high-pressure-treated skim milk (600 MPa/30 min)	26
Figure 2.3- Effect of thermal treatment and emerging technologies on whey protein structure..	27
Figure 2.4- Effect of thermal treatment and emerging technologies on casein structure..	27
Figure 2.5- Supernatant obtained from milk unsonicated (A) and sonicated at 20 kHz for 60 min (B).....	37

CHAPTER 3 - RESEARCH ARTICLE 1

Figure 3.1- Particle size distribution of WPI dispersions and different emulsions measured by dynamic light scattering.....	69
Figure 3.2- A-C) Backscattering intensity profiles of emulsions. (t0) immediately after emulsion preparation, (t7) 7 days, and (t14) 14 days after emulsion preparation. The horizontal axis represents the position along the glass tube. D) Destabilization kinetics of emulsions during 14 days of storage	71
Figure 3.3- Representative images of the microstructure of fresh produced emulsions and after 14 days of storage at room temperature (25 °C) under lighted conditions.....	72
Figure 3.4- A) Color parameter b* and (B) color difference of emulsions during 14 days of storage under light. C) Appearance of fresh produced emulsions.....	75

CHAPTER 4 - RESEARCH ARTICLE 2

Figure 4.1- Particle size distribution and average hydrodynamic diameter of WPI, WPI particles and WPI particles prepared in the presence of lutein of W-L/O/W measured by DLS.....	91
Figure 4.2- A) Mean squared displacement of the emulsion droplets and B) Macroscopic viscosity index as a function of time for the various W/O/W emulsions, measured using the Rheolaser under quiescent conditions..	93

Figure 4.3- A) Visual appearance and color difference (calculated from the difference in color parameters L*, a* and b* values before and after storage under light at 33,340 lx and 24 °C). B) b* color parameter in fresh emulsions, as well as after 14 days of storage under light	95
Figure 4.4- Representative confocal microscopy images of emulsions before and after digestion. Lipids were labelled with Nile red (red color), and proteins were labelled with FITC (green color).....	96
Figure 4.5- A) Free amino acids released after <i>in vitro</i> intestinal digestion expressed as L-glutamine equivalents (mM) per g of protein and B) Free fatty acids of emulsions after digestion expressed as palmitic acid equivalents (mM)	97

CHAPTER 5 - RESEARCH ARTICLE 3

Figure 5.1- Representative T _{gr} curves for each one of the analyzed IFs. Arrows indicate the position of T _{gr}	112
Figure 5.2- Sorption isotherms of (A) milk-IF, (B) soy-IF, (C) rice-IF at 0 and 120 days of storage at 50 °C.....	115
Figure 5.3- Increment of AMP (A) and Browning Index (B) of the different IFs during aging at 50 °C. (B) The visual aspect of powdered samples at 0 and 120 days of storage at 50 °C of the milk-IF (1-2), soy-IF (3-4), rice-IF (5-6).....	117
Figure 5.4- Confocal microscopy images of the different IFs at (A) 0 and (B) after 120 days of storage at 50 °C with the percentage of increase of the free fat content.....	119
Figure 5.5- Particle size distribution characterized by the volume (%) occupied by the particles in relation to their size (A) and the cumulative volume diameters D ₉₀ (B) after rehydration of the different IFs before and after 60 and 120 days of aging at 50 °C	121

LIST OF TABLES

CHAPTER 2 - LITERATURE REVIEW

Table 2.1- Effects of different treatments on milk, milk protein dispersions and rehydrated high-protein dairy ingredients.	29
Table 2.2- Summary of treatments conditions.....	32

CHAPTER 3 - RESEARCH ARTICLE 1

Table 3.1- Hydrodynamic diameter (D_h , nm) and ζ -potential (mV) of WPI dispersions and different emulsions..	69
Table 3.2- Concentration of lutein in the emulsions, encapsulation efficiency and lutein loss after 14 days of storage under lighted conditions at room temperature.	73

CHAPTER 4 - RESEARCH ARTICLE 2

Table 4.1- Average hydrodynamic diameter measured by dynamic light scattering for primary emulsions, and $D_{4,3}$ average measured by static light scattering of the final emulsions.	92
Table 4.2- Amount of lutein measured in fresh emulsions, as well as after storage for 14 days under light. The encapsulation efficiency of the fresh emulsions is also shown.....	94
Table 4.3- Recovery and bioaccessibility after <i>in vitro</i> digestion	98

CHAPTER 5 - RESEARCH ARTICLE 3

Table 5.1- Composition of the different IFs according to the information provided by the manufacturer.....	109
Table 5.2- Water activity (a_w) and moisture content and free-fat content of milk-IF, soy-IF and rice-IF at 0 and 120 days of storage in different temperatures	114

TABLE OF CONTENTS

CHAPTER 1 – GENERAL INTRODUCTION	17
CHAPTER 2 - LITERATURE REVIEW	20
2.1. Introduction.....	21
2.2. Milk proteins and high-protein dairy ingredients	22
2.3. How do thermal treatments affect the structure and techno-functionality of milk proteins?	25
2.3.1. Effects on the structure	25
2.3.2. Effects on techno-functionalities	28
2.4. How do emerging technologies affect the structure and techno-functionality of milk proteins?	31
2.4.1. What are the emerging technologies?.....	31
2.4.2. Effects on the structure and techno-functionalities	34
2.5. How does the addition of organic solvents affect the structure of proteins?	40
2.6. How do different treatments modulate the binding properties and allergenicity of milk proteins?	41
2.7. Carotenoids: structure, bioactivities and fortification in formulated food products ..	42
2.8. How all this information connects into formulated products: the case of infant formulas	44
2.9. Perspectives	46
2.10. References	47
CHAPTER 3 - RESEARCH ARTICLE 1	61
3.1. Introduction.....	63
3.2. Materials and methods	64
3.2.1. Materials	64
3.2.2. Preparation of emulsions	65
3.2.3. Particle size and ζ -potential measurements	66

3.2.4.	Optical microscopy.....	66
3.2.5.	Physical stability of the emulsions	66
3.2.6.	Lutein encapsulation and photo-stability.....	67
3.2.7.	Color of emulsions over time	67
3.2.8.	Statistics.....	68
3.3.	Results.....	68
3.3.1.	Characterization of emulsions	68
3.3.2.	Physical stability of the emulsions	70
3.3.3.	Lutein encapsulation and photo-stability.....	72
3.4.	Conclusions.....	75
3.5.	References.....	76
CHAPTER 4 - RESEARCH ARTICLE 2.....		79
4.1.	Introduction.....	82
4.2.	Material and methods.....	83
4.2.1.	Materials	83
4.2.2.	Preparation of emulsions	84
4.2.3.	Particle size.....	85
4.2.4.	Rheological behavior.....	86
4.2.5.	Lutein encapsulation efficiency.....	86
4.2.6.	Lutein stability.....	86
4.2.7.	<i>In vitro</i> digestion.....	87
4.2.8.	Lutein recovery and bioaccessibility	88
4.2.9.	Confocal microscopy	89
4.2.10.	Protein hydrolysis	89
4.2.11.	Lipid hydrolysis	90
4.2.12.	Statistics	90
4.3.	Results.....	90

4.3.1.	Emulsion stability	90
4.3.2.	Lutein stability	93
4.3.3.	<i>In vitro</i> digestion.....	95
4.4.	Conclusions.....	99
4.5.	References.....	100
CHAPTER 5 - RESEARCH ARTICLE 3.....		104
5.1.	Introduction.....	107
5.2.	Material and methods.....	108
5.2.1.	Material.....	108
5.2.2.	Storage conditions	109
5.2.3.	Determination of glass–rubber transition temperature (T_{gr}) by rheological method.....	109
5.2.4.	Analysis of moisture content, water activity, and sorption isotherms.....	110
5.2.5.	Advanced Maillard Products (AMP) fluorescence and Browning Index.....	110
5.2.6.	Free fat content	110
5.2.7.	Confocal Laser Scanning Microscopy (CLSM)	111
5.2.8.	Particle size distribution	111
5.2.9.	Statistical data analysis.....	112
5.3.	Results and discussion	112
5.3.1.	Glass–rubber transition temperature (T_{gr}) determined by rheological method	112
5.3.2.	Water activity (a_w), moisture content and sorption isotherms of IFs during aging.....	113
5.3.3.	Development of the Maillard reaction.....	116
5.3.4.	Free fat.....	118
5.3.5.	Particle size distribution during rehydration	120
5.4.	Conclusions.....	122
5.5.	References.....	123
CHAPTER 6 - GENERAL DISCUSSION		128

CHAPTER 7 - GENERAL CONCLUSION AND PERSPECTVES	131
CHAPTER 8 - REFERENCES	132
CHAPTER 9 - ANNEXES	134

CHAPTER 1 – GENERAL INTRODUCTION

Nowadays, there is a great interest and demand for healthy and functional ingredients and food that contribute to consumers' health and life quality, being a global concern for food industries, consumers, and government agencies (Mantovani et al., 2021; Paiva et al., 2020). This trend is driven by high-quality food products, so considerable research has been completed aiming to preserve food products and to ensure their quality, safety, and high nutritional properties using minimal processing and minimal or no added chemical preservatives (Borad et al., 2017). In this context, various technologies have been studied and tested to optimize the biological and sensory properties of food products, guaranteeing their preservation and minimizing collateral effects associated with intense treatments (Mirmoghtadaie, Aliabadi, & Hosseini, 2016). Because of the wide consumption and availability of milk and dairy products, they have been used as preferable models to explore and validate the effects of these treatments, from a structural and techno-functional point of view. The information that follows may aid in the development of innovative dairy products/ingredients in alignment with consumer's demands.

The development of these functional products is very often based also on the supplementation of food matrices with a bioactive compound, such as carotenoids, for example, lutein, since such compounds cannot be synthesized by the human body and have numerous benefits, especially for children and elderly (Miranda-Dominguez et al., 2022; Stephenson et al., 2021). Nevertheless, the development of such food products is not a simple task. Several drawbacks are associated with their addition to food products, such as poor water solubility and low stability during processing and storage (Teo et al., 2017; Zhao et al., 2018). In this scenario, the design of delivery systems based on emulsions shows great potential for improving their stability and bioaccessibility with reduced adverse effects on food sensory properties (McClements & Li, 2010). The choice of structuring material and method of delivery are important points to be considered (Stephenson et al., 2021). Milk proteins are pointed out as those preferable for binding carotenoids since they are known to be natural vehicles that deliver essential nutrients from the mother to the newborn (Mantovani et al., 2021). Furthermore, they are natural food matrices with great availability, GRAS (generally recognized as safe), and great nutritional value (Tavares et al., 2014).

The development of functional products can also be based on the design of blends that try to mimic natural foods, such as in the case of infant formulas (IFs), whose main purpose of replacing or complementing breast milk for infant nutrition (Blanchard, Zhu, & Schuck,

2013). Traditional IFs available on the market are formulated using cow's milk and cow's milk-based ingredients as the main protein source (Bocquet et al., 2019), but soy protein isolate, or hydrolyzed rice protein could be used as alternative protein sources. Processing and storage parameters applied to IFs containing alternative protein sources derived from those consolidated for cow's milk-based IFs (Le Roux, Chacon, et al., 2020), however, the replacement of dairy proteins by plant proteins, even partially, has a great impact on IFs properties, which means that process parameters should be adapted for each formulation to provide satisfactory quality for the obtained IFs (Le Roux, Mejean, et al., 2020). To understand the relationship between aging conditions and the physicochemical changes of IFs, it is important to identify their critical storage conditions, which will be highly influenced by their composition (Masum et al., 2020; Saxena et al., 2019; Tham, Yeoh, et al., 2017).

In this context, the aim of this thesis was to evaluate the relationship between physicochemical properties, bioaccessibility, and possible applications of emulsions stabilized by whey proteins containing lutein. To achieve this, this thesis was structured into eight chapters:

- i. Chapter 1 displays a General Introduction to the thesis subject.
- ii. Chapter 2 contains a literature review of milk proteins and how different treatments, and reaction parameters affect their structure, techno-functionality, and binding properties. Besides to presenting the structure, bioactivity, and fortification of carotenoids in formulated food products. Finally, a case study on formulated food products, infant formulas.
- iii. Chapter 3 discusses delivery systems in which lutein is incorporated into whey protein stabilized emulsions evaluating how the steps of addition and evaporation of ethanol affect the obtained systems.
- iv. Chapter 4 discusses other types of delivery systems in which lutein is incorporated into simple and double emulsions containing protein nanoparticles, to evaluate the effects on stability and bioaccessibility.
- v. Chapter 5 presents a case study on infant formula with valuable information about the relationship between aging conditions and the physicochemical changes in infant formulas, to identify their critical storage conditions.
- vi. Chapter 6 brings the General Discussion that connects the main results described in Chapters 3 to 5.
- vii. Chapter 7 has a General Conclusion which also brings some future perspectives.

- viii. Chapter 8 contains the references cited in the Introduction and General Discussion.

CHAPTER 2 - LITERATURE REVIEW

The content of the literature review (chapter 2) was mostly extracted from the review article “Thermal treatments and emerging technologies: Impacts on the structure and techno-functional properties of milk proteins”, written by the author of this thesis. This review was published in the Journal Trends in Food Science and Technology (IF 2023: 16.002) and it can be accessed through the link <https://doi.org/10.1016/j.tifs.2019.06.004>, and the license to reuse this content in this thesis is in Annex 1. In addition, some topics on structure, bioactivity and fortification of carotenoids in formulated food products are covered. As well as a case study on formulated food products, infant formulas.

2.1.Introduction

Milk and dairy products are among the most important sources of proteins for adults and children, being the main raw material and protein source in infant formulas (Borad et al., 2017). Proteins are important for various human metabolic functions because they (i) provide essential amino acids and bioactive peptides, (ii) bind and transport metals and vitamins and (iii) perform specific functions such as antibodies and hormones (Borad, Kumar, & Singh, 2017). During food processing, proteins are essential compounds because of their nutritional value and techno-functional properties, which determine food quality and stability (Han, Cai, Cheng, & Sun, 2018).

Due to the great demand for healthy and functional ingredients, the development of functional products has grown with wide applications of carotenoids as bioactive ingredients in food. Similar to adults, carotenoid consumption has been linked with a number of health benefits in infants. Between them, lutein has an important role in ocular development and supporting brain development and enhanced cognitive functioning, emphasizing the importance of carotenoid consumption in infants and the need for supplementation in infant formulas (Miranda-Dominguez et al., 2022; Stephenson et al., 2021). However, due to their low solubility in an aqueous medium, low bioavailability, and sensitivity to heat, oxygen, and light, which can even be worsened depending on the process and storage conditions, their incorporation in formulated food products is somehow limited (Teo et al., 2017; Zhao et al., 2018). In this context, the encapsulation of carotenoids as a method to optimize carotenoid delivery has been proposed as viable to overcome the aforementioned drawbacks and will be addressed in the following chapters.

Infant formulas (IFs) have the main purpose of replacing or complementing breast milk for infant nutrition (Blanchard, Zhu, & Schuck, 2013). Even though, formulas should mimic the composition of breast milk as much as possible, carotenoid concentrations are mainly low and most formulas are not supplemented to match the higher levels found in human milk (Miranda-Dominguez et al., 2022; Stephenson et al., 2021). Traditional IFs available on the market are formulated using cow's milk and cow's milk-based ingredients as the main protein source. However, the replacement of dairy raw materials with plant protein-based ones is recommended in formulating IFs for infants with cow's milk protein allergy (Bocquet et al., 2019). In this context, soy protein isolate or hydrolyzed rice protein is often used as preferable alternative protein sources. Processing and storage parameters applied to IFs containing alternative protein sources derived from those consolidated for cow's milk-

based IFs (Le Roux, Chacon, et al., 2020), however, the replacement of dairy proteins by plant proteins, even partially, has a great impact on IFs properties, which means that process parameters should be adapted for each formulation to provide satisfactory quality for the obtained IFs (Le Roux, Mejean, et al., 2020).

2.2. Milk proteins and high-protein dairy ingredients

Milk proteins can be divided into two main groups (i) caseins, which are insoluble at pH 4.6 and represent 80 % of the total protein content of bovine milk, and (ii) whey proteins, which are globular proteins with an approximate pI of 5.0 and represent the other 20 % of the total protein content of bovine milk (Beliciu & Moraru, 2013; Tavares & Malcata, 2016).

Caseins in milk are naturally present as supramolecular structures of approximately 150-200 nm in hydrodynamic diameter, termed casein micelles. These casein micelles contain four different polypeptide chains, α_{S1} -, α_{S2} -, β - and κ -casein, in the following proportion: 4.0-1.0-3.5-1.5 (Beliciu & Moraru, 2013). To stabilize the micelles, casein molecules are assembled together by protein-protein interactions (hydrophobic, hydrogen, and electrostatic interaction) and by the presence of calcium phosphate nanoclusters (6–8 % by weight) (Broyard & Gaucheron, 2015).

However, whey proteins are a group formed by a complex mix of different proteins containing mostly, β -lactoglobulin (β -LG) (~ 55 %), α -lactalbumin (α -LA) (~ 20 %), bovine serum albumin (BSA) (~ 7 %), immunoglobulins (~ 13 %) and several other minor proteins such as lactoferrin (~ 5 %) (Tavares & Malcata, 2016). In addition, for whey obtained through the enzymatic separation of casein micelles catalyzed by chymosin, caseinomacropeptide (CMP) released from the κ -casein can be observed (Abd El-Salam & El-Shibiny, 2018). When present, this peptide may represent up to 20 % of the total whey protein content (Tavares & Malcata, 2016). Compared to casein micelles, whey proteins are much smaller with a hydrodynamic diameter of no longer than 10 nm (O'Mahony & Fox, 2013).

Despite the theoretical classification of milk proteins, these proteins are typically incorporated in food products as commercial ingredients in powder, popularly as concentrates or isolates of milk protein or its fractions. Milk protein concentrate (MPC) usually presents a total protein concentration of approximately 40-85 % and milk protein isolate (MPI) presents greater than 90 % protein (Agarwal, Beausire, Patel, & Patel, 2015). A proportion of approximately 80 % casein and 20 % whey protein is maintained in these products. From the casein fraction, isolated casein micelles, calcium caseinate (CaCas), and sodium caseinate

(NaCas) can be obtained, among which NaCas is the most used because of its better solubility (Silva, Ahrné, Ipsen, & Hougaard, 2018). Whey protein concentrates (WPCs) of a total protein content typically between 35 and ≥ 80 % and whey protein isolates (WPIs) of a total protein content ≥ 90 % can be produced from whey (Carter & Drake, 2018).

These ingredients are widely used in a great variety of food products because of their unique techno-functional properties, e.g., emulsification, gelation, thickening, foaming, and flavor binding capacity, and because of their high nutritive value and Generally Recognized as Safe (GRAS) status (Frydenberg, Hammershøj, Andersen, Greve, & Wiking, 2016; Jambrak, Mason, Lelas, Paniwnyk, & Herceg, 2014).

Figure 2.1 summarizes the major processes involved in the production of several high-protein dairy ingredients. MPC powders are obtained from pasteurized skim milk ultrafiltration to concentrate its proteins by removing water, lactose, and soluble minerals (Yanjun et al., 2014). To produce milk protein powders (MPPs) of greater than 65 % total protein content, diafiltration is required (Figure 2.1). After ultrafiltration and/or diafiltration, MPP can be obtained by spray drying (Agarwal et al., 2015). The caseins present in MPP have a micellar structure similar to the native form found in milk, and whey proteins are present in a globular native form or may undergo subtle modifications in their tertiary structure according to processing conditions (O'Sullivan et al., 2014).

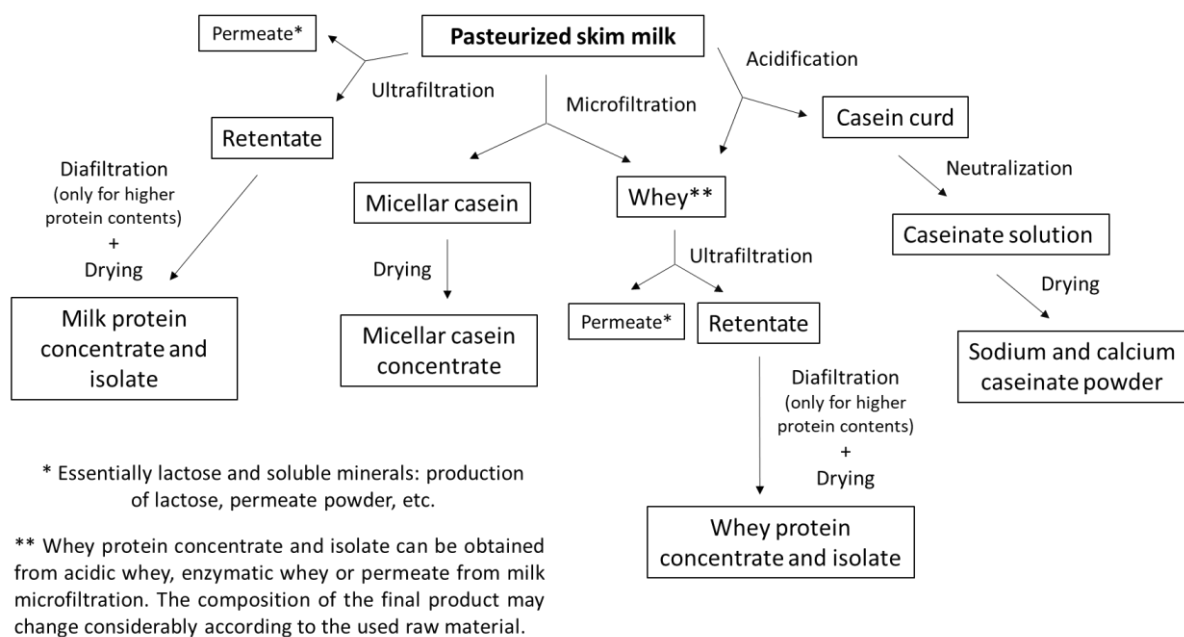


Figure 2.1- Production of high-protein dairy ingredients. Obtained from Nunes et al. (2019) with authorization of use (Annex 1).

Native phosphocaseinate or micellar casein concentrate (MCC) is produced by microfiltration of pasteurized skim milk with a membrane pore size of approximately 0.1 μm to concentrate casein micelles (Figure 2.1) (Silva et al., 2018). Diafiltration may be used before spray drying to increase whey protein removal, which varies from 60 to 95 % (Agarwal et al., 2015). After complete rehydration of MCC powders, individual casein micelles approximately 150-200 nm in hydrodynamic diameter and a structure similar to the native ones are expected (Zhang et al., 2018).

However, caseinates consist of salts derived from the partial disruption of the native micellar structure of the casein micelles. NaCas is produced from skim milk by acidic precipitation of micellar caseins and their resuspension under alkaline conditions (NaOH) (Silva et al., 2018). During this process, calcium phosphate is partially removed from the casein micelle, and the structure is damaged producing smaller structures of approximately 65 nm in hydrodynamic diameter (Hadjسادok, Pitkowski, Nicolai, Benyahia, & Moulai-Mostefa, 2008). CaCas is produced exactly as NaCas only replacing sodium hydroxide with calcium hydroxide ($\text{Ca}(\text{OH})_2$). CaCas shows poor hydration and a compact structure because of the amount of calcium bound to strong anionic sites of the caseins (O'Mahony & Fox, 2013).

The whey obtained as a permeate of milk microfiltration, acidic whey from casein micelle precipitation, and sweet whey obtained from milk enzymatic coagulation are potential raw materials to produce WPCs and WPIs (Abd El-Salam, El-Shibiny, & Salem, 2009). To produce WPC and WPI, microfiltration may be used to pretreat the whey, ultrafiltration/diafiltration is used to concentrate whey proteins, vacuum evaporation may also be used for concentration, and spray drying is used to obtain powdered ingredients (Carter & Drake, 2018).

Spray drying is the most widespread drying process used to produce high-protein dairy ingredients, generating particles with dense structures and heterogeneity in size, shape, and porosity as a function of the drying conditions and the nature of the proteins in the powder (Schuck, le Floch-Fouere, & Jeantet, 2013). During spray drying, the outlet air temperature is noted as a critical parameter that dictates the maximal temperature reached by the product droplets/particles; it generally does not exceed 70 $^{\circ}\text{C}$ (Meena, Singh, & Panjagar, 2017). Spray drying has been reported to promote at some level whey protein denaturation, with a significant negative impact on the solubility of high-protein dairy ingredients (Schuck et al., 2013; Udabage, Puvanenthiran, Yoo, Versteeg, & Augustin, 2012). Solubility is an important primary techno-functional property as it affects other properties such as emulsifying, gelling,

and foaming (Higuera-Barraza et al., 2016). Thus, the intensity of the thermal treatments associated with the pasteurization of the raw material, concentration by vacuum evaporation, and spray drying may affect the techno-functional behavior of the obtained high-protein dairy ingredients.

2.3. How do thermal treatments affect the structure and techno-functionality of milk proteins?

2.3.1. Effects on the structure

Thermal treatment is the most applied method of food processing used to prevent deterioration caused by microorganisms and to provide a safer food product with an extended shelf life (Raikos, 2010). The two most commonly applied thermal treatments in milk currently are the high-temperature short time (HTST) and ultra-high temperature (UHT) treatments. During the HTST treatment, milk is heated to a minimum of 72 °C for 15 s, whereas the UHT treatment maintains the milk at temperatures ranging from 135 to 145 °C for 2 - 4 s (Qi et al., 2015).

The effectiveness of a treatment applied to food products depends on the target variable, thus the effects of this treatment may vary as a function of the associated physical parameters, as well as product characteristics (composition, protein concentration, conductivity, pH, ionic strength, water activity, etc.).

Generally, the energy associated with the treatments discussed in this review is sufficient to (i) disrupt non-covalent interactions, such as hydrogen bonds and hydrophobic interactions, and (ii) change protein conformation exposing hydrophobic amino acid residues (aliphatic/aromatic) and/or free sulfhydryl groups. However, excessively intense treatments may induce the formation of new inter and intramolecular interactions, leading to aggregation (Frydenberg et al., 2016; Qi et al., 2015). cc (Beliciu et al., 2012).

In addition, during thermal treatment, α -terminal amino groups from proteins and ϵ -amino groups from lysine residues may react with reducing carbohydrates via a Maillard reaction. Thus, depending on the intensity of the thermal treatment, sensory properties (aroma, flavor, and appearance) as well as the nutritional value of the products may be negatively affected (Abd El-Salam & El-Shibiny, 2018).

Whey proteins submitted to thermal treatment may suffer conformational changes leading to a more random structure and in the function of the intensity of the treatment, irreversible changes leading to protein aggregation and precipitation may be observed

(Dissanayake & Vasiljevic, 2009). Rehydrated WPI treated at 72 °C for 10 min and 90 °C for 1 and 10 min showed a substantial decrease in both α -LA and β -LG monomers, indicating their aggregation, which was not observed under mild conditions (63 °C for 30 min and 72 °C for 15 s) (Sui et al., 2011). UHT treatments seem to induce disruption of nearly all of the tertiary structure of whey proteins, as well as a significant loss of the secondary structure, in particular, antiparallel β -sheet and α -helix (Qi et al., 2015). In contrast, HTST pasteurization (72 - 75 °C for 15 - 20 s) seems to have minimal or no impact on the secondary structure of whey proteins in milk (Bogahawaththa et al., 2018; Qi et al., 2015).

In general, mild thermal treatments such as HTST pasteurization do not sensibly disturb the structure of the casein micelle in skim milk, which shows high heat stability because of its lack of tertiary structure (Bogahawaththa et al., 2018; Broyard & Gaucheron, 2015). In contrast, severe thermal treatments (at temperatures above 100 °C) induce considerable precipitation of soluble calcium and solubilization of colloidal calcium phosphate. In addition, extensive heat induces the dissociation of κ -casein, as well as some α_s -caseins from micelles, reducing their steric and electrostatic repulsion, leading to aggregation. When whey proteins are present during thermal treatment, complexes between β -LG and casein micelles or individual caseins (particularly κ -casein) are formed via disulfide bonds (Dalgleish & Corredig, 2012). As shown in Figure 2.2 (A and B), these structural changes induced in skim milk by intense thermal treatment may impact its appearance, appearing whiter (Considine et al., 2007).

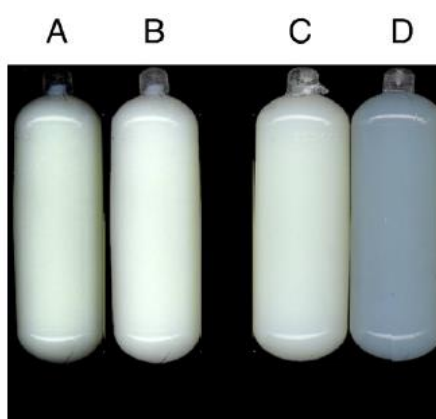


Figure 2.2- Changes in milk appearance after heat and high-pressure treatments. (A) and (C) untreated skim milk; (B) heated skim milk (100 °C/3 min); (D) high-pressure-treated skim milk (600 MPa/30 min) (Considine et al., 2007).

These structural changes are summarized in Figure 2.3 for whey proteins and in Figure 2.4 for caseins.

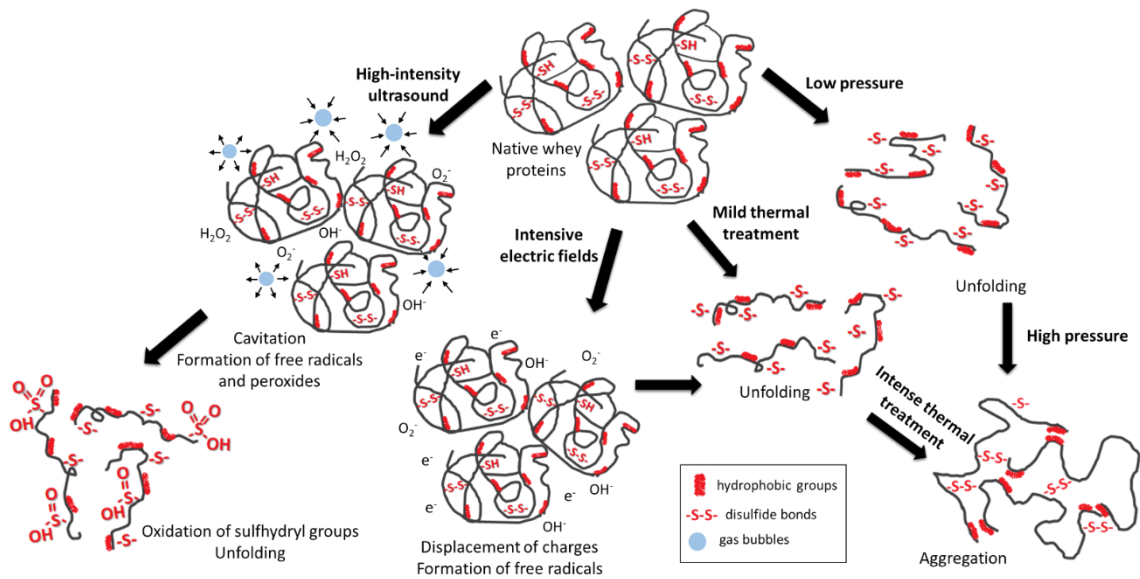


Figure 2.3- Effect of thermal treatment and emerging technologies on whey protein structure. Obtained from Nunes et al. (2019) with authorization of use (Annex 1).

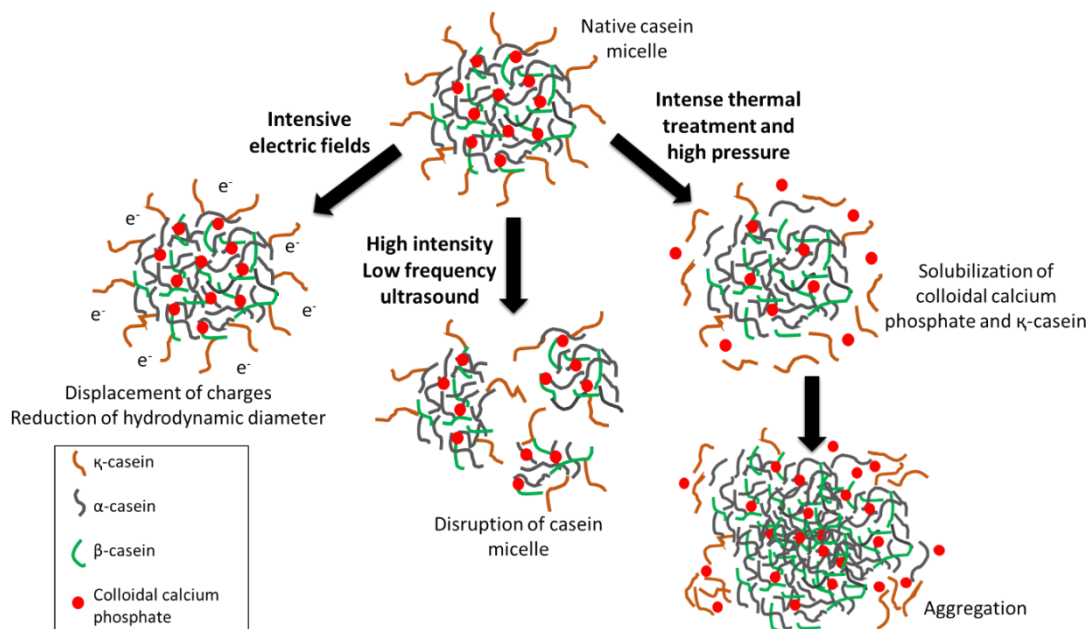


Figure 2.4- Effect of thermal treatment and emerging technologies on casein structure. Obtained from Nunes et al. (2019) with authorization of use (Annex 1).

2.3.2. Effects on techno-functionalities

As previously discussed, protein structure may change when submitted to different treatments; these changes may also be translated as different techno-functional behaviors (Mirmoghtadaie et al., 2016), as shown in Table 2.1. Generally, the increase in the flexibility and the superficial hydrophobicity of milk proteins because of a specific treatment results in a better orientation and faster adsorption of these proteins on polar/nonpolar interfaces (Mirmoghtadaie et al., 2016). For example, Nicorescu et al. (2010) observed a strong increase in the stability of the foam from rehydrated WPI submitted to a continuous flow thermal treatment at 80 °C for 300 s, because of the formation of heat-induced soluble protein aggregates. In this study, the best foam stability was found when approximately 10 % of soluble aggregates were present, supposedly via their effect on drainage retardation (Nicorescu et al., 2009). Nevertheless, the formation of large protein aggregates leads to emulsion and foam instability, as observed in heat-treated milk protein systems (Raikos, 2010) or the impairment of the emulsification and gelation properties of WPI (Sui et al., 2011). Thus, this equilibrium needs to be attended to improve milk protein interfacial properties.

In the same manner, the increase in the superficial hydrophobicity because of the protein unfolding induced by different treatments has been positively correlated with an improvement in protein gelling properties (Frydenberg et al., 2016). Allied with protein unfolding, the manner in which the different treatments are capable of exposing protein active sites to form protein networks seems to be a determinant of the strength of the gel obtained (Frydenberg et al., 2016; Shen, Fang, Gao, & Guo, 2017). However, intense thermal treatment can increase the gelation time and decrease gel firmness during enzymatic coagulation, mainly associated with heat denaturation of whey protein, which impacts rennin hydrolysis kinetics (Broyard & Gaucheron, 2015; Perreault et al., 2017).

Table 2.1- Effects of different treatments on milk, milk protein dispersions, and rehydrated high-protein dairy ingredients.

Treatment	Product	Effects	References
Thermal treatment	Rehydrated MCC, Rehydrated WPC, raw milk	- Pasteurization did not affect the secondary structure of whey proteins nor disturb the supramolecular structure of the casein micelles. - High temperatures caused loss of the secondary structure, disrupted the tertiary structure, unfolding and/or aggregation of whey proteins. It also induced the solubilization of colloidal calcium phosphate and CMs aggregation.	Beliciu et al., 2012; Bogahawaththa et al., 2018; Laiho et al., 2015; Qi et al., 2015
	Rehydrated WPI, Rehydrated WPC	- Under severe conditions (90 °C/1-10 min) emulsification and gelation properties worsened.	Perreault et al., 2017; Sui et al., 2011
	Rehydrated WPI	- Foam stabilization improved.	Nicorescu et al., 2010
Ultrasound	Reconstituted skim milk	- Casein micelles were ruptured with a consequent reduction in the particle diameter.	Liu et al., 2014a
	Reconstituted skim milk; Rehydrated: MCC, NaCas, MPI, MPC, WPI, WPC, hydrolyzed whey proteins	- Superficial hydrophobicity increased while the intrinsic viscosity decreased. - The rehydration process and the emulsifying, foaming, and gelation properties improved.	Furtado et al., 2017; Jambrak et al., 2008, 2014; Liu et al., 2014b; Madadlou et al., 2010; O'Sullivan et al., 2014; YanJun et al., 2014; Zhang et al., 2018
	Whey protein dispersions, Rehydrated WPC; Rehydrated WPI	- Turbidity of suspensions decreased. - Gel strength increased while the gelation time and gel syneresis decreased.	Martini et al., 2010; Zisu et al., 2011
Pulsed electric fields	Raw skim milk	- The casein micelle size was not significantly altered.	Shamsi & Sherkat, 2009
	Rehydrated WPI	- Whey proteins unfolded leading to an increase in the superficial	Xiang et al., 2011

		hydrophobicity.	
	Rehydrated WPI, raw milk	- Physicochemical (protein aggregation, surface hydrophobicity, sulfhydryl groups, and thermal stability) or emulsification properties were not affected while the gelation properties improved.	Sui et al., 2011; Yu et al., 2009
	Rehydrated WPI	- Despite the conservation of the secondary structure of whey proteins, their tertiary structure changed.	Bouaouina et al., 2006
High- pressure treatments	Raw skim milk; Rehydrated WPC, Rehydrated WPI, Rehydrated MCC	- Superficial hydrophobicity increased. - The hardness of casein and whey protein gels, as well as the stability of formed emulsions and foams, increased.	Baier et al., 2015; Broyard & Gaucheron, 2015; Lee et al., 2006;
	Raw skim milk; Rehydrated MCC, Rehydrated MPC	Under pressures > 450 MPa: - Large protein aggregates formed and the secondary structure of the proteins was affected. - The casein micelle size decreased and the levels of soluble calcium and phosphorus increased.	Bogahawaththa et al., 2018; Cadesky et al., 2017
	Pasteurized milk	- The increased viscosity observed at \geq 250 MPa is a result of the disintegration of casein micelles and the consequent formation of nonuniform protein aggregates. - Foaming and emulsifying properties improved.	Hettiarachchi et al., 2018; Tran et al., 2018
	Microwave β -LG dispersion	- At low temperatures, microwaves did not induce protein changes. - At high temperatures, significant changes in the secondary and tertiary structure of β -LG were reported, accelerating protein unfolding and	Gomaa et al., 2016, 2013

		aggregation.	
Gamma radiation	β -LG dispersion, Rehydrated WPI	High doses > 20 kGy: - The tertiary and secondary structures of β -LG in solution changed, leading to aggregation. - Protein solubility decreased, and apparent viscosity and turbidity of dispersions increased.	de la Hoz & Netto, 2008; Wang et al., 2018b
Pulsed light	Rehydrated WPI	- Changes in tertiary structure and slight changes in secondary structure were noted. - Excessive doses caused protein aggregation. - Low doses resulted in an enhancement of solubility and foaming properties.	Siddique et al., 2016, 2017
Supercritical fluid extrusion	Rehydrated WPC	- Decreased protein solubility. - Induced cold-set gelation.	Manoi & Rizvi, 2008

2.4. How do emerging technologies affect the structure and techno-functionality of milk proteins?

2.4.1. What are the emerging technologies?

There is an enormous demand for new technologies to replace (or to be combined with) conventional thermal treatment, providing longer shelf life without causing undesirable changes (Raikos, 2010; Shanmugam et al., 2012). Since the intensity of the treatment is a key point concerning its effect on milk proteins, Table 2.2 summarizes the range of processing conditions of all technologies discussed in this review.

Table 2.2- Summary of treatment conditions.

Treatment	Conditions
Thermal treatment	HTST: 72 - 75 °C / 15 - 20 s UHT: 135 - 145 °C / 2 - 4 s
High-pressure treatment	High-pressure processing: 100 - 1000 MPa / 5 - 30 min High-pressure homogenization: 100 - 400 MPa / 10 ⁻⁴ s
High-intensity ultrasound	Low-intensity (< 1 W.cm ⁻²) high-frequency (100 kHz - 1 MHz) High intensity (10 - 1000 W.cm ⁻²) low frequency (20 - 100 kHz)
Pulsed electric field	15 - 50 kV.cm ⁻¹ / few μs
Microwave	300 MHz–300 GHz / cycles
Radio frequency	3 KHz to 300 MHz / cycles
Irradiation	Ionizing irradiation: 1- 50 kGy / h Nonionizing irradiation: 100 – 1100 nm / few minutes to hours
Supercritical fluid extrusion	2 to 30 MPa, 20 - 50 °C, for up to 300 min

In high-pressure processing or high hydrostatic pressure processing, the products are placed in a specially designed vessel containing a pressure-transmitting fluid (e.g., water) where they are exposed to high pressures (100-1000 MPa) for 5 to 30 min. This treatment aids in maintaining food characteristics because of the absence of significant heating (Huppertz, Vasiljevic, Zisu, & Deeth, 2019; Voigt, Kelly, & Huppertz, 2015). High-pressure processing in the range of 300–600 MPa is considered an alternative nonthermal treatment for milk “pasteurization” (Bogahawaththa, Buckow, Chandrapala, & Vasiljevic, 2018; Voigt et al., 2015).

However, in high-pressure homogenization or dynamic high-pressure treatment, the liquid product passes through a homogenizing valve in a continuous flow and is subjected to pressures up to 400 MPa for a much shorter time (approximately 10⁻⁴ s). In the specific case of microfluidization, the homogenizer design forces the collision of two streams of the liquid product at high velocity (up to 50 m.s⁻¹) ensuring its local pressurization (Deeth & Lewis, 2017). Similarly to high-pressure homogenization, recent developments have enabled the conception of high-pressure-jet processing, in which pumps are able to deliver dynamic pressures up to 600 MPa, and a nozzle is used to restrict the flow (Tran, Roberts, Felix, &

Harte, 2018). In these homogenization designs, the products are simultaneously submitted to phenomena induced by cavitation, shear, turbulence, and a temperature increase. Unlike the high-pressure processing treatments, the temperature irreversibly increases by approximately 20 °C for each 100 MPa increase on high-pressure homogenization treatments. Thus, in the latter case, temperature control is highly recommended (Harte, 2016).

High-intensity ultrasound (HIU) has been noted as an environmentally friendly technology since sound waves are considered safe and nontoxic and it requires low energy and short processing time (Frydenberg et al., 2016). This technology is based on the passage of sound waves through the product, creating regions of high and low pressure (O'Sullivan et al., 2017). The pressure differential generated is directly proportional to the amount of energy applied to the system. It can be classified into two categories: low-intensity ($< 1 \text{ W.cm}^{-2}$) with high frequency (100 kHz - 1 MHz), and high intensity ($10 - 1000 \text{ W.cm}^{-2}$) with low frequency (20 - 100 kHz) (Noci, 2017; O'Sullivan et al., 2017).

Pulsed electric field (PEF), in turn, is a technology that offers the advantage of retaining many of the food quality attributes that can be lost during conventional thermal treatment (Xiang, Ngadi, Ochoa-Martinez, & Simpson, 2011). PEF is an ideal alternative treatment for the processing of high-protein foods such as milk and dairy ingredients or products containing heat-sensitive components because of its reduced heating effects (Deeth & Datta, 2011; Zhao, Tang, Lu, Chen, & Li, 2014). For this treatment, high-intensity electrical pulses (15 and 50 kV.cm^{-1}) are applied to the products by electrodes over a very short duration (a few microseconds) (Huppertz et al., 2019). Cooling systems may be associated with PEF treatments to avoid long exposure of the product to elevated temperatures (Deeth & Datta, 2011). Though PEF treatments may have effects on the structure of milk proteins and consequently on their techno-functionality, most studies applied to milk and dairy products have focused on microorganisms (Huppertz, Vasiljevic, Zisu, & Deeth, 2019).

Over the past few decades, microwave technology has gained widespread popularity (Han et al., 2018). It is based on the application of electromagnetic irradiation within the frequency range of 300 MHz–300 GHz, with 915 MHz and 2.45 GHz the most applied frequencies. The electric field component of the microwave induces the rotation of dipoles from water, organic molecules, or ions, and the friction generated by these molecules produces heat that is distributed in a nonuniform manner during the process (Mishra & Ramchandran, 2015). Therefore, uncontrolled microwave heating can generate effects similar to conventional heating (Gomaa, Nsonzi, Sedman, & Ismail, 2016). However, radio frequency

technology covers the frequency range from 3 KHz to 300 MHz and has a lower energy consumption and more uniform heating compared to that of microwaves (Han et al., 2018).

Ionizing irradiation and nonionizing irradiation are other emerging technologies applied to food products, including milk. Gamma-rays, X-rays, or electron beams are the most commonly used sources of ionizing irradiation in food products, which act by freeing electrons from atomic bonds (Deeth & Lewis, 2017; Han et al., 2018). Meanwhile, nonionizing irradiation includes ultraviolet rays (UV-A, B, and C) (100–400 nm), visible light (400–700 nm), and infrared (700–1100 nm) (Kuan, Bhat, Patras, & Karim, 2013). Pulsed light refers to the application of short pulses of high-energy broad-spectrum light (200–1100 nm) (Siddique, Maresca, Pataro, & Ferrari, 2017).

Supercritical fluid extrusion has also been applied to dairy matrices tracking new textures and rheological characteristics. In dairy products, treatments range from 2 to 30 MPa at temperatures from 20 to 50 °C and for up to 300 min duration (Deeth & Lewis, 2017). Supercritical carbon dioxide (Sc-CO₂) is the most often used supercritical fluid because its supercritical conditions can be easily reached ($T_c = 31^\circ\text{C}$, $P_c = 7.38\text{ MPa}$). Its high solubility enhances plasticizing and depressurization promotes the expansion of the material. This technology successfully induces thermal gelation of dairy ingredients (Chauvet, Sauceau, & Fages, 2017).

2.4.2. Effects on the structure and techno-functionalities

Many studies have been completed applying emerging treatments as an alternative to improve protein techno-functional properties by inducing controlled structural changes (Huppertz, Vasiljevic, Zisu, & Deeth, 2019). A summary of these studies is shown in Table 2.1.

2.4.2.1. High-pressure treatment

The effect of high-pressure processing on the structure of milk proteins highly depends on the molecular compression and on the reduction in volume during treatment (Voigt et al., 2015). At a low protein concentration and low pressure (< 300 MPa), reversible denaturation may occur, whereas at higher pressures (> 300 MPa) irreversible and extensive effects on protein structure and techno-functionality may be observed (Abd El-Salam et al., 2009). From a structural perspective, as hydrophobic interactions are very sensitive to pressure, the quaternary structure of proteins is frequently affected by high-pressure processing (Huppertz et al., 2019). Furthermore, significant changes in the tertiary structure of

proteins are observed above 200 MPa, while secondary structure changes occur at very high pressures, leading to irreversible denaturation (Voigt et al., 2015). For example, processing above 400 MPa induced denaturation of whey proteins in skim milk with a reduction in β -sheets and α -helix content. Furthermore, at 600 MPa, the formation of large aggregates mainly stabilized by disulfide bonds involving β -LG and κ -casein has been observed. Under these conditions, the measured structural impact was substantially greater than that associated with HTST pasteurization (Bogahawaththa et al., 2018). These structural changes are summarized in Figure 2.3.

Compared to high-pressure processing, very few studies are available focusing on the effect of high-pressure homogenization on food proteins. Some studies suggest only minor changes in the secondary or tertiary structure of proteins by homogenization at pressures up to 400 MPa when cooling devices are used (Harte, 2016). In high-pressure-jet processing, limited denaturation of whey protein from skim milk was reported at high pressure (500 MPa) (Mohan, Ye, & Harte, 2016).

Regarding the techno-functionality (Table 2.1), high-pressure treatments were useful to (i) improve the gelling, emulsifying and foaming properties of whey proteins dispersions treated at 500 MPa - 20 min and 690 MPa - 5 min (Baier et al., 2015; Lee et al., 2006); (ii) induce an increase in the heat coagulation time and the emulsifying activity index of whey protein when combined with thermal treatments (90 °C for 20 min with 1 and 5 passes at 140 MPa) (Dissanayake & Vasiljevic, 2009) and (iii) stabilize whey protein against heat-induced changes during spray drying of protein-rich products (200 MPa for 10 min was reported as the optimal condition) (Udabage et al., 2012). The increase in pressure levels and the duration of the high-pressure processing applied to whey proteins increased the strength of the formed gels, for example (Abd El-Salam et al., 2009; Lee, Clark, & Swanson, 2006).

Despite their open structure, casein micelles are compressible. Then, they may be disrupted by high-pressure processing at greater than 200 MPa (Voigt et al., 2015). After prolonged treatments at 250–300 MPa, micellar fragments reassemble through hydrophobic interactions to form micelle-like supramolecular structures smaller than the native ones (Huppertz, Fox, de Kruif, & Kelly, 2006). At 10 % casein concentration, treatments at pressures greater than 350 MPa resulted in a homogeneous network similar to a weak gel (Cadesky, Walkling-Ribeiro, Kriner, Karwe, & Moraru, 2017). Summarizing, high-pressure processing (i) decreases the hydrodynamic diameter of casein supramolecular structures, consequently decreasing the turbidity of the suspensions; (ii) increases the hydration of caseins; and (iii) induces slight solubilization of colloidal calcium phosphate (Broyard &

Gaucheron, 2015; Deeth & Lewis, 2017), as shown in Figure 2.4. After high-pressure processing, a reduction in the casein supramolecular structure from ~160 nm to 100 nm was reported, and consequently skim milk becomes translucent (Figure 2.2 C and D) (Bogahawaththa et al., 2018). A significant decrease in rehydrated casein micelle size is often linked to the loss of its colloidal stability (Baier et al., 2015). For the techno-functionality (Table 2.1), increasing the high-pressure processing intensity increased the strength of acidic and rennet milk gels (Broyard & Gaucheron, 2015). In addition, high-pressure processing of casein micelles dispersion at pH 7 slightly increased its foam stabilization activity (Baier et al., 2015). High-pressure-jet processing at 300-500 MPa markedly improved milk foaming and emulsifying properties, which was attributed to casein micelle dissociation (Hettiarachchi et al., 2018; Tran et al., 2018).

2.4.2.2.High-intensity ultrasound

Treatments based on high ultrasound intensities are interested in the cavitation phenomenon, which implies the fast formation and collapse of gas bubbles generated by localized pressure differentials occurring over short periods of time (O'Sullivan et al., 2017). This phenomenon is considered the major mechanism responsible for many of the effects observed by these treatments, including disruption of bacteria and other cells, as well as alterations of several protein attributes (Deeth & Datta, 2011). In addition, cavitation generates hydrogen peroxide that may induce the oxidation of free sulfhydryl groups of proteins into undesirable sulfinic and sulfonic acids. Moreover, free radicals and superoxides can be produced from water, promoting protein cross-linking (Ashokkumar et al., 2010; Mirmoghtadaie et al., 2016).

In the meantime, much of the ultrasound energy is converted to heat, generating high local temperatures up to 5000 K and pressures up to 100 MPa (Ashokkumar et al., 2010; Deeth & Datta, 2011). Temperature control of sonicated milk protein dispersions is therefore critical (Huppertz et al., 2019). In addition to the formation of free radicals and other compounds, ultrasound treatments may also modify the protein hydration state by replacing intramolecular hydrogen bonds with water-protein hydrogen bonds, without essentially altering their secondary structure as reported to rehydrated WPI or MPC (Frydenberg et al., 2016; Jambrak, Mason, Lelas, Herceg, & Herceg, 2008; Yanjun et al., 2014). Depending on the frequency applied, the product is exposed to the following phenomena: (i) low frequencies (~ 20 kHz) generate strong physical forces such as shear and turbulence, but a low number of

reactive radicals or (ii) high frequencies (300-500 kHz) generate less intense physical effects and more radicals (Noci, 2017). These structural changes are summarized in Figure 2.3.

Regarding the techno-functionality (Table 2.1), mild ultrasound treatments increased the solubility of whey protein-rich ingredients by exposing hydrophilic domains and consequently increasing water-protein interaction, while partial unfolding induced by intense ultrasound treatments led to whey protein aggregation and a decrease in their solubility (Jambrak et al., 2008; Noci, 2017). Besides that, the generated cavitation disrupted agglomerated powder particles, increasing their solubilization rate compared to that of the conventional overhead mixer (O'Sullivan et al., 2017). In addition, this treatment can increase protein hydrophobicity and decrease interfacial tension. This may improve the emulsion activity and emulsion stability indices until the intensity of the treatment leads to high protein aggregation (O'Sullivan et al., 2014; O'Sullivan et al., 2017). For example, ultrasound has been associated with a reduction in turbidity, an increase in solubility, improvement in emulsifying and foaming properties, and better gelling behavior of rehydrated whey protein-rich ingredients and MPC (Jambrak et al., 2008; Yanjun et al., 2014; Zisu et al., 2011). Figure 2.5 shows the reduction in turbidity of ultracentrifugation supernatant obtained from skim milk treated using ultrasound (Shanmugam et al., 2012).



Figure 2.5- Supernatant obtained from milk unsonicated (A) and sonicated at 20 kHz for 60 min (B) (Shanmugam et al., 2012).

For casein suspensions or casein-rich dairy ingredients ultrasound treatments are also not associated with changes in their native structure, as shown in Figure 2.4 (Chandrapala, Martin, Zisu, Kentish, & Ashokkumar, 2012). During the rehydration of casein-rich

ingredients, ultrasound treatments were linked to a reduction in the diameter of powder particles and consequently in suspension turbidity, which was more pronounced at a higher pH (Madadlou, Mousavi, Emam-Djomeh, Ehsani, & Sheehan, 2009). The casein micelles naturally show an open hydrated random structure; thus, ultrasound treatments seem to not alter their structure (Zhang et al., 2018). Similar behavior was reported for NaCas since ultrasound treatments reduced the particle diameter in suspension without affecting covalent interactions (Furtado, Mantovani, Consoli, Hubinger, & Cunha, 2017).

Ultrasound has also been reported to improve important parameters (Table 2.1) of reconstituted skim milk coagulation by rennin such as gelation time, gel firmness, curd firming rate, and gel network connectivity (Liu et al., 2014b). The small reduction in the diameter of casein micelles in reconstituted skim milk and the increase in protein hydrophobicity seemed to be responsible for these results (Liu et al., 2014a). Madadlou et al. (2010) indicated an increase in the elasticity of gels formed by sonicated acid casein dispersions, which showed a more interconnected structure. Ultrasound treatment applied to MCCs prior to spray drying also improved its solubility, emulsification activity, and rennet-gelation properties (Zhang et al., 2018).

2.4.2.3. Pulsed electric field

Regarding PEF treatments, after exposure to intensive electric fields, the apparent charge of proteins changes because of the modification of their ionic interactions (Jaeger, Meneses, & Knorr, 2014). In addition, for this and other technologies based on the electromagnetic spectrum, some protein polar groups can absorb energy and generate free radicals. These radicals can cross-link proteins as previously mentioned and disrupt various interactions between protein molecules, including van der Waals, electrostatic and hydrophobic interactions, and hydrogen and disulfide bonds, which may facilitate protein unfolding (Han et al., 2018). Moreover, in general, polypeptide chains possess a strong dipole moment, which has the potential to be affected by electric fields. In complement, these treatments induce an increase in the dielectric “constant” of the proteins, causing their unfolding by dissociation of noncovalent interactions (Zhao et al., 2014). For example, PEF treatment (30-35 kV.cm⁻¹ for 19.2 - 211 μs) did not change the superficial hydrophobicity, the content of free SH groups, or the primary structure of rehydrated WPI, in contrast to the intense thermal treatments (Sui, Roginski, Williams, Versteeg, & Wan, 2011). Their effect on whey protein foaming properties has not been reported; moreover, they apparently do not

affect the emulsification properties (emulsion stability) of rehydrated WPI (Mirmoghtadaie et al., 2016; Sui et al., 2011).

The structural effect reported in the literature for PEF treatments applied to caseins is contradictory. Shamsi & Sherkat, (2009) did not observe any significant change in the casein micelle structure after PEF treatment (35 kV.cm^{-1}) of skim milk, while Floury et al., (2006) reported a reduction in the size of casein micelles by increasing the electric field intensity ($45\text{--}55 \text{ kV.cm}^{-1}$), which negatively affected their coagulation behavior.

All these structural changes are summarized in Figures 2.3 and 2.4.

2.4.2.4.Microwave

Microwave treatment at 2.45 GHz applied to reach temperatures between $70\text{--}90 \text{ }^\circ\text{C}$ accelerated the unfolding of β -LG dispersions and provoked more extensive protein aggregation than that of the conventional thermal treatment (Gomaa et al., 2016; Gomaa, Sedman, & Ismail, 2013; Mishra & Ramchandran, 2015). Besides that, they have been suggested as capable of promoting L to D amino acid isomerization. Since amino acids in a D configuration are not well metabolized, this may have a major impact on protein nutritional quality. However, some evidence suggests that such amino acid isomerization does not occur in milk and infant foods treated with microwaves (Mishra & Ramchandran, 2015).

2.4.2.5.Irradiation

As shown so far, changes in the secondary and tertiary structure of the protein largely depend upon the intensity of the treatment. In the case of irradiation, the dosage level to induce such changes should be greater than 35 kGy (Borad et al., 2017; de la Hoz & Netto, 2008). However, the changes in surface hydrophobicity and disulfide bonds induced to β -LG dispersions by a high irradiation dose (50 kGy) were less pronounced than those induced by thermal treatment (de la Hoz & Netto, 2008). Regarding the techno-functionality, gamma-radiation in high doses reduced the solubility of milk protein dispersions but increased their apparent viscosity and turbidity because of protein aggregation (Wang et al., 2018b). Slight structural changes in milk proteins were also reported when submitted to pulsed light treatment (PL). This technology induced an increase in the concentration of sulfhydryl and carbonyl groups in whey proteins, consequently modifying their tertiary structure and slightly modifying their secondary structure (Siddique, Maresca, Pataro, & Ferrari, 2016). In adequate dosages, PL enhanced the solubility and foaming properties of rehydrated WPI because of partial unfolding (Siddique et al., 2016), but excessive doses caused an increase in the

turbidity of the rehydrated WPI because of the increase in the mean particle size and the aggregation index (Siddique et al., 2017). Concerning UV irradiation, it caused less extensive denaturation of dispersed whey proteins than that of the UHT or HTST heating treatments (Kristo, Hazizaj, & Corredig, 2012), and NaCas treated in a powder form did not undergo significant structural changes before 4 h of treatment (Kuan, Bhat, & Karim, 2011).

2.5. How does the addition of organic solvents affect the structure of proteins?

Protein nanoparticles represent a potential system for encapsulation and delivery of bioactive compounds. They can be optimized to enable site-specific delivery and generate an elevated ratio of encapsulated material. Several techniques have been employed to prepare protein particles, such as emulsification and solvent extraction, salting out, complex formation, desolvation, and spray drying (Gülseren et al., 2012a). In particular, desolvation offers notable advantages such as no need for employing any special equipment, easy handling, and fast production (Hejri et al., 2013). This technique is perhaps the simplest method for the preparation of the nanodispersions of water-insoluble bioactive compounds (Chu et al., 2007). The method generally consists by adding a desolvating agent such as ethanol or acetone with a dissolved bioactive compound drop by drop into the protein solution (Sadeghi et al., 2014). The effect of solvent on protein structure relates to the changes in the dielectric constant of the solvent, solvation forces, and affects hydrophobic interactions, hydrogen bonding, dipolar moments, and salt bridging (Gülseren et al., 2012a). The protein undergoes conformational changes that lead to protein unfolds, amine groups, thiol groups, and hydrophobic regions relocate to the surface of the molecule and cause an increase in intramolecular binding along with the reduction in hydrophobic interactions. Strong binding interactions among protein molecules lead to the formation of particles with the potential to entrap bioactive compounds (Sadeghi et al., 2014). Then, the organic solvent is evaporated from the nanodispersion under reduced pressure. The technique allows the preparation of nanodispersions in one step at low energy input with a high yield of encapsulation (Chu et al., 2007). The preparation conditions can strongly affect particle characteristics such as size and surface properties of protein particles that can be significantly changed by the number of disulfide bonds and thiol groups, degree of unfolding, electrostatic repulsion between protein molecules, ionic strength, and pH. So, it is necessary to design an optimized formulation for each application that is able to satisfy the requirements (Hejri et al., 2013; Sadeghi et al., 2014).

An advantage of this approach is that various food-grade molecules can be used to prepare nanoparticles, including whey proteins, sodium caseinate, and small molecule surfactants (Lee et al., 2011; Teo et al., 2017). For example, whey protein isolate (WPI) nanoparticles prepared using ethanol desolvation showed high zinc incorporation efficiencies and remained stable after 30 days of storage at 22 °C (Gülseren et al., 2012b). Moreover, Jain et al., (2018) formulated lycopene-loaded whey protein isolate nanoparticles by ethanol desolvation. These authors obtained nanoparticles of around 110 nm diameter and over 60 % of lycopene incorporation.

Nanoemulsions can be prepared using the desolvation approach. It consists of mixing an aqueous phase containing an emulsifier with an organic phase consisting of oil, water-miscible organic solvent, and may be also a bioactive compound. The organic solvent is then removed from the emulsions by evaporation, which causes the oil droplets to shrink and incorporate the bioactive compound into a water-based formulation with a high loading capacity. The use of organic solvent in this method is advantageous over traditional oil carriers as the organic solvent can potentially improve the solubility of lipophilic compounds in the dispersed phase.

2.6. How do different treatments modulate the binding properties and allergenicity of milk proteins?

As previously discussed, some treatments may induce structural changes in milk proteins which may lead to (i) exposure of previously buried sites capable of binding small ligands (e.g., bioactive compounds) and (ii) destruction or exposure of allergenic sites (epitopes), respectively decreasing or increasing their immunoreactivity (Ekezie, Cheng, & Sun, 2018). In this framework, the application of different treatments to milk proteins has been used to improve their encapsulation properties and reduce their allergenicity (Tavares, Croguennec, Carvalho, & Bouhallab, 2014; Yazdi & Corredig, 2012).

Structural changes induced by thermal treatments on β -LG improved its ability to bind and preserve the antioxidant capacity of epigallocatechin gallate (EGCG) (Li, Du, Jin, & Du, 2012), while those induced in caseins micelles improved their affinity and the protective effect of curcumin and β -carotene (Sáiz-Abajo, González-Ferrero, Moreno-Ruiz, Romo-Hualde, & González-Navarro, 2013; Yazdi & Corredig, 2012). The observed behavior was associated with an enhancement of hydrophobic interactions between the ligands and proteins because of an exposition of hydrophobic patches. In the same manner, high-pressure

homogenization alone or combined with mild thermal treatments improved the ability of whey proteins to entrap and protect α -tocopherol (Relkin & Shukat, 2012) and improved the ability of caseins to bind α -tocopherol acetate and retinyl acetate (Blayo et al., 2014; Chevalier-Lucia, Blayo, Gràcia-Julià, Picart-Palmade, & Dumay, 2011).

In complement to structural changes, even thermal treatments as high as 120 °C for 15 min did not affect the allergenicity of bovine casein (Borad et al., 2017). However, the structural changes induced by thermal treatments above 90 °C led to the irreversible aggregation of α -LA and β -LG in rehydrated WPI that masked and/or destroyed conformational epitopes, which reduced the allergenicity of these proteins. Conversely, mild thermal treatments (50–90 °C) induced protein unfolding which increased their antigenicity because of exposure of previously buried epitopes (Bu, Luo, Zheng, & Zheng, 2009).

The same logic was observed for high-pressure processing applied to β -LG. The antigenicity of β -LG increased by increasing the severity of the treatment within the range of 200–600 MPa for 10–30 min (Kleber, Maier, & Hinrichs, 2007). Nevertheless, pressures greater than 600 MPa reduced allergenicity by masking linear epitopes because of protein aggregation (Bogahawaththa et al., 2018; Hu, Zheng, Liu, Deng, & Zhao, 2016). No correlation was reported between the enhancement of enzymatic digestion associated with high-pressure processing and observed structural changes (Kurpiewska et al., 2019).

Other technologies have also been applied to whey proteins aiming to reduce their antigenicity. Gamma radiation at doses up to 10 kGy efficiently reduced the allergenicity of α -LA and β -LG because of extensive protein denaturation and aggregation (Lee et al., 2001); however, in more complex matrices this result was not reproduced (Kaddouri et al., 2008). Pulsed light treatments also reduced milk allergenicity (Hu et al., 2016), and ultrasound treatments were reported to be potentially able to reduce β -LG allergenicity by increasing its digestibility (Stanic-Vucinic et al., 2012). However, except for hydrolysis, typically applied treatments do not completely eliminate protein allergenicity and its reduction requires extreme treatments that are often linked to a loss of nutritional and techno-functional properties (Ekezie et al., 2018; Verhoeckx et al., 2015).

2.7. Carotenoids: structure, bioactivities, and fortification in formulated food products

Carotenoids are natural pigments, usually yellow, orange, and red, distributed in plants, algae, and various bacteria and fungi. They are lipophilic biomolecules and classified as carotenes, exclusively composed of hydrogen and carbons, such as β -carotene, α -carotene,

and lycopene or xanthophylls, that possess at least one functional group containing oxygen, the most common being lutein, zeaxanthin and β -cryptoxanthin (Li et al., 2015; Stephenson et al., 2021).

An important characteristic of the structure of this group of molecules is their extensive system of conjugated double bonds, which is responsible for absorbing light in the UV–visible region, as well as for their antioxidant capacity, translated by scavenging free radicals or quenching singlet oxygen (Mantovani et al., 2021; Mora-Gutierrez et al., 2018). Numerous studies have shown the potential health benefits associated with carotenoid consumption. For example, carotenoids such as β -carotene, α -carotene, and β -cryptoxanthin have provitamin A activity. This vitamin contributes to vision and growth and is one of the major micronutrient deficiencies worldwide, particularly in developing countries (Rodriguez-Concepcion et al., 2018). Lutein and zeaxanthin have recently come into the limelight because of animal and epidemiological studies that support their lower risk of eye diseases, such as age-related macular degeneration (AMD) and cataracts when consumed daily at reasonable amounts (Eggersdorfer & Wyss, 2018; Eisenhauer et al., 2017; Krinsky & Johnson, 2005; Moran et al., 2018; Paiva et al., 2020). In infants, lutein is the predominant carotenoid in the brain, while in older adults, has been linked to improved cognitive health (Miranda-Dominguez et al., 2022; Rodriguez-Concepcion et al., 2018).

Since most animals, including humans, cannot synthesize carotenoids in the body, they must be acquired through the ingestion of food, mainly associated with fruit and vegetable consumption or food supplements (Zhao et al., 2018). Unfortunately, the application of lutein in formulated food products is limited due to its low solubility in the aqueous phase and sensitivity to heat, oxygen, and light, making this carotenoid easily oxidized, isomerized, and/or degraded (Teo et al., 2017; Zhao et al., 2018). Besides that, the bioaccessibility, and consequently the bioavailability of lutein is also low and variable according to many diet-related factors, such as the food microstructure and composition, which may impair its absorption (Mantovani et al., 2022; Mora-Gutierrez et al., 2018). Furthermore, the manufacturing process, particularly those involving heat treatments, can alter the microstructure of food, influencing the retention of carotenoids and their bioaccessibility (Stephenson et al., 2021). Findings by Wang et al., (2018a) in bovine milk fortified with lutein showed little effect of HTST on the lutein, whereas UHT resulted in reductions of 8 % in the lutein content and up to 63 % in the bioaccessibility.

2.8. How all this information connects into formulated products: the case of infant formulas

The main purposes of infant formulas are to replace or supplement breast milk in infants whose mothers cannot breastfeed, choose not to breastfeed, or do not breastfeed exclusively. They are also indicated in cases where breastfeeding is medically contraindicated or when exclusive intake of breast milk is not sufficient to provide the infant's ideal weight gain (Blanchard et al., 2013; Contreras-Calderón et al., 2009).

Infant formulas are produced using adequate amounts of proteins, fats, carbohydrates, minerals, and vitamins to try to mimic the composition of breast milk as much as possible (McCarthy et al., 2013). Most of the products available on the market have cow's milk as a raw material and protein source, but the proportion between whey protein and casein needs to be adjusted to 60:40, to coincide with that of human milk (Lemaire et al., 2018; Tham et al., 2016), while the main carbohydrates present are lactose and oligosaccharides (Blanchard et al., 2013).

Soy protein isolates are also a protein source widely used in infant formulas, being suitable for infants allergic to cow's milk protein, and for vegan families. However, about 10 – 14 % of babies with cow's milk protein allergy may be allergic to soy protein, in these cases the best indication is to use hydrolyzed protein formulas (Bhatia & Greer, 2008). Therefore, infant formulas based on hydrolyzed rice protein have been proposed for the treatment of cow's milk protein allergy (CMPA), since rice is considered one of the least allergenic cereals. Proteins are hydrolyzed to increase their solubility, and protein quality is improved by amino acid supplementation (Bocquet et al., 2019). These two types of formulas usually replace lactose with carbohydrates such as maltodextrins, glucose syrup, sucrose, and starches, and can be consumed by infants with lactose intolerance and/or galactosemia, although there are lactose-free or reduced-content cow's milk formulas that are more suitable in these cases (Blanchard et al., 2013; Bocquet et al., 2019).

Combinations of vegetable oils such as palm, coconut, soy, and sunflower oils are optimized to provide a fatty acid profile similar to that of breast milk, in addition to providing the ideal energy content. During the production of infant formulas, the oil phase is stabilized by proteins to form an oil-in-water emulsion (Tham et al., 2017). In addition, vitamins and minerals are added to compensate for the low content present in these sources, compared to human milk (Damjanovic Desic & Birlouez-Aragon, 2011).

Infant formulas are products with several compounds with antioxidant properties, such as nucleotides, carotenoids, phenolic compounds, some vitamins, and minerals (Li et al., 2009). These provide oxidative stability and delay the initiation and propagation of reactive oxygen species that can deteriorate the quality of formulas (Tijerina Sáenz et al., 2009). However, the carotenoid concentrations in infant formulas vary but are mainly low and most formulas are not supplemented to match the higher levels found in human milk (Miranda-Dominguez et al., 2022; Stephenson et al., 2021). The major carotenoids in human milk are lutein, zeaxanthin, β -carotene, lycopene, α -carotene, and β -cryptoxanthin. Similar to adults, carotenoid consumption has been linked with a number of health benefits in infants. In total, 50 % of the carotenoid content (α -carotene, β -carotene, and β -cryptoxanthin) in milk has provitamin A activity. Lutein and zeaxanthin have been implicated in ocular development. More recently, lutein has been identified as the predominant (59 %) carotenoid in the infant brain, supporting brain development as well as enhanced cognitive functioning (Rodriguez-Concepcion et al., 2018; Stephenson et al., 2021). For this reason and taking into account that carotenoids have many biological functions, an adequate concentration in dietary sources and fortification of products such as infant formula should be considered (Miranda-Dominguez et al., 2022; Stephenson et al., 2021).

As mentioned before, heat treatment has been widely studied as it is one of the most used methods in food processing and this is no different for infant formulas (Shen et al., 2017). The production of this product includes different steps, such as mixing ingredients in water or skimmed milk, homogenization, heat treatment, spray drying, and storage (Blanchard et al., 2013; Sabater et al., 2018). Heat treatments that can be used include high-temperature short-time pasteurization (HTST, 72 °C, 15 s), ultra-high temperature treatment (UHT, 130 – 140 °C, 3 – 6 s) and containerized sterilization (110 °C, 10 min) (Wang et al., 2018c). These treatments are very important to minimize the risks associated with contaminants such as microorganisms and enzymes (Mediwaththe et al., 2018). Because of some of these treatments, the IFs have a long shelf life (12 - 24 months), however, their stability during storage is highly dependent on factors such as composition and storage conditions (e.g. temperature, relative humidity, time) (Drapala et al., 2017; McCarthy et al., 2013; Wang et al., 2018c). It is reported in the literature that these products may be subjected to temperatures above 45 °C, reaching 57 °C inside containers, over periods of 3 months during continental or intercontinental transport (Leinberger, 2006; Norwood et al., 2016).

All these aforementioned conditions can result in several physicochemical changes in infant formulas, such as protein denaturation and aggregation, protein-lipid and protein-

protein interactions, destabilization of protein-stabilized emulsions, isomerization of sugars, and a series of chemical reactions, in particular the Maillard reaction (Damjanovic Desic & Birlouez-Aragon, 2011; Wang et al., 2018c). All these changes are important as they can influence the functional, sensory, rheological properties and particle size of infant formulas and their subsequent nutrient absorption (Gómez-Gallego et al., 2016; Tham et al., 2016). This is very relevant when one takes into account that most of the nutrition of infants fed infant formula in the first months of life is obtained from the digestion of the reconstituted powdered formula (Sabater et al., 2018).

Several processing and storage parameters are applied to IFs containing alternative protein sources derived from those consolidated for cow's milk-based IFs since published scientific reports appear to be limited for the former. Most of the available reports on the use of plant proteins in IFs focus on their encapsulation capacity, digestibility, and/or allergenicity (Le Roux, Chacon, et al., 2020). However, the replacement of dairy proteins by plant proteins, even partially, has a great impact on IFs properties, which means that process parameters should be adapted for each formulation to provide satisfactory quality for the obtained IFs (Le Roux, Mejean, et al., 2020).

2.9. Perspectives

Each one of the reviewed treatments has a specific means to alter the structure of milk proteins, and, as presented, the mechanism of alteration may differ for caseins and whey proteins. In general, (i) exposing previously buried sites improves the ability of the protein to bind bioactive compounds; (ii) immunoreactivity may be reduced by irreversible protein aggregation; (iii) the increase in the superficial hydrophobicity and flexibility of proteins is positively correlated with interfacial properties, even though the presence of some soluble aggregates may be relevant and (iv) the increase in the reactivity of the proteins by exposition of reactive sites may improve the network organization during protein gelation.

Since nowadays there is a great interest in healthy ingredients and food with nutritional quality, there is a great demand for fortification of food products formulated with bioactive compounds, such as carotenoids, for example, lutein, since such compounds cannot be synthesized by the human body and have numerous benefits, especially for children. However, when designing a fortified food, the stability of carotenoids within the food matrix and the subsequent bioaccessibility should be examined. Furthermore, how to perform this fortification and their interaction with processing should be investigated.

Regarding the case of infant formulas, is important to understand the relationship between aging conditions and the physicochemical changes of infant formulas, to identify their critical storage conditions, and how this can be influenced by their composition.

2.10. References

- Abd El-Salam, M. H., & El-Shibiny, S. (2018). Glycation of whey proteins: Technological and nutritional implications. *International Journal of Biological Macromolecules*, *112*, 83–92. <https://doi.org/10.1016/j.ijbiomac.2018.01.114>
- Abd El-Salam, M. H., El-Shibiny, S., & Salem, A. (2009). Factors Affecting the Functional Properties of Whey Protein Products: A Review. *Food Reviews International*, *25*(3), 251–270. <https://doi.org/10.1080/87559120902956224>
- Agarwal, S., Beausire, R. L. W., Patel, S., & Patel, H. (2015). Innovative Uses of Milk Protein Concentrates in Product Development. *Journal of Food Science*, *80*(S1), A23–A29. <https://doi.org/10.1111/1750-3841.12807>
- Ashokkumar, M., Bhaskaracharya, R., Kentish, S., Palmer, M., Zisu, B., Ashokkumar, M., ... Zisu, B. (2010). The ultrasonic processing of dairy products - An overview. *Dairy Science & Technology*, *90*, 147–168. <https://doi.org/10.1051/dst/2009044>
- Baier, D., Schmitt, C., & Knorr, D. (2015). Changes in functionality of whey protein and micellar casein after high pressure - Low temperature treatments. *Food Hydrocolloids*, *44*, 416–423. <https://doi.org/10.1016/j.foodhyd.2014.10.010>
- Beliciu, C. M., & Moraru, C. I. (2013). Physico-chemical changes in heat treated micellar casein - Soy protein mixtures. *LWT - Food Science and Technology*, *54*, 469–476. <https://doi.org/10.1016/j.lwt.2013.06.013>
- Beliciu, C. M., Sauer, A., & Moraru, C. I. (2012). The effect of commercial sterilization regimens on micellar casein concentrates. *Journal of Dairy Science*, *95*(10), 5510–5526. <https://doi.org/10.3168/jds.2011-4875>
- Bhatia, J., & Greer, F. (2008). Use of Soy Protein-Based Formulas in Infant Feeding. *Pediatrics*, *121*(5), 1062–1068. <https://doi.org/10.1542/peds.2008-0564>
- Blanchard, E., Zhu, P., & Schuck, P. (2013). Infant formula powders. In B. Bhandari, N. Bansal, M. Zhang, & P. Schuck (Eds.), *Handbook of Food Powders: Processes and properties* (1st ed., pp. 465–483). Woodhead Publishing Limited. <https://doi.org/10.1533/9780857098672.3.465>
- Blayo, C., Puentes-Rivas, D., Picart-Palmade, L., Chevalier-Lucia, D., Lange, R., & Dumay,

- E. (2014). Binding of retinyl acetate to whey proteins or phosphocasein micelles: Impact of pressure-processing on protein structural changes and ligand embedding. *Food Research International*, *66*, 167–179. <https://doi.org/10.1016/j.foodres.2014.09.005>
- Bocquet, A., Dupont, C., Chouraqui, J. P., Darmaun, D., Feillet, F., Frelut, M. L., Girardet, J. P., Hankard, R., Lapillonne, A., Rozé, J. C., Simeoni, U., Turck, D., & Briend, A. (2019). Efficacy and safety of hydrolyzed rice-protein formulas for the treatment of cow's milk protein allergy. *Archives de Pédiatrie*, *26*(4), 238–246. <https://doi.org/10.1016/j.arcped.2019.03.001>
- Bogahawaththa, D., Buckow, R., Chandrapala, J., & Vasiljevic, T. (2018). Comparison between thermal pasteurization and high pressure processing of bovine skim milk in relation to denaturation and immunogenicity of native milk proteins. *Innovative Food Science and Emerging Technologies*, *47*, 301–308. <https://doi.org/10.1016/j.ifset.2018.03.016>
- Borad, S. G., Kumar, A., & Singh, A. K. (2017). Effect of processing on nutritive values of milk protein. *Critical Reviews in Food Science and Nutrition*, *57*(17), 3690–3702. <https://doi.org/10.1080/10408398.2016.1160361>
- Bouaouina, H., Desrumaux, A., Loisel, C., & Legrand, J. (2006). Functional properties of whey proteins as affected by dynamic high-pressure treatment. *International Dairy Journal*, *16*, 275–284. <https://doi.org/10.1016/j.idairyj.2005.05.004>
- Broyard, C., & Gaucheron, F. (2015). Modifications of structures and functions of caseins: a scientific and technological challenge. *Dairy Science & Technology*, *95*, 831–862. <https://doi.org/10.1007/s13594-015-0220-y>
- Bu, G. H., Luo, Y. K., Zheng, Z., & Zheng, H. (2009). Effect of heat treatment on the antigenicity of bovine α -lactalbumin and β -lactoglobulin in whey protein isolate. *Food and Agricultural Immunology*, *20*, 195–206.
- Cadesky, L., Walkling-Ribeiro, M., Kriner, K. T., Karwe, M. V., & Moraru, C. I. (2017). Structural changes induced by high-pressure processing in micellar casein and milk protein concentrates. *Journal of Dairy Science*, *100*(9), 7055–7070. <https://doi.org/10.3168/jds.2016-12072>
- Carter, B. G., & Drake, M. A. (2018). The effects of processing parameters on the flavor of whey protein ingredients. *Journal of Dairy Science*, *101*(8), 1–12. <https://doi.org/10.3168/jds.2018-14571>
- Chandrapala, J., Martin, G. J. O., Zisu, B., Kentish, S. E., & Ashokkumar, M. (2012). The effect of ultrasound on casein micelle integrity. *Journal of Dairy Science*, *95*(12), 6882–

6890. <https://doi.org/10.3168/jds.2012-5318>
- Chauvet, M., Sauceau, M., & Fages, J. (2017). Extrusion assisted by supercritical CO₂: A review on its application to biopolymers. *Journal of Supercritical Fluids*, *120*, 408–420. <https://doi.org/10.1016/j.supflu.2016.05.043>
- Chevalier-Lucia, D., Blayo, C., Gràcia-Julià, A., Picart-Palmade, L., & Dumay, E. (2011). Processing of phosphocasein dispersions by dynamic high pressure: Effects on the dispersion physico-chemical characteristics and the binding of α -tocopherol acetate to casein micelles. *Innovative Food Science and Emerging Technologies*, *12*, 416–425. <https://doi.org/10.1016/j.ifset.2011.07.007>
- Chu, B. S., Ichikawa, S., Kanafusa, S., & Nakajima, M. (2007). Preparation and characterization of β -carotene nanodispersions prepared by solvent displacement technique. *Journal of Agricultural and Food Chemistry*, *55*(16), 6754–6760. <https://doi.org/10.1021/jf063609d>
- Considine, T., Patel, H. A., Anema, S. G., Singh, H., & Creamer, L. K. (2007). Interactions of milk proteins during heat and high hydrostatic pressure treatments — A Review. *Innovative Food Science and Emerging Technologies*, *8*, 1–23. <https://doi.org/10.1016/j.ifset.2006.08.003>
- Contreras-Calderón, J., Guerra-Hernández, E., & García-Villanova, B. (2009). Utility of some indicators related to the Maillard browning reaction during processing of infant formulas. *Food Chemistry*, *114*(4), 1265–1270. <https://doi.org/10.1016/j.foodchem.2008.11.004>
- Dalgleish, D. G., & Corredig, M. (2012). The Structure of the Casein Micelle of Milk and Its Changes During Processing. *Annual Review of Food Science and Technology*, *3*, 449–467. <https://doi.org/10.1146/annurev-food-022811-101214>
- Damjanovic Desic, S., & Birlouez-Aragon, I. (2011). The FAST index - A highly sensitive indicator of the heat impact on infant formula model. *Food Chemistry*, *124*(3), 1043–1049. <https://doi.org/10.1016/j.foodchem.2010.07.071>
- de la Hoz, L., & Netto, F. M. (2008). Structural modifications of β -lactoglobulin subjected to gamma radiation. *International Dairy Journal*, *18*, 1126–1132. <https://doi.org/10.1016/j.idairyj.2008.06.005>
- Deeth, H. C., & Datta, N. (2011). Non-Thermal Technologies: Pulsed Electric Field Technology and Ultrasonication. In J. W. Fuquay (Ed.), *Encyclopedia of Dairy Sciences* (2nd ed., pp. 738–743). Mississippi: Elsevier.
- Deeth, H. C., & Lewis, M. J. (2017). Non-Thermal Technologies. In H. C. Deeth & M. L. Lewis (Eds.), *High Temperature Processing of Milk and Milk Products* (1st ed., p. 584).

Wiley-Blackwell.

- Dissanayake, M., & Vasiljevic, T. (2009). Functional properties of whey proteins affected by heat treatment and hydrodynamic high-pressure shearing. *Journal of Dairy Science*, 92(4), 1387–1397. <https://doi.org/10.3168/jds.2008-1791>
- Drapala, K. P., Auty, M. A. E., Mulvihill, D. M., & O'Mahony, J. A. (2017). Influence of emulsifier type on the spray-drying properties of model infant formula emulsions. *Food Hydrocolloids*, 69, 56–66. <https://doi.org/10.1016/j.foodhyd.2016.12.024>
- Eggersdorfer, M., & Wyss, A. (2018). Carotenoids in human nutrition and health. *Archives of Biochemistry and Biophysics*, 652, 18–26. <https://doi.org/10.1016/j.abb.2018.06.001>
- Eisenhauer, B., Natoli, S., Liew, G., & Flood, V. M. (2017). Lutein and zeaxanthin — Food sources, bioavailability and dietary variety in age-related macular degeneration protection. *Nutrients*, 9(2). <https://doi.org/10.3390/nu9020120>
- Ekezie, F.-G. C., Cheng, J.-H., & Sun, D.-W. (2018). Effects of nonthermal food processing technologies on food allergens: A review of recent research advances. *Trends in Food Science and Technology*, 74, 12–25. <https://doi.org/10.1016/j.tifs.2018.01.007>
- Floury, J., Grosset, N., Leconte, N., Pasco, M., Madec, M. N., & Jeantet, R. (2006). Continuous raw skim milk processing by pulsed electric field at non-lethal temperature: effect on microbial inactivation and functional properties. *Lait*, 86, 43–57.
- Frydenberg, R. P., Hammershøj, M., Andersen, U., Greve, M. T., & Wiking, L. (2016). Protein denaturation of whey protein isolates (WPIs) induced by high intensity ultrasound during heat gelation. *Food Chemistry*, 192, 415–423. <https://doi.org/10.1016/j.foodchem.2015.07.037>
- Furtado, G. D. F., Mantovani, R. A., Consoli, L., Hubinger, M. D., & Cunha, R. L. da. (2017). Structural and emulsifying properties of sodium caseinate and lactoferrin influenced by ultrasound process. *Food Hydrocolloids*, 63, 178–188. <https://doi.org/10.1016/j.foodhyd.2016.08.038>
- Gomaa, A. I., Nsonzi, F., Sedman, J., & Ismail, A. A. (2016). Enhanced Unfolding of Bovine β -Lactoglobulin Structure Using Microwave Treatment: a Multi-Spectroscopic Study. *Food Biophysics*, 11, 370–379. <https://doi.org/10.1007/s11483-016-9451-6>
- Gomaa, A. I., Sedman, J., & Ismail, A. A. (2013). An investigation of the effect of microwave treatment on the structure and unfolding pathways of β -lactoglobulin using FTIR spectroscopy with the application of two-dimensional correlation spectroscopy (2D-COS). *Vibrational Spectroscopy*, 65, 101–109. <https://doi.org/10.1016/j.vibspec.2012.11.019>

- Gómez-Gallego, C., Recio, I., Gómez-Gómez, V., Ortuño, I., Bernal, M. J., Ros, G., & Periago, M. J. (2016). Effect of processing on polyamine content and bioactive peptides released after in vitro gastrointestinal digestion of infant formulas. *Journal of Dairy Science*, *99*(2), 924–932. <https://doi.org/10.3168/jds.2015-10030>
- Gülseren, I., Fang, Y., & Corredig, M. (2012a). Whey protein nanoparticles prepared with desolvation with ethanol: Characterization, thermal stability and interfacial behavior. *Food Hydrocolloids*, *29*(2), 258–264. <https://doi.org/10.1016/j.foodhyd.2012.03.015>
- Gülseren, I., Fang, Y., & Corredig, M. (2012b). Zinc incorporation capacity of whey protein nanoparticles prepared with desolvation with ethanol. *Food Chemistry*, *135*(2), 770–774. <https://doi.org/10.1016/j.foodchem.2012.04.146>
- Hadjsadok, A., Pitkowski, A., Nicolai, T., Benyahia, L., & Moulai-Mostefa, N. (2008). Characterisation of sodium caseinate as a function of ionic strength, pH and temperature using static and dynamic light scattering. *Food Hydrocolloids*, *22*, 1460–1466. <https://doi.org/10.1016/j.foodhyd.2007.09.002>
- Han, Z., Cai, M., Cheng, J., & Sun, D. (2018). Effects of electric fields and electromagnetic wave on food protein structure and functionality: A review. *Trends in Food Science & Technology*, *75*, 1–9. <https://doi.org/10.1016/j.tifs.2018.02.017>
- Harte, F. (2016). Food Processing by High-Pressure Homogenization. In V. M. Balasubramaniam, G. V Barbosa-Cánovas, & H. L. M. Lelieveld (Eds.), *High Pressure Processing of Food: Principles, Technology and Applications* (1st ed., p. 762). New York: Springer.
- Hejri, A., Khosravi, A., Gharanjig, K., & Hejazi, M. (2013). Optimisation of the formulation of β -carotene loaded nanostructured lipid carriers prepared by solvent diffusion method. *Food Chemistry*, *141*(1), 117–123. <https://doi.org/10.1016/j.foodchem.2013.02.080>
- Hettiarachchi, C. A., Corzo-Martínez, M., Mohan, M. S., & Harte, F. M. (2018). Enhanced foaming and emulsifying properties of high-pressure-jet-processed skim milk. *International Dairy Journal*, *87*, 60–66. <https://doi.org/10.1016/j.idairyj.2018.06.004>
- Higuera-Barraza, O. A., Toro-Sanchez, C. L. Del, Ruiz-Cruz, S., & Márquez-Ríos, E. (2016). Effects of high-energy ultrasound on the functional properties of proteins. *Ultrasonics Sonochemistry*, *31*, 558–562. <https://doi.org/10.1016/j.ultsonch.2016.02.007>
- Hu, G., Zheng, Y., Liu, Z., Deng, Y., & Zhao, Y. (2016). Structure and IgE-binding properties of α -casein treated by high hydrostatic pressure, UV-C, and far-IR radiations. *Food Chemistry*, *204*, 46–55. <https://doi.org/10.1016/j.foodchem.2016.02.113>
- Huppertz, T., Fox, P. F., de Kruif, K. G., & Kelly, A. L. (2006). High pressure-induced

- changes in bovine milk proteins: A review. *Biochimica et Biophysica Acta*, 1764, 593–598. <https://doi.org/10.1016/j.bbapap.2005.11.010>
- Huppertz, T., Vasiljevic, T., Zisu, B., & Deeth, H. (2019). Novel Processing Technologies: Effects on Whey Protein Structure and Functionality. In H. C. Deeth & N. Bansal (Eds.), *Whey Proteins: From Milk to Medicine* (pp. 281–334). Elsevier Inc. <https://doi.org/10.1016/B978-0-12-812124-5.00009-6>
- Jaeger, H., Meneses, N., & Knorr, D. (2014). Food Technologies: Pulsed Electric Field Technology. In Y. Motarjemi (Ed.), *Encyclopedia of Food Safety* (1st ed., Vol. 3, pp. 239–244). Elsevier. <https://doi.org/10.1016/B978-0-12-378612-8.00260-2>
- Jain, A., Sharma, G., Ghoshal, G., Kesharwani, P., Singh, B., Shivhare, U. S., & Katare, O. P. (2018). Lycopene loaded whey protein isolate nanoparticles: An innovative endeavor for enhanced bioavailability of lycopene and anti-cancer activity. *International Journal of Pharmaceutics*, 546, 97–105. <https://doi.org/10.1016/j.ijpharm.2018.04.061>
- Jambrak, A. R., Mason, T. J., Lelas, V., Herceg, Z., & Herceg, I. L. (2008). Effect of ultrasound treatment on solubility and foaming properties of whey protein suspensions. *Journal of Food Engineering*, 86, 281–287. <https://doi.org/10.1016/j.jfoodeng.2007.10.004>
- Jambrak, A. R., Mason, T. J., Lelas, V., Paniwnyk, L., & Herceg, Z. (2014). Effect of ultrasound treatment on particle size and molecular weight of whey proteins. *Journal of Food Engineering*, 121, 15–23. <https://doi.org/10.1016/j.jfoodeng.2013.08.012>
- Kaddouri, H., Mimoun, S., El-Mecherfi, K. E., Chekroun, A., Kheroua, O., & Saidi, D. (2008). Impact of γ -Radiation on Antigenic Properties of Cow's Milk β -Lactoglobulin. *Journal of Food Protection*, 71(6), 1270–1272.
- Kleber, N., Maier, S., & Hinrichs, J. (2007). Antigenic response of bovine β -lactoglobulin influenced by ultra-high pressure treatment and temperature. *Innovative Food Science and Emerging Technologies*, 8(1), 39–45.
- Krinsky, N. I., & Johnson, E. J. (2005). Carotenoid actions and their relation to health and disease. *Molecular Aspects of Medicine*, 26(6), 459–516. <https://doi.org/10.1016/j.mam.2005.10.001>
- Kristo, E., Hazizaj, A., & Corredig, M. (2012). Structural changes imposed on whey proteins by UV irradiation in a continuous UV light reactor. *Journal of Agricultural and Food Chemistry*, 60, 6204–6209. <https://doi.org/10.1021/jf300278k>
- Kuan, Y. H., Bhat, R., & Karim, A. A. (2011). Emulsifying and foaming properties of ultraviolet-irradiated egg white protein and sodium caseinate. *Journal of Agricultural and*

- Food Chemistry*, 59, 4111–4118. <https://doi.org/10.1021/jf104050k>
- Kuan, Y. H., Bhat, R., Patras, A., & Karim, A. A. (2013). Radiation processing of food proteins - A review on the recent developments. *Trends in Food Science and Technology*, 30, 105–120. <https://doi.org/10.1016/j.tifs.2012.12.002>
- Kurpiewska, K., Biela, A., Loch, J. I., Lipowska, J., Siuda, M., & Lewiński, K. (2019). Towards understanding the effect of high pressure on food protein allergenicity: β -lactoglobulin structural studies. *Food Chemistry*, 270, 315–321. <https://doi.org/10.1016/j.foodchem.2018.07.104>
- Laiho, S., Ercili-Cura, D., Forssell, P., Myllärinen, P., & Partanen, R. (2015). The effect of dynamic heat treatments of native whey protein concentrate on its dispersion characteristics. *International Dairy Journal*, 49, 139–147. <https://doi.org/10.1016/j.idairyj.2015.05.002>
- Le Roux, L., Chacon, R., Dupont, D., Jeantet, R., Deglaire, A., & Nau, F. (2020). In vitro static digestion reveals how plant proteins modulate model infant formula digestibility. *Food Research International*, 130, 108917.
- Le Roux, L., Mejean, S., Chacon, R., Lopez, C., Dupont, D., Deglaire, A., Nau, F., & Jeantet, R. (2020). Plant proteins partially replacing dairy proteins greatly influence infant formula functionalities. *LWT - Food Science and Technology*, 120, 108891. <https://doi.org/10.1016/j.lwt.2019.108891>
- Lee, J.-W., Kim, J.-H., Yook, H.-S., Kang, K.-O., Lee, S.-Y., Hwang, H.-J., & Byun, M.-W. (2001). Effects of Gamma Radiation on the Allergenic and Antigenic Properties of Milk Proteins. *Journal of Food Protection*, 64(2), 272–276.
- Lee, S. J., Choi, S. J., Li, Y., Decker, E. A., & McClements, D. J. (2011). Protein-stabilized nanoemulsions and emulsions: Comparison of physicochemical stability, lipid oxidation, and lipase digestibility. *Journal of Agricultural and Food Chemistry*, 59(1), 415–427. <https://doi.org/10.1021/jf103511v>
- Lee, W., Clark, S., & Swanson, B. G. (2006). Functional properties of high hydrostatic pressure-treated whey protein. *Journal of Food Processing and Preservation*, 30(509), 488–501.
- Leinberger, D. (2006). Temperature and humidity in ocean containers. In *Proceedings of Dimensions*. International Safe Transit Association.
- Lemaire, M., Le Huërou-Luron, I., & Blat, S. (2018). Effects of infant formula composition on long-term metabolic health. *Journal of Developmental Origins of Health and Disease*, 9(6), 573–589. <https://doi.org/10.1017/s2040174417000964>

- Li, B., Du, W., Jin, J., & Du, Q. (2012). Preservation of (-)-Epigallocatechin-3-gallate Antioxidant Properties Loaded in Heat Treated β -Lactoglobulin Nanoparticles. *Journal of Agricultural and Food Chemistry*, *30*, 3477–3484. <https://doi.org/10.1021/jf300307t>
- Li, W., Hosseinian, F. S., Tsopmo, A., Friel, J. K., & Beta, T. (2009). Evaluation of antioxidant capacity and aroma quality of breast milk. *Nutrition*, *25*, 105–114. <https://doi.org/10.1016/j.nut.2008.07.017>
- Li, X., Wang, G., Chen, D., & Lu, Y. (2015). β -Carotene and astaxanthin with human and bovine serum albumins. *Food Chemistry*, *179*, 213–221. <https://doi.org/10.1016/j.foodchem.2015.01.133>
- Liu, Z., Juliano, P., Williams, R. P. W., Niere, J., & Augustin, M. A. (2014a). Ultrasound effects on the assembly of casein micelles in reconstituted skim milk. *Journal of Dairy Research*, *81*, 146–155. <https://doi.org/10.1017/S0022029913000721>
- Liu, Z., Juliano, P., Williams, R. P. W., Niere, J., & Augustin, M. A. (2014b). Ultrasound improves the renneting properties of milk. *Ultrasonics - Sonochemistry*, *21*, 2131–2137. <https://doi.org/10.1016/j.ultsonch.2014.03.034>
- Madadlou, A., Emam-Djomeh, Z., Mousavi, M. E., Mohamadifar, M., & Ehsani, M. (2010). Acid-induced gelation behavior of sonicated casein solutions. *Ultrasonics - Sonochemistry*, *17*(1), 153–158. <https://doi.org/10.1016/j.ultsonch.2009.06.009>
- Madadlou, A., Mousavi, M. E., Emam-Djomeh, Z., Ehsani, M., & Sheehan, D. (2009). Sonodisruption of re-assembled casein micelles at different pH values. *Ultrasonics Sonochemistry*, *16*, 644–648. <https://doi.org/10.1016/j.ultsonch.2008.12.018>
- Manoi, K., & Rizvi, S. S. H. (2008). Rheological characterizations of texturized whey protein concentrate-based powders produced by reactive supercritical fluid extrusion. *Food Research International*, *41*, 786–796. <https://doi.org/10.1016/j.foodres.2008.07.001>
- Mantovani, R. A., Rasera, M. L., Vidotto, D. C., Mercadante, A. Z., & Tavares, G. M. (2021). Binding of carotenoids to milk proteins: Why and how. *Trends in Food Science and Technology*, *110*, 280–290. <https://doi.org/10.1016/j.tifs.2021.01.088>
- Mantovani, R. A., Xavier, A. A. O., Tavares, G. M., & Mercadante, A. Z. (2022). Lutein bioaccessibility in casein-stabilized emulsions is influenced by the free to acylated carotenoid ratio, but not by the casein aggregation state. *Food Research International*, *161*, 111778. <https://doi.org/10.1016/j.foodres.2022.111778>
- Martini, S., Potter, R., & Walsh, M. K. (2010). Optimizing the use of power ultrasound to decrease turbidity in whey protein suspensions. *Food Research International*, *43*(10), 2444–2451. <https://doi.org/10.1016/j.foodres.2010.09.018>

- McCarthy, N. A., Gee, V. L., Hickey, D. K., Kelly, A. L., O'Mahony, J. A., & Fenelon, M. A. (2013). Effect of protein content on the physical stability and microstructure of a model infant formula. *International Dairy Journal*, *29*, 53–59. <https://doi.org/10.1016/j.idairyj.2012.10.004>
- Mediwaththe, A., Bogahawaththa, D., Grewal, M. K., Chandrapala, J., & Vasiljevic, T. (2018). Structural changes of native milk proteins subjected to controlled shearing and heating. *Food Research International*, *114*, 151–158. <https://doi.org/10.1016/j.foodres.2018.08.001>
- Meena, G. S., Singh, A. K., & Panjagar, N. R. (2017). Milk protein concentrates: opportunities and challenges. *Journal of Food Science and Technology*, *54*(10), 3010–3024. <https://doi.org/10.1007/s13197-017-2796-0>
- Miranda-Dominguez, O., Ramirez, J. S. B., Mitchell, A. J., Perrone, A., Earl, E., Carpenter, S., Feczko, E., Graham, A., Jeon, S., Cohen, N. J., Renner, L., Neuringer, M., Kuchan, M. J., Erdman, J. W., & Fair, D. (2022). Carotenoids improve the development of cerebral cortical networks in formula-fed infant macaques. *Scientific Reports*, *12*(1), 1–13. <https://doi.org/10.1038/s41598-022-19279-1>
- Mirmoghtadaie, L., Aliabadi, S. S., & Hosseini, S. M. (2016). Recent approaches in physical modification of protein functionality. *Food Chemistry*, *199*, 619–627. <https://doi.org/10.1016/j.foodchem.2015.12.067>
- Mishra, V. K., & Ramchandran, L. (2015). Novel Thermal Methods in Dairy Processing. In N. Datta & P. M. Tomasula (Eds.), *Emerging Dairy Processing Technologies: Opportunities for the Dairy Industry* (p. 360). Wiley-Blackwell.
- Mohan, M. S., Ye, R., & Harte, F. (2016). Initial study on high pressure jet processing using a modified waterjet on physicochemical and rennet coagulation properties of pasteurized skim milk. *International Dairy Journal*, *55*, 52–58. <https://doi.org/10.1016/j.idairyj.2015.12.004>
- Mora-Gutierrez, A., Attaie, R., Núñez de González, M. T., Jung, Y., Woldesenbet, S., & Marquez, S. A. (2018). Complexes of lutein with bovine and caprine caseins and their impact on lutein chemical stability in emulsion systems: Effect of arabinogalactan. *Journal of Dairy Science*, *101*(1), 18–27. <https://doi.org/10.3168/jds.2017-13105>
- Moran, N. E., Mohn, E. S., Hason, N., Erdman, J. W., & Johnson, E. J. (2018). Intrinsic and extrinsic factors impacting absorption, metabolism, and health effects of dietary carotenoids. *Advances in Nutrition*, *9*(4), 465–492. <https://doi.org/10.1093/ADVANCES/NMY025>

- Nicorescu, I., Loisel, C., Riaublanc, A., Vial, C., Djelveh, G., Cuvelier, G., & Legrand, J. (2009). Effect of dynamic heat treatment on the physical properties of whey protein foams. *Food H*, 23, 1209–1219. <https://doi.org/10.1016/j.foodhyd.2008.09.005>
- Nicorescu, I., Vial, C., Loisel, C., Riaublanc, A., Djelveh, G., Cuvelier, G., & Legrand, J. (2010). Influence of protein heat treatment on the continuous production of food foams. *Food Research International*, 43, 1585–1593. <https://doi.org/10.1016/j.foodres.2010.03.015>
- Noci, F. (2017). Dairy Products Processed With Ultrasound. In D. Bermudez-Aguirre (Ed.), *Ultrasound: Advances in Food Processing and Preservation* (1st ed., p. 556). Academic Press.
- Norwood, E.-A., Chevallier, M., Le Floch-Fouéré, C., Schuck, P., Jeantet, R., & Croguennec, T. (2016). Heat-Induced Aggregation Properties of Whey Proteins as Affected by Storage Conditions of Whey Protein Isolate Powders. *Food and Bioprocess Technology*, 9, 993–1001. <https://doi.org/10.1007/s11947-016-1686-1>
- Nunes, L., Martins, E., Perrone, Í. T., & Carvalho, A. F. De. (2019). The Maillard Reaction in Powdered Infant Formula. *Journal of Food and Nutrition Research*, 7(1), 33–40. <https://doi.org/10.12691/jfnr-7-1-5>
- O'Mahony, J. A., & Fox, P. F. (2013). Milk Proteins: Introduction and Historical Aspects. In P. L. H. McSweeney & P. F. Fox (Eds.), *Advanced Dairy Chemistry-IA: Proteins: Basic Aspects* (4th ed.). New York: Springer.
- O'Sullivan, J., Arellano, M., Pichot, R., & Norton, I. (2014). The effect of ultrasound treatment on the structural, physical and emulsifying properties of dairy proteins. *Food Hydrocolloids*, 42, 386–396. <https://doi.org/10.1016/j.foodhyd.2014.05.011>
- O'Sullivan, J. J., Park, M., Beevers, J., Greenwood, R. W., & Norton, I. T. (2017). Applications of ultrasound for the functional modification of proteins and nanoemulsion formation: A review. *Food Hydrocolloids*, 71, 299–310. <https://doi.org/10.1016/j.foodhyd.2016.12.037>
- Paiva, P. H. C., Coelho, Y. L., da Silva, L. H. M., Pinto, M. S., Vidigal, M. C. T. R., & Pires, A. C. dos S. (2020). Influence of protein conformation and selected Hofmeister salts on bovine serum albumin/lutein complex formation. *Food Chemistry*, 305, 125463. <https://doi.org/10.1016/j.foodchem.2019.125463>
- Perreault, V., Morin, P., Pouliot, Y., & Britten, M. (2017). Effect of denatured whey protein concentrate and its fractions on rennet-induced milk gels. *International Dairy Journal*, 64, 48–55. <https://doi.org/10.1016/j.idairyj.2016.09.005>

- Qi, P. X., Ren, D., Xiao, Y., & Tomasula, P. M. (2015). Effect of homogenization and pasteurization on the structure and stability of whey protein in milk. *Journal of Dairy Science*, 98(5), 1–14. <https://doi.org/10.3168/jds.2014-8920>
- Raikos, V. (2010). Effect of heat treatment on milk protein functionality at emulsion interfaces. A review. *Food Hydrocolloids*, 24, 259–265. <https://doi.org/10.1016/j.foodhyd.2009.10.014>
- Relkin, P., & Shukat, R. (2012). Food protein aggregates as vitamin-matrix carriers: Impact of processing conditions. *Food Chemistry*, 134, 2141–2148. <https://doi.org/10.1016/j.foodchem.2012.04.020>
- Rodriguez-Concepcion, M., Avalos, J., Bonet, M. L., Boronat, A., Gomez-Gomez, L., Hornero-Mendez, D., Limon, M. C., Meléndez-Martínez, A. J., Olmedilla-Alonso, B., Palou, A., Ribot, J., Rodrigo, M. J., Zacarias, L., & Zhu, C. (2018). A global perspective on carotenoids: Metabolism, biotechnology, and benefits for nutrition and health. *Progress in Lipid Research*, 70, 62–93. <https://doi.org/10.1016/j.plipres.2018.04.004>
- Sabater, C., Montilla, A., Ovejero, A., Prodanov, M., Olano, A., & Corzo, N. (2018). Furosine and HMF determination in prebiotic-supplemented infant formula from Spanish market. *Journal of Food Composition and Analysis*, 66, 65–73. <https://doi.org/10.1016/j.jfca.2017.12.004>
- Sadeghi, R., Moosavi-Movahedi, A. A., Emam-Jomeh, Z., Kalbasi, A., Razavi, S. H., Karimi, M., & Kokini, J. (2014). The effect of different desolvating agents on BSA nanoparticle properties and encapsulation of curcumin. *Journal of Nanoparticle Research*, 16(9), 2565. <https://doi.org/10.1007/s11051-014-2565-1>
- Sáiz-Abajo, M.-J., González-Ferrero, C., Moreno-Ruiz, A., Romo-Hualde, A., & González-Navarro, C. J. (2013). Thermal protection of β -carotene in re-assembled casein micelles during different processing technologies applied in food industry. *Food Chemistry*, 138, 1581–1587. <https://doi.org/10.1016/j.foodchem.2012.11.016>
- Schuck, P., le Floch-Fouere, C., & Jeantet, R. (2013). Changes in Functional Properties of Milk Protein Powders: Effects of Vacuum Concentration and Drying. *Drying Technology*, 31(13–14), 1578–1591. <https://doi.org/10.1080/07373937.2013.816316>
- Shamsi, K., & Sherkat, F. (2009). Application of pulsed electric field in non-thermal processing of milk. *Asian Journal of Food and Agro-Industry*, 2(3), 216–244.
- Shanmugam, A., Chandrapala, J., & Ashokkumar, M. (2012). The effect of ultrasound on the physical and functional properties of skim milk. *Innovative Food Science and Emerging Technologies*, 16, 251–258. <https://doi.org/10.1016/j.ifset.2012.06.005>

- Shen, X., Fang, T., Gao, F., & Guo, M. (2017). Effects of ultrasound treatment on physicochemical and emulsifying properties of whey proteins pre- and post-thermal aggregation. *Food Hydrocolloids*, *63*, 668–676. <https://doi.org/10.1016/j.foodhyd.2016.10.003>
- Siddique, M. A. B., Maresca, P., Pataro, G., & Ferrari, G. (2016). Effect of pulsed light treatment on structural and functional properties of whey protein isolate. *Food Research International*, *87*, 189–196. <https://doi.org/10.1016/j.foodres.2016.07.017>
- Siddique, M. A. B., Maresca, P., Pataro, G., & Ferrari, G. (2017). Influence of pulsed light treatment on the aggregation of whey protein isolate. *Food Research International*, *99*, 419–425. <https://doi.org/10.1016/j.foodres.2017.06.003>
- Silva, D. F. da, Ahrné, L., Ipsen, R., & Hougaard, A. B. (2018). Casein-Based Powders: Characteristics and Rehydration Properties. *Comprehensive Reviews in Food Science and Food Safety*, *17*, 240–254. <https://doi.org/10.1111/1541-4337.12319>
- Stanic-Vucinic, D., Stojadinovic, M., Atanaskovic-Markovic, M., Ognjenovic, J., Grönlund, H., van Hage, M., ... Velickovic, T. C. (2012). Structural changes and allergenic properties of β -lactoglobulin upon exposure to high-intensity ultrasound. *Molecular Nutrition & Food Research*, *56*, 1894–1905. <https://doi.org/10.1002/mnfr.201200179>
- Stephenson, R. C., Ross, R. P., & Stanton, C. (2021). Carotenoids in Milk and the Potential for Dairy Based Functional Foods. *Foods*, *10*, 1263. <https://doi.org/10.1016/B978-0-12-384731-7.00172-0>
- Sui, Q., Roginski, H., Williams, R. P. W., Versteeg, C., & Wan, J. (2011). Effect of pulsed electric field and thermal treatment on the physicochemical and functional properties of whey protein isolate. *International Dairy Journal*, *21*(4), 206–213. <https://doi.org/10.1016/j.idairyj.2010.11.001>
- Tavares, G. M., Croguennec, T., Carvalho, A. F., & Bouhallab, S. (2014). Milk proteins as encapsulation devices and delivery vehicles: Applications and trends. *Trends in Food Science and Technology*, *37*, 5–20. <https://doi.org/10.1016/j.tifs.2014.02.008>
- Tavares, T., & Malcata, F. X. (2016). Whey and Whey Powders: Protein Concentrates and Fractions. In B. Caballero, P. Finglas, & F. Toldra (Eds.), *Encyclopedia of Food and Health* (1st ed., pp. 506–513). Elsevier Ltd. <https://doi.org/10.1016/B978-0-12-384947-2.00748-0>
- Teo, A., Lee, S. J., Goh, K. K. T., & Wolber, F. M. (2017). Kinetic stability and cellular uptake of lutein in WPI-stabilised nanoemulsions and emulsions prepared by emulsification and solvent evaporation method. *Food Chemistry*, *221*, 1269–1276.

- <https://doi.org/10.1016/j.foodchem.2016.11.030>
- Tham, T. W. I., Wang, C., Yeoh, A. T. H., & Zhou, W. (2016). Moisture sorption isotherm and caking properties of infant formulas. *Journal of Food Engineering*, *175*, 117–126. <https://doi.org/10.1016/j.jfoodeng.2015.12.014>
- Tham, T. W. Y., Yeoh, A. T. H., & Zhou, W. (2017). Characterisation of aged infant formulas and physicochemical changes. *Food Chemistry*, *219*, 117–125. <https://doi.org/10.1016/j.foodchem.2016.09.107>
- Tijerina Sáenz, A., Elisia, I., Innis, S. M., Friel, J. K., & Kitts, D. D. (2009). Use of ORAC to assess antioxidant capacity of human milk. *Journal of Food Composition and Analysis*, *22*(7–8), 694–698. <https://doi.org/10.1016/j.jfca.2009.01.021>
- Tran, M., Roberts, R., Felix, T. L., & Harte, F. M. (2018). Effect of high-pressure-jet processing on the viscosity and foaming properties of pasteurized whole milk. *Journal of Dairy Science*, *101*(5), 3887–3899. <https://doi.org/10.3168/jds.2017-14103>
- Udabage, P., Puvanenthiran, A., Yoo, J. A., Versteeg, C., & Augustin, M. A. (2012). Modified water solubility of milk protein concentrate powders through the application of static high pressure treatment. *Journal of Dairy Research*, *79*, 76–83. <https://doi.org/10.1017/S0022029911000793>
- Verhoeckx, K. C. M., Vissers, Y. M., Baumert, J. L., Faludi, R., Feys, M., Flanagan, S., ... Kimber, I. (2015). Food processing and allergenicity. *Food and Chemical Toxicology*, *80*, 223–240. <https://doi.org/10.1016/j.fct.2015.03.005>
- Voigt, D. D., Kelly, A. L., & Huppertz, T. (2015). High-Pressure Processing of Milk and Dairy Products. In N. Datta & P. M. Tomasula (Eds.), *Emerging Dairy Processing Technologies: Opportunities for the Dairy Industry* (1st ed., p. 360). Wiley-Blackwell.
- Wang, C., Liu, J., Duan, B., Lao, Y., Qi, P. X., & Ren, D. (2018a). Effects of dietary antioxidant supplementation of feed, milk processing and storage on the lutein content and sensory quality of bovine milk. *International Journal of Dairy Technology*, *71*(4), 849–856. <https://doi.org/10.1111/1471-0307.12532>
- Wang, X. B., Wang, C. N., Zhang, Y. C., Liu, T. T., Lv, J. P., Shen, X., & Guo, M. R. (2018b). Effects of gamma radiation on microbial, physicochemical, and structural properties of whey protein model system. *Journal of Dairy Science*, *101*(6), 1–12. <https://doi.org/10.3168/jds.2017-14085>
- Wang, X., Esquerre, C., Downey, G., Henihan, L., O'Callaghan, D., & O'Donnell, C. (2018c). Assessment of infant formula quality and composition using Vis-NIR, MIR and Raman process analytical technologies. *Talanta*, *183*, 320–328.

<https://doi.org/10.1016/j.talanta.2018.02.080>

- Xiang, B. Y., Ngadi, M. O., Ochoa-Martinez, L. A., & Simpson, M. V. (2011). Pulsed Electric Field-Induced Structural Modification of Whey Protein Isolate. *Food and Bioprocess Technology*, 4, 1341–1348. <https://doi.org/10.1007/s11947-009-0266-z>
- Yanjun, S., Jianhang, C., Shuwen, Z., Hongjuan, L., Jing, L., Lu, L., ... Jiaping, L. (2014). Effect of power ultrasound pre-treatment on the physical and functional properties of reconstituted milk protein concentrate. *Journal of Food Engineering*, 124, 11–18. <https://doi.org/10.1016/j.jfoodeng.2013.09.013>
- Yazdi, S. R., & Corredig, M. (2012). Heating of milk alters the binding of curcumin to casein micelles. A fluorescence spectroscopy study. *Food Chemistry*, 132, 1143–1149. <https://doi.org/10.1016/j.foodchem.2011.11.019>
- Yu, L. J., Ngadi, M., & Raghavan, G. S. V. (2009). Effect of temperature and pulsed electric field treatment on rennet coagulation properties of milk. *Journal of Food Engineering*, 95, 115–118. <https://doi.org/10.1016/j.jfoodeng.2009.04.013>
- Zhang, R., Pang, X., Lu, J., Liu, L., Zhang, S., & Lv, J. (2018). Effect of high intensity ultrasound pretreatment on functional and structural properties of micellar casein concentrates. *Ultrasonics - Sonochemistry*, 47, 10–16. <https://doi.org/10.1016/j.ultsonch.2018.04.011>
- Zhao, C., Shen, X., & Guo, M. (2018). Stability of lutein encapsulated whey protein nano-emulsion during storage. *PLoS ONE*, 13(2), 1–10. <https://doi.org/10.1371/journal.pone.0192511>
- Zhao, W., Tang, Y., Lu, L., Chen, X., & Li, C. (2014). Pulsed Electric Fields Processing of Protein-Based Foods. *Food and Bioprocess Technology*, 7, 114–125. <https://doi.org/10.1007/s11947-012-1040-1>
- Zisu, B., Lee, J., Chandrapala, J., Bhaskaracharya, R., Palmer, M., Kentish, S., & Ashokkumar, M. (2011). Effect of ultrasound on the physical and functional properties of reconstituted whey protein powders. *Journal of Dairy Research*, 78, 226–232. <https://doi.org/10.1017/S0022029911000070>

CHAPTER 3 - RESEARCH ARTICLE 1

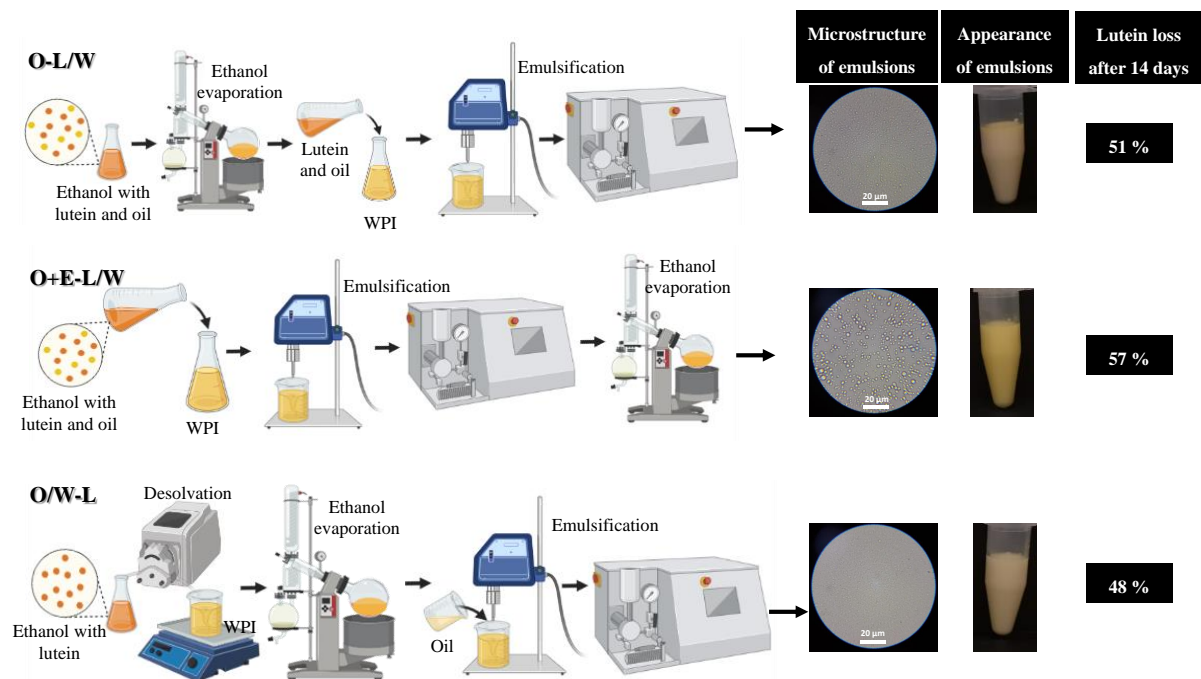
Title: Ethanol assisted incorporation of lutein into whey protein stabilized emulsions: how the steps of addition and evaporation of the solvent affect the obtained systems.

Authorship: Lauane Nunes, Milena Corredig, Guilherme M. Tavares.

The manuscript will be submitted to Food and Bioprocess Technology (IF 2023: 5.581).

The objective of this study was to provide an understanding of the influence of the steps applied for incorporation of lutein into oil/water emulsions stabilized by whey proteins regarding lutein stability and emulsion physical stability. One important highlight of the study regards the improved chemical and physical stability of the emulsion O/W-L. This sample was produced by adding the ethanolic lutein solution into the aqueous dispersion of whey proteins, then the ethanol was eliminated by rotary evaporation and the emulsification step was performed.

Graphical abstract



Abstract

Lutein is a bioactive compound associated with several health benefits, but its incorporation into formulated products is challenging due to its low water solubility. To produce emulsified systems containing lutein, different studies use organic solvents to assist its incorporation into the emulsions, however low attention has been given to the influence of the order of the emulsification step and solvent evaporation on the stability of the obtained systems. Thus, the objective of this study was to provide an understanding of the influence of these steps for the incorporation of lutein into oil/water emulsions stabilized by whey proteins. Ethanolic lutein solution was added to the oil phase of the emulsion, which was removed by rotary evaporation before (O-L/W) or after (O+E-L/W) the emulsification step. Another system was produced by adding the ethanolic lutein solution into the aqueous dispersion of whey proteins, then the ethanol was eliminated by rotary evaporation and the emulsification step was performed (O/W-L). The high encapsulation efficiency observed for O-L/W and O+E-L/W emulsions indicates the successful incorporation of lutein within the oil droplets, while lutein in the O/W-L emulsion was distributed in the dispersed and continuous phase. No differences could be noticed in the lutein degradation over 14 days of storage under lighted conditions between O-L/W and O/W-L samples, however, it was more pronounced for O+E-L/W. Regarding the creaming stability, the O/W-L sample was the most stable one. The results highlight the importance of rationalizing the incorporation of bioactive compounds as a useful strategy to improve the stability of the obtained systems.

Keywords: carotenoid, desolvation, emulsification, whey proteins nanoparticles, simple emulsions.

3.1.Introduction

A variety of bioactive compounds can be incorporated into foods and beverages in order to functionalize them and contribute to maintaining the health and well-being of consumers (McClements & Li, 2010). Lutein is one of these bioactive compounds, which has been reported for reducing the risk of chronic diseases such as cataracts and age-related macular degeneration when consumed regularly in appropriate amounts (Teo et al., 2017). This yellow-orange oxygenated carotenoid contains a series of conjugated double bonds conferring to the molecule antioxidant properties and its ability to absorb light in the UV-visible region (Ochoa Becerra et al., 2020; Yi et al., 2016). The hydrophobic nature of lutein and its susceptibility to be degraded when exposed to light, oxygen and heat makes its incorporation into formulated foods challenging (Mantovani et al., 2020). In addition, the tendency of lutein to aggregate beyond its solubility limit impacts several of its properties, such as its pigmentation, its antioxidant properties, and its interaction with other molecules of the formulated product (Rasera et al., 2023; Yi et al., 2016). In this scenario, to produce emulsified systems containing lutein, several studies describe the solubilization of the carotenoid into an organic solvent prior to its incorporation into the oil phase of the emulsion, followed by a complementary step of solvent evaporation before the emulsification step. For example, Iddir et al., (2020) produced emulsions with β -carotene, lycopene and lutein dissolved in hexane and peanut oil, with subsequent evaporation of the solvent and emulsification with soy proteins, whey protein, gelatin or sodium caseinate. Conversely Mantovani et al., (2022) incorporated different lutein-rich carotenoids extracts into sunflower oil assisted with ethyl acetate, which was eliminated by vacuum evaporation before emulsification.

Since organic solvents are often employed as a coadjutant for the production of emulsified systems containing carotenoids, the question about how the addition and evaporation of the solvent could be applied to modulate the characteristics of the obtained emulsions arises. Although the elimination of the solvent from the oil phase before emulsification is more often described in the literature, some reports pointed out the positive effect of some organic solvents on improving the stability of emulsions when eliminated after the emulsification step. Through this method and using ethyl acetate Lee et al., (2011) and Teo et al., (2017) obtained nanoemulsions with sizes smaller than 70 nm, which were stable during storage and to salt addition, thermal treatment, and freezing/thawing. Despite the

advantages of using ethyl acetate, in this study ethanol was used because it is a substance Generally Recognized as Safe (GRAS) for use in food products (McClements & Li, 2010).

Moreover, the controlled addition of organic solvents to protein dispersions followed by the solvent evaporation, known as desolvation, has been applied to produce protein nanoparticles displaying promising characteristics for the encapsulation and delivery of bioactive compounds (Gülseren et al., 2012a). Whey protein isolate (WPI) nanoparticles prepared using ethanol desolvation showed high zinc incorporation efficiencies and remained stable after 30 days of storage at 22 °C (Gülseren et al., 2012b). Moreover, Jain et al., (2018) formulated lycopene-loaded whey protein isolate nanoparticles by ethanol desolvation. These authors obtained nanoparticles of around 110 nm diameter and over 60 % of lycopene incorporation.

In this scenario, to understand the influence of the different combinations of emulsification and solvent evaporation to produced lutein-load oil/water whey protein stabilized emulsions, different systems were produced (i) the first emulsion was produced by adding the ethanolic solution of lutein into the oil phase of the emulsion, then the solvent was eliminated by rotary evaporation before the emulsification step; (ii) the second one was produced by adding the ethanolic solution of lutein into the oil phase of the emulsion, which was emulsified into the aqueous dispersion of whey proteins, then the solvent was eliminated from the emulsion by rotary evaporation, and (iii) the third one was produced by adding the ethanolic solution of lutein into the aqueous dispersion of whey proteins, then the ethanol was eliminated by rotary evaporation and the emulsification step was performed. The different samples were evaluated regarding their encapsulation efficiency and physical and chemical stability over time. This investigation will provide insights regarding the rationalization of the emulsification process to produce tailored lutein-load emulsions.

3.2. Materials and methods

3.2.1. Materials

Whey protein isolate (WPI) was obtained from a commercial source (containing, according to manufacturer, 94 % protein; 0.9 % fat; 2 % lactose and 0.44 % minerals). Lutein standard and sodium azide were purchased from Sigma-Aldrich (Darmstadt, Germany). Ethanol and solvents used in the lutein extraction were reagent grade acquired from Synth (Brazil). Corn oil (Liza[®], Cargill Agrícola S.A., Brazil) was acquired at a local market in the city of Campinas (Brazil). Ultrapure water was used to prepare all dispersions.

3.2.2. Preparation of emulsions

In order to compare how the order of addition and evaporation of ethanol would affect the characteristics of whey protein stabilized oil-in-water emulsions containing lutein, three different emulsions were prepared. All different emulsions contained equivalent lutein, whey protein and oil concentrations. In all cases, the addition of lutein was assisted using ethanol (ethanolic lutein solutions), which was removed by rotary evaporation, at different moments according to the different samples.

The first emulsion, referred to as O-L/W, was prepared by solubilizing lutein in ethanol, which was added to corn oil at a ratio of 1:9 w.w⁻¹ (ethanolic lutein solution:oil). Then, the mixture was stirred, and the solvent was removed by rotary evaporation under reduced pressure at a temperature below 35 °C (Yi et al., 2014). The aqueous phase was prepared by dispersing 2 % w.w⁻¹ of WPI in Milli-Q water (pH 7.0) containing 0.02 % w.w⁻¹ sodium azide, followed by stirring for 2 h at room temperature (25 °C) and overnight at 8 °C to ensure protein solubilization (Lee et al., 2011; Teo et al., 2017). Then, the oil phase containing 0.001 % w.w⁻¹ lutein but free from ethanol was mixed with the aqueous phase at a ratio of 1:9 w.w⁻¹ (oil:aqueous WPI dispersion) using a high-speed disperser (T25, IKA, Staufen, Germany) at 12,000 rpm for 3 min to form a coarse emulsion, which was subjected to 3 cycles of a high-pressure microfluidization at 600 bar (Microfluidics, model 110-P, corp. Newton, MA, USA) to obtain a fine emulsion (Gumus et al., 2017; Zhao et al., 2020).

Regarding the second emulsion, referred to as O+E-L/W, the lutein prepared in ethanol was added to corn oil at the ratio 1:9 w.w⁻¹. The organic phase was added to the aqueous phase containing 2 % w.w⁻¹ of WPI and 0.02 % w.w⁻¹ sodium azide at a mass ratio of 1:9 oil:aqueous WPI dispersion with a final lutein concentration of 0.001 % w.w⁻¹. Then a coarse emulsion was prepared by using a high-speed disperser, followed by high-pressure microfluidization to obtain a fine emulsion. Ethanol was then removed from the fine emulsion by rotary evaporation. The applied emulsification and rotary evaporation parameters were the same employed to produce the O-L/W sample.

The third emulsion, referred to as O/W-L, was prepared by the addition of the 0.001 % w.w⁻¹ ethanolic lutein solution drop-by-drop to 2 % w.w⁻¹ WPI aqueous dispersion (pH 7.0) containing 0.02 % w.w⁻¹ of sodium azide. The WPI dispersion was kept under magnetic stirring and the ethanolic lutein solution was added at a constant flow rate of 1 mL.min⁻¹ assured by a peristaltic pump (PRR-2A, Shimadzu, Kyoto, Japan) until a final ethanol to aqueous phase volumetric ratio of 1:1 (Jain et al., 2018; Sadeghi et al., 2014). The mixture was then subjected to rotary evaporation for solvent removal. The corn oil was mixed with the

obtained desolvated protein dispersion containing lutein at a ratio of 1:9 w.w⁻¹ using a high-speed disperser to produce a coarse emulsion, and then a fine emulsion was obtained using high-pressure microfluidization. The applied emulsification and rotary evaporation parameters were the same employed to produce the O-L/W sample.

All emulsions were prepared in triplicate, transferred to glass bottles, and stored at 4 °C until analysis.

3.2.3. Particle size and ζ -potential measurements

The particle size and ζ -potential of the proteins before and after desolvation, as well as, of the different emulsions were measured using a Zetasizer Nano ZS 90 (Malvern Instruments, Worcestershire, UK). For particle size measurements, emulsions were diluted 1000-fold and proteins after desolvation 100-fold in Milli-Q water (pH 7), proteins before desolvation were only filtered through 0.45 μ m syringe filters (Pall, New York, USA), then 1 mL of samples was transferred into the measuring cell and analyzed at a wavelength of 633 nm at a backscattering of 90°, using a refractive index of 1.45 and 1.33 for particles and water, respectively (Shen et al., 2018; Zhao et al., 2020). Each sample was analyzed in triplicate, and the particle size was expressed as hydrodynamic diameter (D_h) and particle size distribution.

Regarding the ζ -potential of the samples, measurements were conducted according to Santiago et al., (2021). The samples were diluted in the same way as above. Measurements were performed at 25 °C employing the refractive index, the dielectric constant, and the viscosity of the dispersant of 1.33, 78.5, and 0.887 mPa.s, respectively. Each sample was analyzed three times.

3.2.4. Optical microscopy

The microstructure of the emulsions was analyzed right after production and after 14 days of storage using an optical microscope. One droplet of each sample was placed on the microscope slide, covered with a glass cover slip, and observed using a Digilab model DI-136 M optical microscope (Digilab Comercial, Brazil) with the magnification of 2000 times and at least 5 representative images of the emulsions were taken.

3.2.5. Physical stability of the emulsions

The physical stability of emulsions was followed through its tendency of phase separation during 14 days of storage. The fresh produced emulsions were placed into glass

tubes (height 45 mm) and the backscattering intensity of laser light was monitored over time at 25 °C, using a Turbiscan LAB® Expert (Formulation, France).

3.2.6. Lutein encapsulation and photo-stability

Lutein quantification was performed as described in Xavier et al., (2012). The volume of 4 mL of tetrahydrofuran was sequentially added to 1 mL of the sample, followed by vortexing. Then lutein was partitioned to diethyl ether/petroleum ether (1:1 v.v⁻¹) and the tetrahydrofuran was removed by water washing. The extract obtained after evaporation of the ether phase was dissolved in ethanol and the absorbance was measured at 445 nm with a UV–visible spectroscopy system (8453E, Agilent Technologies Deutschland GmbH, Waldbronn, Germany). The lutein concentration was calculated according to the Lambert-Beer law.

To determine the encapsulation efficiency of lutein in the different emulsions, lutein was quantified in the emulsions and also in their respective oil phase obtained after centrifugation (Allegra 64R centrifuge, Beckman Coulter Inc., CA, United States of America) at 9,450 g per 15 min. Results were expressed as the ratio between the amount of lutein extracted from the oil phase obtained after centrifugation and the total amount of lutein extracted from the emulsion.

To follow the photo-stability of lutein in the different samples, the volume of 12 mL of fresh produced emulsions were exposed to lighted conditions (fluorescent, daylight type; 33,000 Lx) at 25 °C for 14 days. The lutein loss was expressed as the ratio between the amount of lutein extracted from the emulsions after 14 days of storage, and the initial amount of lutein extracted from the fresh produced emulsions. For the emulsions O/W-L, the lutein loss was also determined in the oil phase obtained after centrifugation at 9,450 g/15 min.

3.2.7. Color of emulsions over time

The color of emulsions was measured using a Color Quest XE colorimeter (Hunter Associates Lab., 146 Reston, VA, USA). The measurements were obtained in triplicate and taken for the fresh produced samples and over 14 days of storage at lighted conditions (fluorescent, daylight type; 33,000 Lx) at 25 °C with specular component using illuminant D65, angle 10°. The color difference was calculated according to the color parameters L*, a* and b* measured into the following equation:

$$\Delta E^* = \sqrt{(L^* - L_0^*)^2 + (a^* - a_0^*)^2 + (b^* - b_0^*)^2} \quad \text{Eq. 3.1}$$

where ΔE^* is the color difference; L^* , a^* , and b^* are the lightness, red-green value, and yellow-blue value of the emulsions after storage of 14 days; and L_0^* , a_0^* , and b_0^* are the equivalent color parameters before the storage, respectively (Teo et al., 2017; Zhao et al., 2020).

3.2.8. Statistics

The experiments and analysis were carried out in triplicate and the results were reported as the mean \pm standard deviation. Analysis of variance (ANOVA) and Tukey's test was performed using the statistical program R, version 4.0.2. (R Foundation for Statistical Computing, Vienna, Austria) with a level of significance of $p < 0.05$.

3.3. Results

3.3.1. Characterization of emulsions

Table 3.1 displays the average hydrodynamic diameter and ζ -potential of the original WPI dispersion, and the dispersion obtained after desolvation (WPI-desolvation), as well as, of the different fresh produced emulsions. In the case of the O+E-L/W sample, data obtained after high-pressure microfluidization and before solvent evaporation, referred to as O+E-L/W b.evap., and the final emulsion (after solvent evaporation), referred to as O+E-L/W are shown in Table 3.1. Conversely, Figure 3.1 displays the particle size distribution of the different samples. The average hydrodynamic diameter of the WPI dispersion was 5 ± 0.2 nm, and it displayed a bimodal distribution, which is consistent with literature reports (Gülseren et al., 2012a; Kotchabhakdi & Vardhanabhuti, 2020). After desolvation, the average D_h observed for the dispersion was 294.24 ± 2.37 nm evidencing the formation of protein nanoparticles containing lutein. These nanoparticles displayed a monomodal distribution. To compare, Gülseren et al., (2012a) obtained particle sizes smaller than 10 nm for WPI particles produced by desolvation with ethanol, while Jain et al., (2018) obtained WPI nanoparticles of around 350 nm after ethanol desolvation in the presence of lycopene. The presence of the carotenoid induced the formation of larger particles compared to the system in absence of this molecule. This is aligned with the finds of the present study. It is important to note that the formation of smaller particles rather than larger ones increases the total surface area of the obtained particles, which is presumed to improve their emulsifying properties (Ho et al., 2017). Comparing the ζ -potentials of WPI dispersion (-19.30 ± 0.36) and of the dispersion obtained after desolvation (-24.36 ± 0.46) in Table 3.1, the desolvation lead to an increase of the ζ -potential of the obtained nanoparticles compared to the individual proteins. This behavior is

associated to protein denaturation followed by protein aggregation induced by the changes of dielectric constant during desolvation.

Table 3.1- Hydrodynamic diameter (D_h , nm) and ζ -potential (mV) of WPI dispersions and different emulsions. Different letters in a same column mean a significant difference ($p < 0.05$) between samples.

Sample	D_h (nm)	ζ -potential (mV)
WPI	5.07 ± 0.19^f	-19.30 ± 0.36^a
O-L/W	247.5 ± 6.13^d	-28.32 ± 0.45^e
O+E-L/W b.evap.	1278.8 ± 4.4^a	-25.97 ± 0.27^c
O+E-L/W	952.8 ± 5.2^b	-27.49 ± 0.35^d
WPI-desolvation	294.24 ± 2.37^c	-24.36 ± 0.46^b
O/W-L	222.6 ± 5.88^e	-27.10 ± 0.35^d

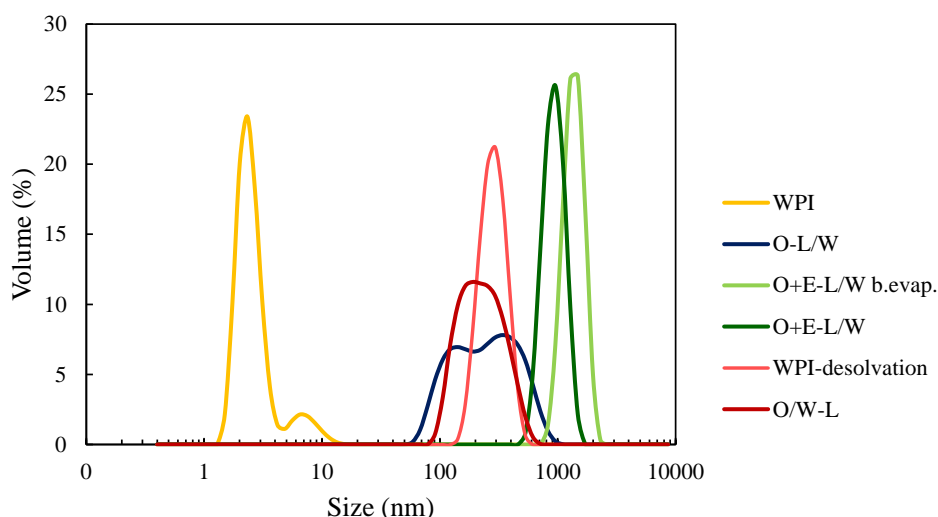


Figure 3.1- Particle size distribution of WPI dispersions and different emulsions measured by dynamic light scattering.

Regarding the emulsions, the smallest average size (222 nm) was observed for the O/W-L emulsion and the largest (953 nm) for the O+E-L/W, both with monomodal distributions. The O-L/W emulsion displayed an intermediate average particle size (248 nm) with a bimodal distribution. Despite the larger size of the particles used for stabilizing the O/W-L compared to the WPI dispersion used for stabilizing the other samples, the O/W-L emulsions had the smallest droplet size. The particle size of the O+E-L/W emulsion being larger compared to the other emulsions shows that the solvent evaporation step applied after

the emulsification played a major role on the obtained emulsion. Comparing the particle sizes of the O+E-L/W emulsion before and after evaporation there was a significant reduction from 1279 to 953 nm, probably promoted by the shrinkage of the droplets when the ethanol was removed by evaporation. In the case of the O-L/W emulsion, the absence of ethanol during the emulsification leads to the formation of small droplets varying from 60 to 955 nm. Differently from the observed when ethyl acetate was used as a coadjutant to produce nanoemulsions, the same effect was not promoted by ethanol, probably due to the lower hydrophobic character and higher viscosity of the latter (Lee et al., 2011; McClements, 2007; Teo et al., 2017). For instance, Teo et al., (2017) achieved particle sizes of 68.8 nm for WPI-stabilized nanoemulsions containing lutein, prepared through a similar method but using ethyl acetate instead ethanol.

The ζ -potential of the different emulsions (Table 3.1) is close to each other and indicates a negatively global charged surface at pH 7. These findings suggest the contribution of electrostatic repulsion on stabilizing the emulsions, along with the steric hindrance provided by the proteins. Values in the same range as those measured in this study were also observed by Teo et al., (2017), who reported ζ -potential of -28.7 mV for WPI-stabilized nanoemulsions containing lutein.

3.3.2. Physical stability of the emulsions

The physical stability of the emulsions was evaluated using the backscattering intensity profiles for samples immediately after preparation (t_0), and after 7 (t_7) and 14 days (t_{14}) of storage at room temperature (25 °C). The obtained data are shown in Figure 3.2A, 3.2B and 3.2C, respectively for O-L/W, O+E-L/W and O/W-L samples. In the case of the O-L/W and O+E-L/W emulsions, an increase in backscattering flux at the top of the emulsions was observed after 7 days of storage, and this trend continued until the 14th day. This increase in backscattering flux indicates a creaming process, where the oil phase tends to migrate and accumulate at the top of the emulsion. This behavior was more intense for O+E-L/W samples. On the other, the backscattering of O/W-L emulsion remained unchanged during all 14 days of storage. Figure 3.2D shows a comparison of the destabilization processes of the emulsions. It confirms that the destabilization process was more accelerated for the O+E-L/W emulsion, followed by the O-L/W emulsion, while the destabilization was almost negligible for the O/W-L emulsion. The small droplet size observed in the O/W-L emulsion (Table 3.1) suggests good stability against phase separation. This indicates that the method used to produce the O/W-L emulsion may contribute to extending the shelf life of products by

minimizing instability and maintaining emulsion integrity over time. Despite the differences pointed-out in Figure 3.2, it was not evident to visually distinguish the formed cream layer.

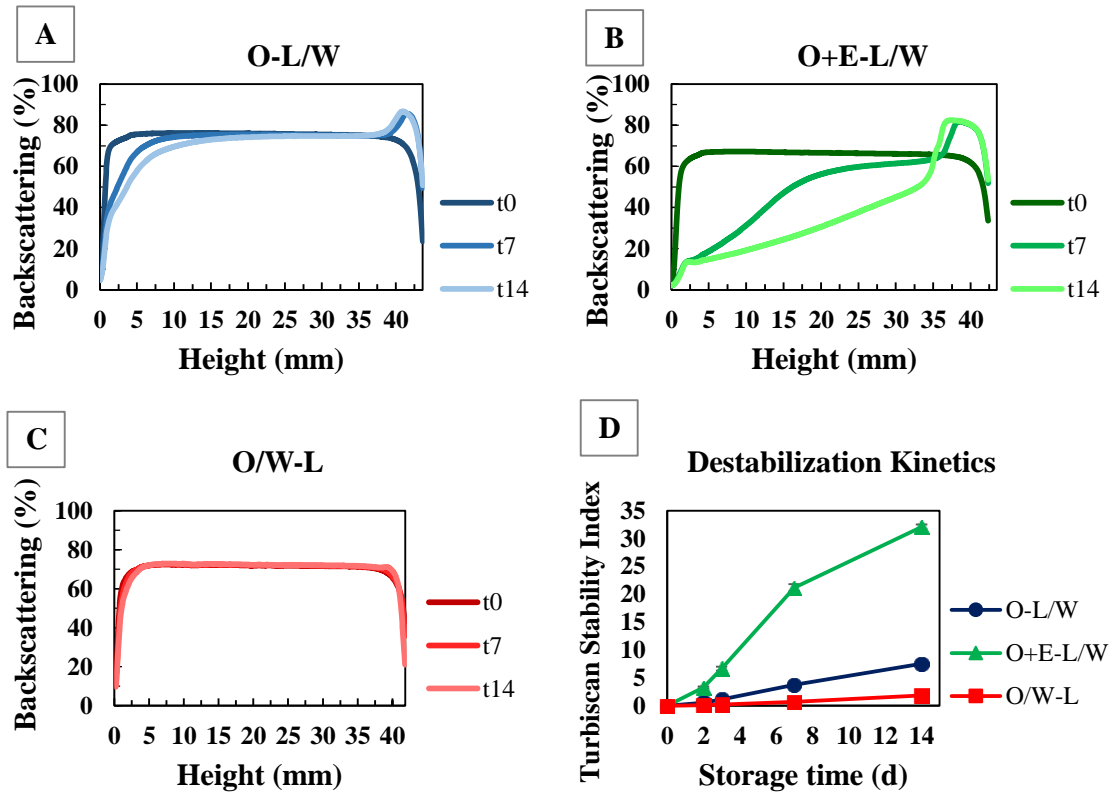


Figure 3.2- A-C) Backscattering intensity profiles of emulsions. (t0) immediately after emulsion preparation, (t7) 7 days, and (t14) 14 days after emulsion preparation. The horizontal axis represents the position along the glass tube. D) Destabilization kinetics of emulsions during 14 days of storage.

The microstructure of the emulsions was monitored by optical microscopy and the obtained images of the fresh produced emulsions and after 14 days of storage are shown in Figure 3.3. The microstructure of the fresh produced samples is in harmony with the findings reported in Figure 3.1 and Table 3.1, which demonstrate the increasing particle size in the order of O/W-L < O-L/W < O+E-L/W. Moreover, after 14 days of storage, there was no noticeable change in the microstructure of the emulsions. These results, combined with the observation discussed in Figure 3.2, suggest a tendency of flocculation of the droplets, in particular for O+E-L/W, rather than a coalescence process.

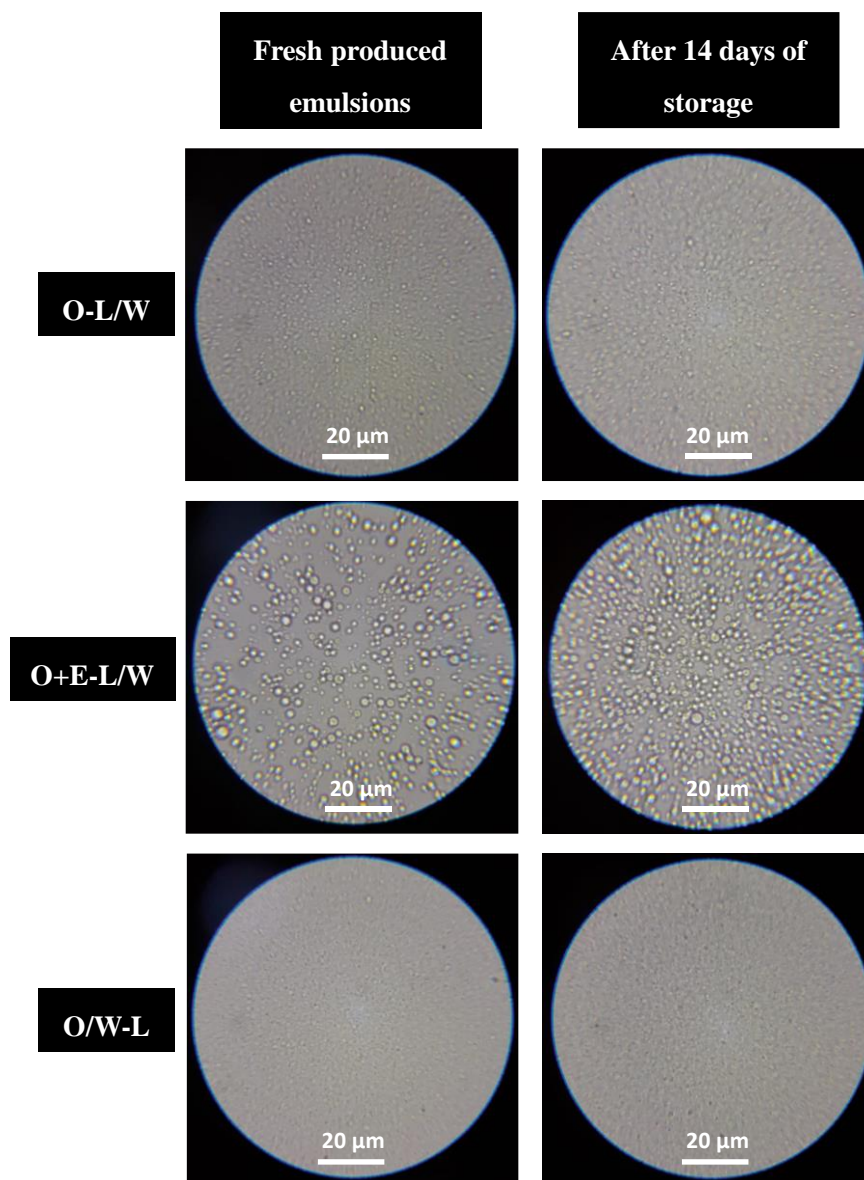


Figure 3.3- Representative images of the microstructure of fresh produced emulsions and after 14 days of storage at room temperature (25 °C) under lighted conditions.

3.3.3. Lutein encapsulation and photo-stability

To determine the lutein encapsulation efficiency in the fresh produced samples, lutein was quantified in the whole emulsions and also only in the cream phase, as shown in Table 3.2. Initially, all emulsions had about $11 \mu\text{g}\cdot\text{mL}^{-1}$ of lutein. The encapsulation efficiency, which indicates the amount of lutein effectively trapped and retained within the oil droplets, varied among the different emulsions. The O+E-L/W emulsion exhibited the highest encapsulation efficiency, exceeding 98 %. Similarly, the O-L/W emulsion displayed a relatively high encapsulation efficiency of approximately 96 %. These results indicate that both emulsions effectively trapped and retained lutein within the oil phase, resulting in high

encapsulation efficiencies. In contrast, the O/W-L emulsion showed a significantly lower encapsulation efficiency of 64 %. During the desolvation process, the conformational changes of the protein (WPI) can lead to selective aggregation, which has the potential to entrap bioactive compounds such as lutein (Sadeghi et al., 2014). In this case, part of the lutein entrapped by the WPI particles remained in the continuous phase rather than in the oil-water interface, resulting in lower encapsulation efficiency. This suggests that lutein was not solely encapsulated within the oil droplets but rather distributed throughout the oil phase, aqueous phase, and/or the emulsion interface. This result was already expected due to the production method.

Table 3.2- Concentration of lutein in the emulsions, encapsulation efficiency and lutein loss after 14 days of storage under lighted conditions at room temperature. Lowercase letters indicate statistically significant differences ($p < 0.05$) within a row.

Analysis	O-L/W	O+E-L/W	O/W-L
Lutein in emulsion ($\mu\text{g.mL}^{-1}$)	11.1 ± 0.1^a	10.9 ± 0.1^a	10.9 ± 0.1^a
Encapsulation efficiency (%)	95.9 ± 1.14^a	98.6 ± 1.0^a	64.4 ± 1.0^b
Lutein in emulsion - 14 days ($\mu\text{g.mL}^{-1}$)	5.5 ± 0.1^a	4.7 ± 0.1^b	5.6 ± 0.1^a
Lutein loss (%) - 14 days	50.5 ± 0.5^b	56.7 ± 0.7^a	48.3 ± 0.5^b (emulsion) 26.8 ± 0.1 (oil phase) 87.3 ± 0.8 (aqueous phase)

To evaluate the photo-stability and consequently the loss of lutein in the different samples, they were exposed to lighted conditions during 14 days. The data are shown in Table 3.2 and it is evident that there was a considerable loss of lutein in all evaluated emulsions over the 14 days of storage under lighted condition. The degradation rates for the O+E-L/W and O-L/W are reported as 57 % and 51 %, respectively. Since lutein is encapsulated within the oil droplets, a significant portion of lutein degradation occurs within this phase. On the other hand, in the O/W-L emulsion, where lutein is distributed between the phases and/or the interface, a significant portion of the degradation (87 %) takes place in the aqueous phase. This suggests that lutein remaining in the aqueous environment is more prone to photo-degradation. For this sample a global lutein loss of around 48 % was observed, which was not significantly different from the one observed for O-L/W samples. Nevertheless, lutein loss of the O+E-L/W sample was significantly higher compared to the other samples.

The stability of the emulsions to storage was also assessed by evaluating through color change over time. Figure 3.4 shows the color parameter b^* , representing the yellow-blue value, color difference of emulsions during storage under lighted condition and the appearance of fresh emulsions. Initially, all emulsions exhibited a yellow color, reflecting the presence of lutein, which is known for its intense yellow-orange pigment. Among the emulsions, the O+E-L/W emulsion displayed a significantly greater yellow color (higher b^* value) compared to the others (Figure 3.4A, 3.4C), even though all emulsions have the same concentration of lutein. These color differences may be linked to the largest hydrodynamic diameter of particles of O+E-L/W samples compared to the other samples (Table 3.1 and Figure 3.1). In addition, potential differences in the aggregation state of lutein comparing samples may also contribute to explain the observed differences, since it plays a major role in lutein color (Rasera et al., 2023; Zhu et al., 2019). For instance, lutein in O+E-L/W was subjected to high shear stress in the presence of large amounts of ethanol which could promote better lutein dispersion before solvent elimination, increasing the yellow character of this sample. The color of all the emulsions faded over time and became lighter, as assessed both for the b^* color parameter and for the color difference, mainly for the O+E-L/W emulsion, which converge to the monitored lutein photo-degradation.

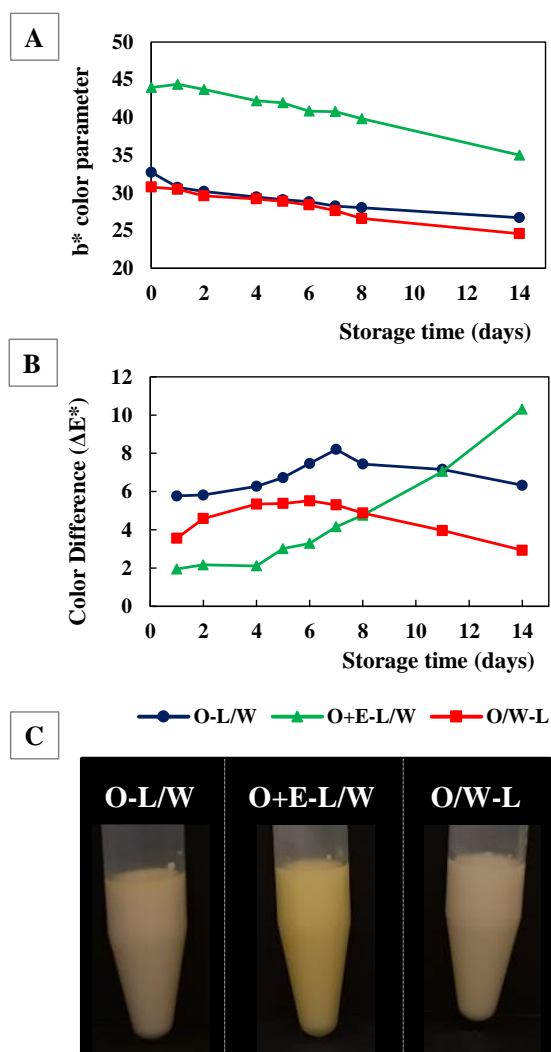


Figure 3.4- A) Color parameter b^* and (B) color difference of emulsions during 14 days of storage under light. C) Appearance of fresh produced emulsions.

3.4. Conclusions

Encapsulation efficiencies higher than 96 % were observed in the O-L/W and O+E-L/W emulsions indicates the successful incorporation of lutein within the oil droplets. On the other hand, only 64 % of encapsulation efficiency was observed for O/W-L emulsion, indicating that lutein was not solely encapsulated within the oil droplets but rather distributed throughout the oil phase, aqueous phase, and/or the emulsion interface. Despite the high lutein degradation during storage observed when it was found in the continuous aqueous phase, the overall lutein degradation of O-L/W and O/W-L emulsions was not significantly different, but smaller compared with O+E-L/W samples. Moreover, the small droplet size observed in the O/W-L emulsion promoted a good stability against phase separation, better than the one observed for the other samples. This indicates that the method used to produce the O/W-L

emulsion may contribute to extending the shelf life of products by maintaining the integrity over time of emulsions containing bioactive molecules. Overall, this study discusses useful insights for using WPI nanoparticles incorporated with lutein to produce lutein-enriched emulsions.

Acknowledgements

We are grateful for the financial support from the CNPq (National Council for Scientific and Technological Development, grant 141708/2018-2), São Paulo Research Foundation (FAPESP, grant 2017/09214-4), Support Fund for Teaching Research and Extension (FAEPEX)/UNICAMP and CAPES (Coordination for the Improvement of Higher Education Personnel).

3.5. References

- Gülseren, I., Fang, Y., & Corredig, M. (2012a). Whey protein nanoparticles prepared with desolvation with ethanol: Characterization, thermal stability and interfacial behavior. *Food Hydrocolloids*, *29*(2), 258–264. <https://doi.org/10.1016/j.foodhyd.2012.03.015>
- Gülseren, I., Fang, Y., & Corredig, M. (2012b). Zinc incorporation capacity of whey protein nanoparticles prepared with desolvation with ethanol. *Food Chemistry*, *135*(2), 770–774. <https://doi.org/10.1016/j.foodchem.2012.04.146>
- Gumus, C. E., Decker, E. A., & McClements, D. J. (2017). Gastrointestinal fate of emulsion-based ω -3 oil delivery systems stabilized by plant proteins: Lentil, pea, and faba bean proteins. *Journal of Food Engineering*, *207*, 90–98. <https://doi.org/10.1016/j.jfoodeng.2017.03.019>
- Ho, K. K. H. Y., Schroën, K., San Martín-González, M. F., & Berton-Carabin, C. C. (2017). Physicochemical stability of lycopene-loaded emulsions stabilized by plant or dairy proteins. *Food Structure*, *12*, 34–42. <https://doi.org/10.1016/j.foostr.2016.12.001>
- Iddir, M., Dingeo, G., Yaruro, J. F. P., Hammaz, F., Borel, P., Schlee, T., Desmarchelier, C., Larondelle, Y., & Bohn, T. (2020). Influence of soy and whey protein, gelatin and sodium caseinate on carotenoid bioaccessibility. *Food & Function*, *11*, 5446–5459. <https://doi.org/10.1039/d0fo00888e>
- Jain, A., Sharma, G., Ghoshal, G., Kesharwani, P., Singh, B., Shivhare, U. S., & Katare, O. P. (2018). Lycopene loaded whey protein isolate nanoparticles: An innovative endeavor for enhanced bioavailability of lycopene and anti-cancer activity. *International Journal of*

- Pharmaceutics*, 546, 97–105. <https://doi.org/10.1016/j.ijpharm.2018.04.061>
- Kotchabhakdi, A., & Vardhanabhuti, B. (2020). Formation of heated whey protein isolate-pectin complexes at pH greater than the isoelectric point with improved emulsification properties. *Journal of Dairy Science*, 103(8), 6820–6829. <https://doi.org/10.3168/jds.2019-17745>
- Lee, S. J., Choi, S. J., Li, Y., Decker, E. A., & McClements, D. J. (2011). Protein-stabilized nanoemulsions and emulsions: Comparison of physicochemical stability, lipid oxidation, and lipase digestibility. *Journal of Agricultural and Food Chemistry*, 59(1), 415–427. <https://doi.org/10.1021/jf103511v>
- Mantovani, R. A., Hamon, P., Rousseau, F., Tavares, G. M., Mercadante, A. Z., Croguennec, T., & Bouhallab, S. (2020). Unraveling the molecular mechanisms underlying interactions between caseins and lutein. *Food Research International*, 138, 109781. <https://doi.org/10.1016/j.foodres.2020.109781>
- Mantovani, R. A., Xavier, A. A. O., Tavares, G. M., & Mercadante, A. Z. (2022). Lutein bioaccessibility in casein-stabilized emulsions is influenced by the free to acylated carotenoid ratio, but not by the casein aggregation state. *Food Research International*, 161, 111778. <https://doi.org/10.1016/j.foodres.2022.111778>
- McClements, D. J. (2007). Critical review of techniques and methodologies for characterization of emulsion stability. *Critical Reviews in Food Science and Nutrition*, 47(7), 611–649. <https://doi.org/10.1080/10408390701289292>
- McClements, D. J., & Li, Y. (2010). Structured emulsion-based delivery systems: Controlling the digestion and release of lipophilic food components. *Advances in Colloid and Interface Science*, 159(2), 213–228. <https://doi.org/10.1016/j.cis.2010.06.010>
- Ochoa Becerra, M., Mojica Contreras, L., Hsieh Lo, M., Mateos Díaz, J., & Castillo Herrera, G. (2020). Lutein as a functional food ingredient: Stability and bioavailability. *Journal of Functional Foods*, 66, 103771. <https://doi.org/10.1016/j.jff.2019.103771>
- Rasera, M. L., de Maria, A. L., & Tavares, G. M. (2023). Co-aggregation between whey proteins and carotenoids from yellow mombin (*Spondias mombin*): Impact of carotenoids' self-aggregation. *Food Research International*, 169, 112855. <https://doi.org/https://doi.org/10.1016/j.foodres.2023.112855>
- Sadeghi, R., Moosavi-Movahedi, A. A., Emam-Jomeh, Z., Kalbasi, A., Razavi, S. H., Karimi, M., & Kokini, J. (2014). The effect of different desolvating agents on BSA nanoparticle properties and encapsulation of curcumin. *Journal of Nanoparticle Research*, 16(9), 2565. <https://doi.org/10.1007/s11051-014-2565-1>

- Santiago, L. A., Fadel, O. M., & Tavares, G. M. (2021). How does the thermal-aggregation behavior of black cricket protein isolate affect its foaming and gelling properties? *Food Hydrocolloids*, *110*, 106169. <https://doi.org/10.1016/j.foodhyd.2020.106169>
- Shen, X., Zhao, C., Lu, J., & Guo, M. (2018). Physicochemical Properties of Whey-Protein-Stabilized Astaxanthin Nanodispersion and Its Transport via a Caco-2 Monolayer. *Journal of Agricultural and Food Chemistry*, *66*, 1472–1478. <https://doi.org/10.1021/acs.jafc.7b05284>
- Teo, A., Lee, S. J., Goh, K. K. T., & Wolber, F. M. (2017). Kinetic stability and cellular uptake of lutein in WPI-stabilised nanoemulsions and emulsions prepared by emulsification and solvent evaporation method. *Food Chemistry*, *221*, 1269–1276. <https://doi.org/10.1016/j.foodchem.2016.11.030>
- Xavier, A. A. O., Mercadante, A. Z., Domingos, L. D., & Viotto, W. H. (2012). Desenvolvimento e validação de método espectrofotométrico para determinação de corante à base de luteína adicionado em iogurte desnatado. *Quimica Nova*, *35*(10), 2057–2062. <https://doi.org/10.1590/S0100-40422012001000028>
- Yi, J., Fan, Y., Yokoyama, W., Zhang, Y., & Zhao, L. (2016). Characterization of milk proteins–lutein complexes and the impact on lutein chemical stability. *Food Chemistry*, *200*, 91–97. <https://doi.org/10.1016/J.FOODCHEM.2016.01.035>
- Yi, J., Lam, T. I., Yokoyama, W., Cheng, L. W., & Zhong, F. (2014). Cellular uptake of β -carotene from protein stabilized solid lipid nanoparticles prepared by homogenization-evaporation method. *Journal of Agricultural and Food Chemistry*, *62*, 1096–1104. <https://doi.org/10.1021/jf404073c>
- Zhao, C., Wei, L., Yin, B., Liu, F., Li, J., Liu, X., Wang, J., & Wang, Y. (2020). Encapsulation of lycopene within oil-in-water nanoemulsions using lactoferrin: Impact of carrier oils on physicochemical stability and bioaccessibility. *International Journal of Biological Macromolecules*, *153*, 912–920. <https://doi.org/10.1016/j.ijbiomac.2020.03.063>
- Zhu, J., Wang, C., Gao, J., Wu, H., & Sun, Q. (2019). Aggregation of Fucoxanthin and Its Effects on Binding and Delivery Properties of Whey Proteins. *Journal of Agricultural and Food Chemistry*, *67*(37), 10412–10422. <https://doi.org/10.1021/acs.jafc.9b03046>

CHAPTER 4 - RESEARCH ARTICLE 2

Title: Compartmentalization of lutein in simple and double emulsions containing protein nanoparticles: effects on stability and bioaccessibility.

Authorship: Lauane Nunes, Negin Hashemi, Sandra Beyer Gregersen, Guilherme M. Tavares, Milena Corredig.

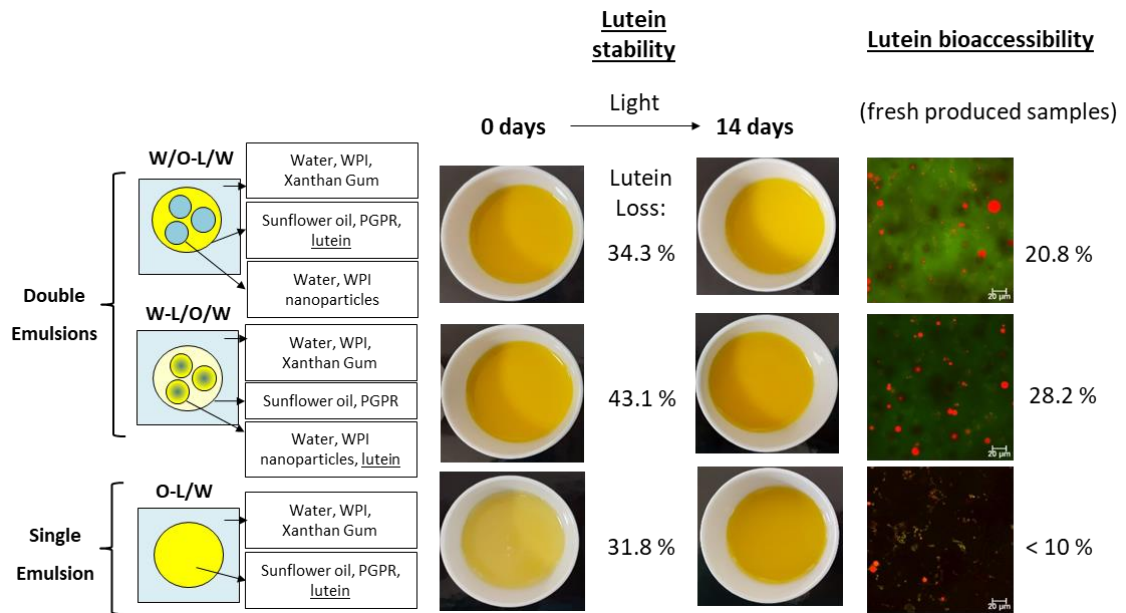
Article published in the Food Research International (IF 2023: 7.425).

The license to reuse this content in the thesis is in Annex 2.

Link for the publication: <https://doi.org/10.1016/j.foodres.2023.113404>

In this study, the impact of lutein localization was extended to water/oil/water double emulsions versus a single oil/water emulsion to evaluate the effects on the stability and *in vitro* bioaccessibility of lutein. Due to the advantages of using desolvation, as discussed in the previous chapter, this method was also incorporated to produce samples studied in this chapter. The inner aqueous phase, which contained whey protein isolate (WPI) nanoparticles obtained by desolvation, was emulsified in sunflower oil stabilized by polyglycerol polyricinoleate (PGPR). The primary emulsion was then emulsified in a continuous aqueous phase containing whey protein isolate (WPI) and xanthan gum. Lutein was incorporated using different strategies: 1) lutein entrapped by WPI nanoparticles using desolvation within the inner water phase of a double emulsion (W-L/O/W); 2) lutein incorporated into the oil phase of the double emulsion (W/O-L/W); 3) lutein incorporated in the oil phase of a single emulsion (O-L/W). The different ways of preparing the emulsions and the location of the lutein in the emulsified systems significantly impacted both lutein chemical stability and bioaccessibility. The W-L/O/W sample showed the lowest lutein stability against light exposure during storage, and the highest lutein bioaccessibility after *in vitro* digestion, for freshly made samples. The incorporation of lutein into the oil phase of the emulsions contributed to the chemical stability of the carotenoid, and beyond that, the high oil fraction may have decreased the extent of incorporation of lutein into the mixed micelles and consequently affected the lutein bioaccessibility.

Graphical abstract



Abstract

Delivery systems designed through protein stabilized emulsions are promising for incorporating carotenoids in different products. Nevertheless, the versatility in structures of such systems raises questions regarding the effect of the bioactive compound localization on their bio-efficacy, in particular for double emulsions. In this context, the aims of this study were to determine the impact of the localization of lutein in different water/oil/water double emulsions versus a single oil/water emulsion on the stability and *in vitro* bioaccessibility of lutein, a lipophilic carotenoid. The inner aqueous phase, which contained whey protein isolate (WPI) nanoparticles obtained by desolvation, was emulsified in sunflower oil stabilized by polyglycerol polyricinoleate (PGPR). The primary emulsion was then emulsified in a continuous aqueous phase containing whey protein isolate (WPI) and xanthan gum, the latter to increase the viscosity of the outer phase and delay creaming. Lutein was incorporated using different strategies: 1) lutein entrapped by WPI nanoparticles within the inner water phase of a double emulsion (W-L/O/W); 2) lutein incorporated into the oil phase of the double emulsion (W/O-L/W); 3) lutein incorporated in the oil phase of a single emulsion (O-L/W). All systems contained similar whey protein concentrations, as well as all other stabilizers. W-L/O/W sample showed the lowest lutein stability against light exposure during storage, and the highest lutein bioaccessibility after *in vitro* digestion, for freshly made samples. Furthermore, the *in vitro* bioaccessibility of lutein incorporated into the single emulsion was considerably lower than those observed for the double emulsions. The results reinforce the importance of designing appropriate structures for delivering improved stability and bioaccessibility of bioactive compounds.

Keywords: INFOGEST protocol, protein nanoparticles, microstructure, double emulsions, carotenoid, delivery systems.

4.1.Introduction

Lutein is a lipophilic natural pigment naturally found in a diversity of fruits and flowers (Rodrigues et al., 2016). This carotenoid cannot be synthesized by the human body, and its regular intake has been associated with benefits for eye health, such as the prevention of age-related macular degeneration and cataracts (Mantovani et al., 2021; Rodrigues et al., 2016). Unfortunately, the amount of lutein consumed through dietary intake is low, raising the opportunity to design foods fortified with this carotenoid, nevertheless, the development of such food products is not a simple task. Lutein has poor water solubility and, is easily susceptible to degradation when exposed to light, oxygen, heat, or humidity (Teo et al., 2017; Zhao et al., 2020). Besides that, the bioaccessibility, and consequently the bioavailability of lutein is also low and variable according to many diet-related factors, such as the food microstructure and composition, which may impair its absorption (Iddir et al., 2020; Mantovani et al., 2022; Mora-Gutierrez et al., 2018). In this scenario, the design of delivery systems based on emulsions shows great potential for improving lutein stability and bioaccessibility (McClements & Li, 2010).

Considering the diversity of emulsified delivery systems which may be used, the benefits of encapsulation of lutein should be evaluated not only in simple oil/water (O/W) emulsions but also in double emulsions which have been proposed as well-suited means to protect compounds prone to oxidation (Marefati et al., 2015). A water/oil/water (W/O/W) double emulsion contains an inner aqueous phase (W), an oil phase (O), and an external continuous aqueous phase (W). Due to the compartmentalized internal structure, double emulsions have some advantages over simple emulsions, for example, in terms of solubilization, protection against chemical degradation, controlled release of different compounds, masking off flavors, production of reduced fat products, and others. Besides that, double emulsions ensure higher encapsulation efficiency of both hydrophilic and lipophilic compounds (Oppermann et al., 2018; Rehman et al., 2020). However, how the localization of the encapsulated bioactive compound on the structure of double emulsions affects its stability and bioaccessibility remains an incipiently addressed question for most bioactive compounds of interest.

Surfactants, proteins, and other hydrocolloids are the main molecules applied as interface stabilizers in double emulsion systems (McClements & Li, 2010). High molecular weight synthetic emulsifiers such as polyglycerol polyricinoleate (PGPR) are effective in stabilizing the internal W/O droplets in double emulsions. Whey protein isolate (WPI)

nanoparticles can also be used to encapsulate hydrophobic molecules and show surface activity (Gülseren et al., 2012; Iddir et al., 2020; Jain et al., 2018; Oppermann et al., 2018; Shen et al., 2018). In addition to the emulsifying properties of WPI, these proteins have been shown to be able to incorporate hydrophobic components when WPI nanoparticles are prepared by the solvent evaporation method that consists of adding a desolvating agent such as ethanol drop by drop into the protein dispersion, then subsequently removing the organic solvent by evaporation (Gülseren et al., 2012; Sadeghi et al., 2014).

In this study, we provide an understanding of the influence of lutein localization in different emulsion systems, with a similar composition, but with very different structures. The effect of the incorporation of lutein in WPI nanoparticles in the internal aqueous phase was compared to the presence of lutein in the oil phase of the double emulsions. Furthermore, a simple emulsion model was also used as a control. In addition to evaluating the stability of the carotenoid in the presence of light, the fate of the lutein and its bioaccessibility, defined as the amount present in the micellar phase, was assessed in the different emulsified systems after the gastric and intestinal stages of *in vitro* digestion following the INFOGEST protocol (Brodkorb et al., 2019; Minekus et al., 2014). To the best of our knowledge, the impact of lutein localization in double emulsions on its chemical stability has yet to be addressed. Furthermore, the difference in the *in vitro* bioaccessibility of this carotenoid using different emulsion structures is unknown, albeit critical in designing optimal oral delivery systems.

4.2. Material and methods

4.2.1. Materials

PGPR 4150 (Palsgaard A/S, Juelsminde, Denmark), whey protein isolate (WPI, 90 % of protein, MyProtein, Magnice, Poland), ethanol absolute (Merck Millipore, Darmstadt, Germany), sunflower oil (Local market, Aarhus, Denmark), lutein (Pharmaceutical Secondary Standard, Merck Millipore, Darmstadt, Germany) and sodium azide (Sigma-Aldrich, Darmstadt, Germany) were used for preparing the emulsions. All emulsions were formulated to contain similar concentrations of PGPR, WPI, and lutein, and to have comparable physical properties. Xanthan gum (XG, Molekymi, Dragør, Denmark) was also added to the outer water phase of all emulsions to delay creaming. Analytical grade solvents (Sigma-Aldrich, Darmstadt, Germany) were used for lutein extraction. The enzymes used during the *in vitro* digestion were pepsin from porcine gastric mucosa (P7000) and pancreatin from porcine pancreas (P7545). Bile extract porcine (B8631) was used in the intestinal phase considering

an average molecular weight of $408.6 \text{ g}\cdot\text{mol}^{-1}$. All the reagents and enzymes used in the *in vitro* digestion were acquired from Sigma-Aldrich (Sigma-Aldrich, Darmstadt, Germany).

4.2.2. Preparation of emulsions

Three different water/oil/water double emulsions were prepared by applying a two-step emulsification procedure. The inner aqueous phase of all double emulsions contained WPI particles obtained by desolvation using ethanol, the oil phase was composed of sunflower oil added with PGPR, while the outer aqueous phase contained WPI and xanthan gum. The first double emulsion, referred to as W/O/W, did not contain lutein. The second double emulsion, referred to as W/O-L/W, contained lutein, which was added to the oil phase. The third double emulsion, referred to as W-L/O/W, also contained lutein in the same final concentration as the previous one, but it was entrapped by the WPI nanoparticles during the desolvation process. A simple oil-in-water emulsion containing lutein was also produced as an additional control.

4.2.2.1. Inner aqueous phase

To prepare the inner aqueous phase of emulsions, ethanol was added drop-by-drop to 2 % $\text{w}\cdot\text{w}^{-1}$ of WPI at a ratio of 1:1 by volume, with subsequent removal of the solvent by rotary evaporation (Buchi, Flawil, Switzerland) under reduced pressure at a temperature below $35 \text{ }^{\circ}\text{C}$ (Jain et al., 2018; Sadeghi et al., 2014). For lutein-loaded nanoparticles, lutein was first solubilized in ethanol and then added to the WPI solution as extensively described (Jain et al., 2018; Sadeghi et al., 2014). In this case, the final WPI suspension contained 0.002 % $\text{w}\cdot\text{w}^{-1}$ lutein after the evaporation step.

4.2.2.2. Emulsification

In the first emulsification step, the inner aqueous phase was slowly added to sunflower oil containing 4 % $\text{w}\cdot\text{w}^{-1}$ PGPR at a ratio of 1:9 $\text{w}\cdot\text{w}^{-1}$, followed by mixing using a shear homogenizer (Ultra-Turrax T25, Ika, Germany) at 20,500 rpm for 2 min to produce coarse emulsions, which were subjected to high-pressure homogenization (Avestin Emulsiflex C5, Ata Scientific Instruments, Caringbah, Australia) at 750 bar for 3 cycles. In the case of W/O-L/W, 0.002 % $\text{w}\cdot\text{w}^{-1}$ lutein was added to the oil phase and stirred until it was completely dissolved before the emulsification step. For the second emulsification step, the primary water in oil emulsions was added dropwise into the outer aqueous phase containing 2 % $\text{w}\cdot\text{w}^{-1}$ WPI

and 0.5 % w.w⁻¹ xanthan gum at a ratio of 2:8 w.w⁻¹, followed by emulsification using a shear mixer Ultra-Turrax at 8,000 rpm/1 min.

A simple oil-in-water emulsion containing lutein was also produced as a control. This emulsion, referred to as O-L/W was prepared by dispersing lutein 0.002 % w.w⁻¹ in sunflower oil with 4 % w.w⁻¹ PGPR, then, the oil phase was emulsified in the aqueous phase prepared with 2 % w.w⁻¹ of the WPI and 0.5 % w.w⁻¹ xanthan gum, at a ratio of 1.8:8.2 w.w⁻¹ using a high-speed disperser at 8,000 rpm for 1 min.

Aqueous phase containing WPI and XG were prepared by dispersing them in Milli-Q water (pH 7.0). Although the physical stability of the emulsion was not within the scope of this work, xanthan gum was added to these emulsions to increase the continuous phase viscosity and delay extensive creaming during storage. Sodium azide 0.02 % w.w⁻¹ was also added to the mixture to inhibit microbial growth. The mixture was continuously stirred at 100 rpm overnight to ensure hydration (Boonlao et al., 2020). All treatments were prepared in duplicates.

4.2.3. Particle size

The mean droplet size of the WPI nanoparticles and primary emulsions was measured by dynamic light scattering (DLS) using a Zetasizer (Malvern Instruments, Worcestershire, UK) model ZSU3100 with the software ZS explorer version 2.0.0.98. For this, the primary emulsion was diluted 50-fold with sunflower oil containing 4 % w.w⁻¹ of PGPR, then, 1 mL of diluted samples was transferred into the measuring cell and analyzed at a wavelength of 633 nm at a backscattering angle of (90°) at 25 °C, using the refractive indices of 1.46 for the oil and 1.33 for the water (Eisinaite et al., 2018; Shen et al., 2018). Each sample was analyzed in triplicate, and the particle size was expressed as average hydrodynamic diameter (nm).

Droplet sizes of secondary and simple emulsions were measured using a static light scattering instrument (Mastersizer 2000, Malvern Instruments, Worcestershire, UK). Enough sample to generate turbidity readings was added to the liquid analysis module tank with water at room temperature (25 °C). The refractive index (RI) values applied for the droplets (sunflower oil) and the dispersant (distilled water) were 1.46 and 1.33, respectively (Eisinaite et al., 2018; Oppermann et al., 2018). The particle size was measured for freshly produced emulsions and after 14 days of storage. The resulting data was presented as particle size distribution, or the volume-weighted average diameter ($D_{4,3}$) of three analyses.

4.2.4. Rheological behavior

The amount of 20 mL of each emulsion was carefully transferred to a flat-bottomed cylindrical glass tube (diameter 25 mm). The tube was immediately placed in the sample chamber of the Rheolaser at 25 °C and the emulsions were measured for 40 min. The instrument measures the change in multiple scattering of the sample under quiescent conditions (Xu et al., 2017). The mean square displacement (MSD) vs. decorrelation time (τ) curves and macroscopic viscosity index (MVI) parameters of the samples were obtained by using the software RheoSoft Master 1.4.0.10 (Xu et al., 2017).

4.2.5. Lutein encapsulation efficiency

Emulsion (1 g) was mixed with 4 mL of tetrahydrofuran (THF) and stirred for 1 minute, then, the extracts were then transferred to a separatory funnel containing 20 mL of ethyl ether and petroleum ether (1:1 v.v⁻¹) and washed with distilled water. The ether phase was collected and dried on a rotary evaporator (temperature < 35 °C), then the extract was dissolved in ethanol and the absorbance was measured at 445 nm with a UV-1700 spectrophotometer (Shimadzu, Duisburg, Germany). Similarly, lutein was also extracted from the cream phase, obtained after centrifugation of an aliquot (1 g) of the same emulsion at 17,400 g for 15 min as previously described (Chen et al., 2020; Zhao et al., 2020).

The lutein concentration was calculated according to the Lambert-Beer law following the equation:

$$[L] = \frac{10^4 \times A_{445} \times DF}{E_{(1\%, 1\text{cm})} \times d} \quad \text{Eq. 4.1}$$

where [L] is the concentration of lutein expressed as $\mu\text{g}\cdot\text{g}^{-1}$; A_{445} : lutein absorbance at 445 nm in ethanol; DF: dilution factor; $E_{(1\%, 1\text{cm})}$: the absorptivity coefficient of lutein in ethanol (2550 $1\%, 1\text{cm}$) (Craft & Soares, 1992); d: the optical path (1 cm) (Xavier et al., 2012).

The encapsulation efficiency (EE) was defined as the total mass of lutein extracted from the initial emulsion (L_{e0}), and the amount of lutein extracted from the oil phase obtained after centrifugation (L_c) using the following equation:

$$EE (\%) = \frac{L_c}{L_{e0}} \times 100 \% \quad \text{Eq. 4.2}$$

4.2.6. Lutein stability

Freshly prepared emulsions (25 mL) were placed into glass tubes and stored for 14 days in a light incubator with an LED sunlight lamp (33,340 lx) at 24 °C. The tubes were placed at a distance of about 70 cm from the lamp. The concentration of lutein, the color

difference (chroma), and the particle size of emulsions were measured at the end of storage as described below, to be compared with values obtained before incubation (Zhao et al., 2020).

4.2.6.1. Lutein loss

The loss of lutein was then calculated as a ratio of the amount of lutein recovered in the emulsion after 14 days (L_{e14}) and that of the initial emulsion (L_{e0}) according to the following equation:

$$\text{Lutein loss (\%)} = \frac{L_{e14}}{L_{e0}} \times 100 \% \quad \text{Eq. 4.3}$$

4.2.6.2. Color

The color of emulsions was measured using a portable colorimeter (CR-400, Konica Minolta, Japan) according to the color parameters L^* , a^* and b^* . The emulsion samples were gently stirred before measurement and then poured into the measurement cup. The color difference was assessed by incorporating the different color parameters into the following equation:

$$\Delta E^* = \sqrt{(L^* - L_0^*)^2 + (a^* - a_0^*)^2 + (b^* - b_0^*)^2} \quad \text{Eq. 4.4}$$

where ΔE^* is the color difference; L^* , a^* , and b^* are the lightness, red-green value, and yellow-blue value of the emulsions after storage of 14 days; and L_0^* , a_0^* , and b_0^* are the equivalent color parameters before the storage, respectively (Teo et al., 2017; Zhao et al., 2020).

4.2.7. *In vitro* digestion

Emulsions containing lutein were subjected to an *in vitro* digestion based on the INFOGEST consensus protocols (Brodkorb et al., 2019; Minekus et al., 2014). The composition of the Simulated Salivary Fluid (SSF), Simulated Gastric Fluid (SGF), and Simulated Intestinal Fluid (SIF) was prepared as described by Brodkorb et al., (2019).

The enzyme activities were experimentally determined as described by the INFOGEST 2.0 protocol (Brodkorb et al., 2019). Pepsin solution had 498.5 U.mg⁻¹ of pepsin activity and was added to achieve an activity of 2,000 U.mL⁻¹ in the final digestion mixture. While pancreatin had 2.33 U.mg⁻¹ and 55.5 ± 2.2 U.mg⁻¹ of trypsin and lipase activity, respectively, it was added to achieve an activity of 100 U.mL⁻¹ of trypsin activity in the final mixture and this was enough to achieve 2,382 U.mL⁻¹ of lipase activity being the recommended 2,000 U.mL⁻¹ (Brodkorb et al., 2019). No additional pancreatic lipase was

added. Furthermore, bile extract was added based on weight, to reach a final concentration of 10 mM, considering an average molecular weight of $408.6 \text{ g}\cdot\text{mol}^{-1}$.

For the oral phase, 5 g of sample, 4 mL of SSF ($\text{pH } 7.0 \pm 0.1$), 25 μL of 0.3 M CaCl_2 , and ultrapure water to reach 10 mL were incubated at 37°C under stirring for 2 min. For the gastric phase, 8 mL of SGF ($\text{pH } 3.0 \pm 0.1$), 0.5 mL of pepsin solution made up in SGF, and 5 μL of 0.3 M CaCl_2 were added, the pH was adjusted to 3.0 ± 0.1 with 1 M HCl and the volume was completed to 20 mL with ultrapure water. The mixture was incubated at 37°C under stirring for 2 h and afterward cooled in an ice bath. To simulate the intestinal conditions, 8.5 mL of SIF stock solution ($\text{pH } 7.0 \pm 0.1$), 5 mL of pancreatin solution made up of SIF, 40 μL of 0.3 M CaCl_2 and 2.5 mL of bile extract solution made up of SIF were added to the gastric chyme. The pH was adjusted to 7.0 ± 0.1 with 1 M NaOH and the final volume was further completed to 40 mL with purified water. The mixture was incubated at 37°C for 2 h under stirring; afterward, the resultant chyme was immediately cooled in an ice bath.

4.2.8. Lutein recovery and bioaccessibility

The lutein recovery and bioaccessibility were determined according to previous studies (Mantovani et al., 2022; Rodrigues et al., 2016). Recovery was expressed as the amount of carotenoid recovered in the chyme relative to that in the samples before digestion. This parameter is important for understanding the fate of lutein during digestion. Bioaccessibility was also evaluated, as the ratio between the amount of carotenoid in the micellar fraction and its respective amount in the sample before digestion. Immediately after *in vitro* digestion, aliquots (5 mL) of chyme were subjected to solvent extraction to quantify the lutein, as described above to estimate lutein's recovery. The remaining chyme (35 mL) was centrifuged (20,000 g at 4°C for 10 min) (Sigma 4-16K, 12169-H Rotor, Germany) to separate the micellar fraction from the insoluble material. Lutein was then extracted and quantified in the micellar fraction, to estimate lutein's bioaccessibility.

Lutein was exhaustively extracted from the chyme and the micellar phase with diethyl ether as previously described (Rodrigues et al., 2016). Organic and aqueous phases were separated in a separation funnel and the aqueous phase with the remaining carotenoids was re-extracted until the extract became colorless. The lutein concentration was then calculated using Eq. 4.1.

The supernatant (micellar aqueous phase) resulting from the centrifugation of the chyme, was exhaustively extracted with diethyl ether in the same way for the chyme. So, bioaccessibility was calculated as the ratio between the amount of carotenoid in the micellar

aqueous phase (supernatant) and its amount in the undigested emulsion, according to the equation:

$$\text{Bioaccessibility (\%)} = \left(\frac{\text{Carotenoid content}_{\text{micellar fraction}}}{\text{Carotenoid content}_{\text{emulsion}}} \right) \times 100 \quad \text{Eq. 4.5}$$

4.2.9. Confocal microscopy

Confocal microscopy of emulsions was carried out at room temperature with a confocal laser scanning microscope (Nikon C2, Nikon Instrument Inc, Tokyo, Japan) using a 60× objective. The samples were dyed with Nile red and fluorescent isothiocyanate (FITC) dissolved in acetone to a concentration of 0.01% w.w⁻¹ to stain fat and proteins, respectively. A small droplet of the dye solutions was placed on a glass slide, allowing the acetone to evaporate before adding the sample, which was left for a minimum of 20 min before visualization. Laser of 488 nm and 561 nm were used for excitation and at least 5 representative images of the emulsions were taken (Grasberger et al., 2021; Iddir et al., 2020).

4.2.10. Protein hydrolysis

The extent of protein hydrolysis was estimated by measuring the level of free amino-terminals using the o-phthaldialdehyde (OPA) spectrophotometric assay (Mulet-Cabero et al., 2017). All the digested samples were pretreated with 5 % trichloroacetic acid (TCA) and centrifuged at 13,000 g for 20 min at 4 °C, to precipitate the insoluble fraction. The supernatant (10 µL) was then added to each well and mixed with 200 µL of freshly prepared OPA. In brief, the reaction was allowed to proceed at 22 °C for 15 min, and then the absorbance was measured at 340 nm using a spectrophotometer (SynergyTM Mx, BioTek, Winooski, VT, USA). A calibration curve was made using different concentrations of L-glutamic acid treated with OPA reagent similarly as for samples. The level of free amino-terminals in the samples was expressed as L-Glutamine equivalents (mmol) per g of protein.

The protein concentration in the fully digested samples was also determined using Pierce BCA Protein Assay Kit (23227 and 23225, Thermo Fisher Scientific, USA). Then 25 µL of the sample was added and mixed with 200 µL of BCA-reagent in each well and incubated at 37 °C for 30 min. The absorbance was measured at 562 nm, and concentration was determined based on a calibration curve made using BSA.

4.2.11. Lipid hydrolysis

Fatty acid release during digestion was determined by colorimetric method using a Free Fatty Acid Quantitation Kit (MAK044, Sigma-Aldrich, St. Louis, USA). The chyme (1 mL) was extracted with 1 mL of chloroform and 0.1 % of triton X-100, vortexed for 15 min, and centrifuged at 13,000 g for 10 min. The supernatant was collected and transferred to a heating block at 50 °C in a fume hood to evaporate the chloroform. The dry pellet was dissolved 100x in FFA assay buffer, then 25 µL of the diluted samples were transferred to the plate and completed with 25 µL of FFA assay buffer. 2 µL of ACS reagent was added to each sample and standard well and incubated for 30 minutes at 37 °C. Afterward, 50 µL of the master reaction mix was added to each of the wells, mixed, and incubated for another 30 minutes at 37 °C with protection from the light. The concentration of free fatty acids was obtained from the absorbance measured at 570 nm and by reference to a standard curve prepared using palmitic acid, with concentrations ranging from 2 to 10 mM.

4.2.12. Statistics

The experiments and analysis were carried out in triplicate and the results were reported as the mean \pm standard deviation. Analysis of variance (ANOVA) and Tukey's test was performed using the statistical program R, version 4.0.2. (R Foundation for Statistical Computing, Vienna, Austria) with a level of significance of $p < 0.05$.

4.3. Results

4.3.1. Emulsion stability

Whey protein nanoparticles were obtained by ethanolic desolvation and their hydrodynamic diameter was about 150 ± 4 nm (Figure 4.1), as measured by dynamic light scattering. In the presence of lutein, the particle size distribution measured by light scattering showed a second larger peak, indicating the presence of some insoluble lutein aggregates. The nanoparticle suspensions were then employed as the inner phase of the primary W/O emulsion, using high-pressure homogenization.

The average hydrodynamic diameter of the primary W/O emulsions, measured by DLS, and the average diameter ($D_{4,3}$) of the final W/O/W emulsions measured by static light scattering are displayed in Table 4.1. The average size of the primary emulsions was around 260 nm, although slightly larger for the primary emulsions containing lutein nanoparticles.

All emulsions had a similar bimodal size distribution, consisting of two populations, one with diameters between 10 and 50 µm and a larger population with a diameter of peak at

around 200 μm . This was caused by the second emulsification process, designed to create large oil droplets, able to encapsulate the primary emulsions. All emulsions had a similar average size, although slightly larger in the case of W-L/O/W, and slightly smaller for W/O-L/W. The similarity in the initial size of the emulsions will facilitate their comparison between treatments in the *in vitro* digestion experiments.

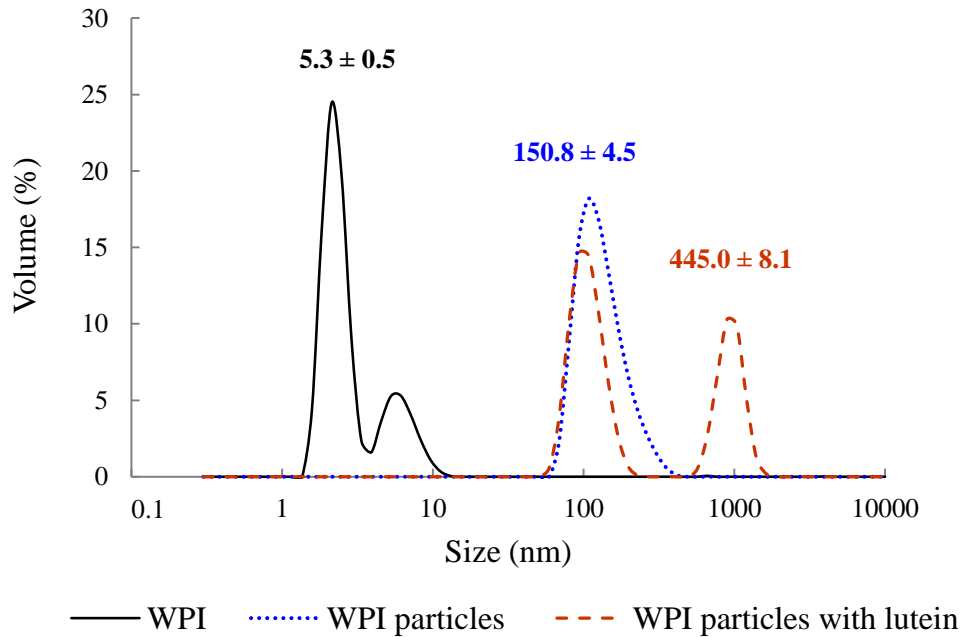


Figure 4.1- Particle size distribution and average hydrodynamic diameter of WPI, WPI particles and WPI particles prepared in the presence of lutein of W-L/O/W measured by DLS. W-L/O/W emulsions with lutein-loaded WPI nanoparticles in the water phase of the primary emulsion.

Table 4.1- Average hydrodynamic diameter measured by dynamic light scattering for primary emulsions, and $D_{4,3}$ average measured by static light scattering of the final emulsions. Different letters indicate statistically significant differences ($p < 0.05$) within a column. W/O/W emulsion control; W/O-L/W emulsion with lutein in the oil phase and WPI nanoparticles in the water phase of the primary emulsion; W-L/O/W emulsions with lutein-loaded WPI nanoparticles in the water phase of the primary emulsion; O-L/W simple emulsion system control containing lutein in the oil phase.

Samples	Primary emulsion (nm)	Final emulsion (μm)
W/O/W	256 ± 4^b	44 ± 2^b
W/O-L/W	258 ± 4^{ab}	40 ± 2^c
W-L/O/W	266 ± 6^a	49 ± 2^a
O-L/W	-	41 ± 2^{bc}

Differences in the emulsions colloidal stability were probed under quiescent conditions using diffusive wave spectrometry. The change in MSD and viscosity index measured over time are shown in Figure 4.2. Double emulsions showed an initial linear behavior followed by a bend in the MSD, when they reached arrested motion (Figure 4.2A). This demonstrated that the particles were slow diffusing, as these decorrelation times are relatively long. There was a clear difference in the MSD behavior between the double emulsions containing lutein (W/O-L/W and W-L/O/W) compared to the W/O/W control, or the single O-L/W emulsion. This difference would suggest a slower diffusivity for the latter treatment. This could suggest an interaction between the carotenoid pigment with the emulsifiers used. Figure 4.2B illustrates the difference in the viscosity parameter (MVI) measured for about 40 min, at zero shear. This parameter also demonstrated that the emulsions were different also in terms of their viscosity, with the double emulsions containing lutein (W/O-L/W and W-L/O/W) showing a lower viscosity index. This may indicate a faster flocculation of these emulsions compared to the two control samples. As these emulsions were prepared with the same concentration of components, these properties were imparted by their interactions. This was not further explored as outside the scope of this research.

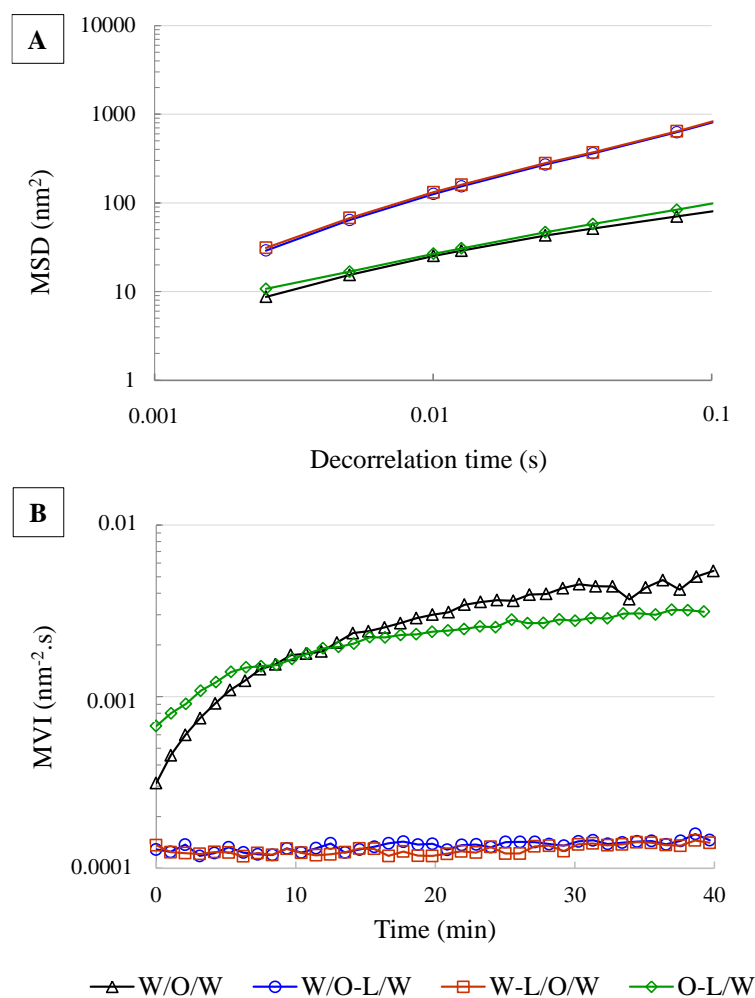


Figure 4.2- A) Mean squared displacement of the emulsion droplets and B) Macroscopic viscosity index as a function of time for the various W/O/W emulsions, measured using the Rheolaser under quiescent conditions. W/O/W emulsion control; W/O-L/W emulsion with lutein in the oil phase and WPI nanoparticles in the water phase of the primary emulsion; W-L/O/W emulsions with lutein-loaded WPI nanoparticles in the water phase of the primary emulsion; O-L/W simple emulsion system control containing lutein in the oil phase.

4.3.2. Lutein stability

The amount of lutein was quantified in the fresh emulsions as well as during storage (Table 4.2). In all initial emulsions, lutein was present in the same concentration range (18 - 20 $\mu\text{g}\cdot\text{g}^{-1}$). All double emulsions showed a high encapsulation efficiency (> 99 %) regardless the lutein location (in the inner water droplets, or in the oil phase). The results suggest lower encapsulation efficiency for the single emulsion (94 %).

Table 4.2- Amount of lutein measured in fresh emulsions, as well as after storage for 14 days under light. The encapsulation efficiency of the fresh emulsions is also shown. Different letters indicate statistically significant differences ($p < 0.05$) within a row. W/O-L/W emulsion with lutein in the oil phase and WPI nanoparticles in the water phase of the primary emulsion; W-L/O/W emulsions with lutein-loaded WPI nanoparticles in the water phase of the primary emulsion; O-L/W simple emulsion system control containing lutein in the oil phase.

Analysis		W/O-L/W	W-L/O/W	O-L/W
Lutein stability	Lutein in emulsion ($\mu\text{g}\cdot\text{g}^{-1}$)	18.8 ± 0.1^a	19.9 ± 0.1^a	18.3 ± 2.9^a
	Encapsulation efficiency (%)	99.4 ± 0.1^a	99.3 ± 0.1^a	94.0 ± 0.6^b
	Lutein in emulsion (14 days) ($\mu\text{g}\cdot\text{g}^{-1}$)	12.3 ± 0.1^a	11.3 ± 0.1^a	12.4 ± 1.8^a
	Lutein loss (%) (14 days)	34.3 ± 0.3^b	43.1 ± 0.8^a	31.8 ± 0.6^b

The amount of remaining lutein after 14 days of storage under light is also shown in Table 4.2, with the respective % of lutein loss during storage. Lowest values were observed for the emulsions prepared by dispersing lutein into the oil phase (W/O-L/W and O-L/W), with the greatest loss for W-L/O/W (43 %). This could be related to a protective effect of the oil and/or PGPR for the chemical stability of lutein. This happens because when dispersed in water, carotenoids tend to form aggregates due to their high hydrophobicity. For lutein, free hydroxyl groups at both ends of the molecule promoted the formation of strongly coupled (H-type) aggregates due to the formation of intermolecular hydrogen bonds (Mantovani et al., 2020).

The stability of the emulsions to storage was also assessed by evaluating the color change over time. Figure 4.3 shows the visual appearance of the fresh emulsions, and after 14 days of storage under light. In addition, the changes in yellow color index (b^*) are also shown. The fresh O-L/W emulsion appeared less yellow initially, possibly due to a larger population of smaller droplets, however, it was the one with the largest color difference after storage. The double emulsions were more yellow at start, but they showed a smaller change after storage. The aggregation state of lutein is known to impact the color in food products (Schex et al., 2020). It is important to point out that the O-L/W emulsion also showed a 37% reduction in particle size after 14 days under light, which may contribute to explain the significant color difference observed for this sample, while no changes in the particle size of the other emulsions were observed over storage (data not shown).

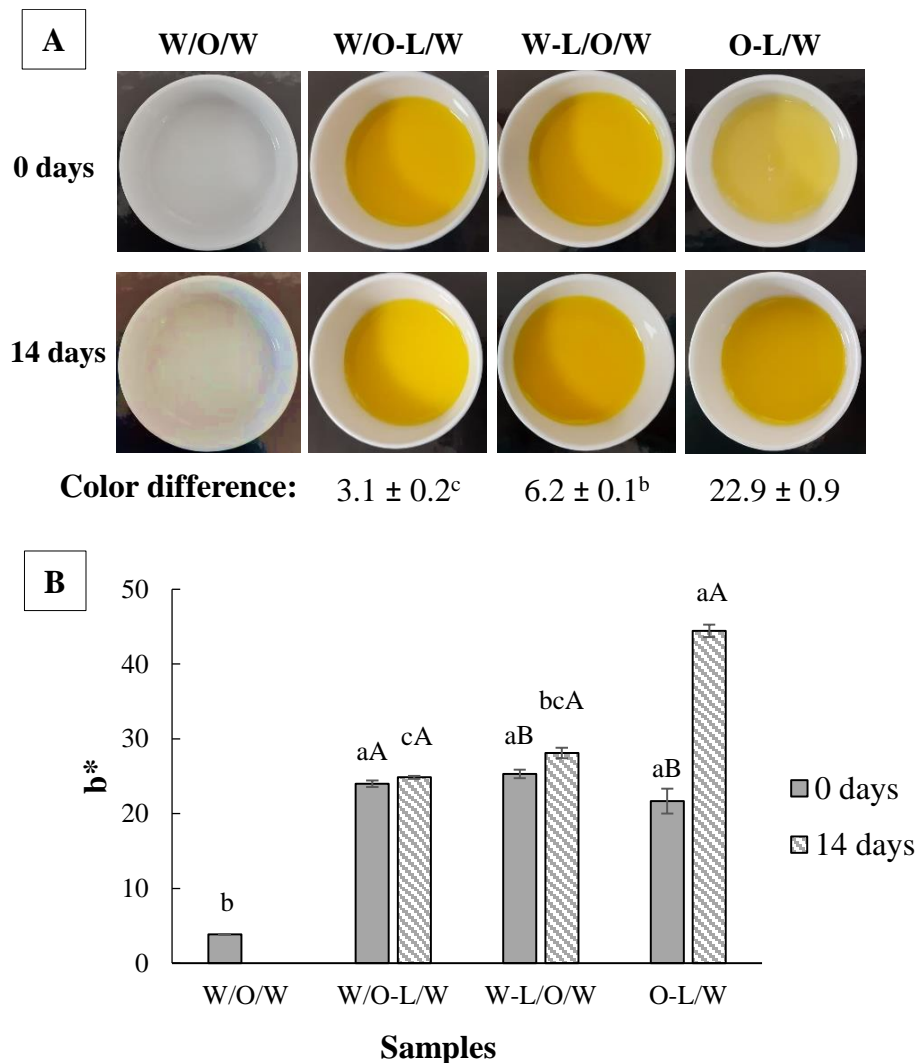


Figure 4.3- A) Visual appearance and color difference (calculated from the difference in color parameters L^* , a^* and b^* values before and after storage under light at 33,340 lx and 24 °C). B) b^* color parameter in fresh emulsions, as well as after 14 days of storage under light. Capital letters indicate statistically significant values within a treatment, while small letters indicate significant difference between treatments ($p < 0.05$). W/O/W emulsion control; W/O-L/W emulsion with lutein in the oil phase and WPI nanoparticles in the water phase of the primary emulsion; W-L/O/W emulsions with lutein-loaded WPI nanoparticles in the water phase of the primary emulsion; O-L/W simple emulsion system control containing lutein in the oil phase.

4.3.3. *In vitro* digestion

Through confocal microscopy (Figure 4.4) it is possible to visualize the evolution of the microstructure of the various emulsions. Samples before digestion showed large droplets,

as expected, confirming the particle size distribution data. It was possible to still detect the presence of oil droplets after digestion, but much less in number and only very few could be seen in the intestinal stage, suggesting extensive digestion for all treatments. The images would suggest the presence of more oil droplets in the double emulsions than in the single O-L/W emulsion after intestinal digestion. Constituents from the emulsions or the gastrointestinal tract fluids are present in the digesta and assemble into different types of colloidal particles with different dimensions, morphologies, and aggregation states. This is more susceptible to occur during the intestinal phase, the stage where lipid digestion takes place (Gasa-Falcon et al., 2017; Gumus et al., 2017; Zhang et al., 2015).

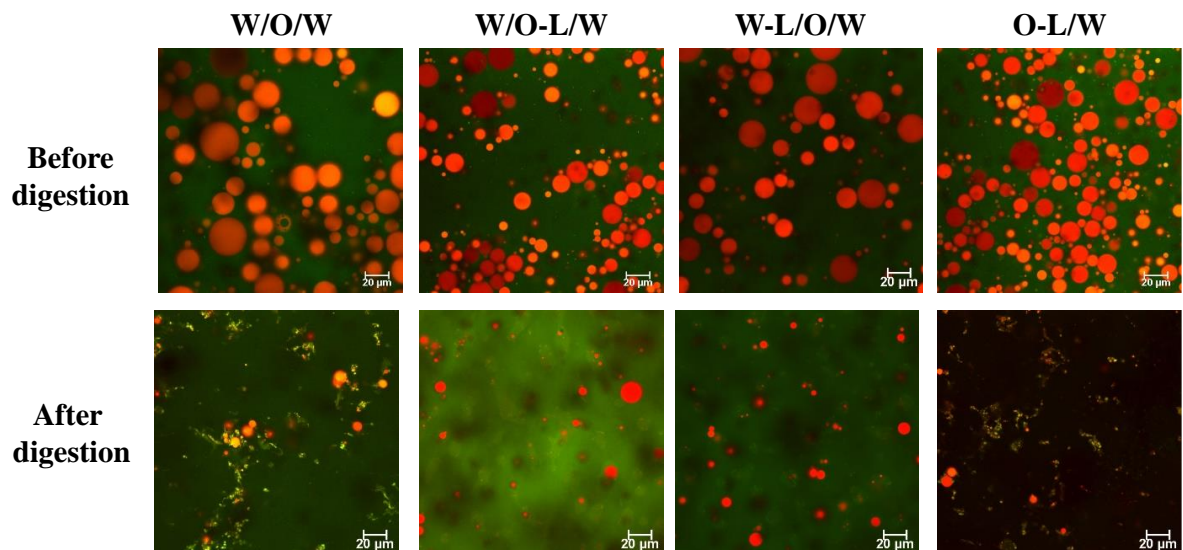


Figure 4.4- Representative confocal microscopy images of emulsions before and after digestion. Lipids were labelled with Nile red (red color), and proteins were labelled with FITC (green color). The white bar indicates 20 μm . W/O/W emulsion control; W/O-L/W emulsion with lutein in the oil phase and WPI nanoparticles in the water phase of the primary emulsion; W-L/O/W emulsions with lutein-loaded WPI nanoparticles in the water phase of the primary emulsion; O-L/W simple emulsion system control containing lutein in the oil phase.

Figure 4.5 shows the results of the free N-terminals and free fatty acids of emulsions after digestion. The W/O/W control emulsion displayed the highest amount of free amino acids after digestion, but also the lowest concentration of free fatty acids compared with the other samples, which did not significantly differ between each other for these parameters. The decrease in the lipolysis rate for W/O/W can be related to the aggregation of the digestion

products or remaining peptide chains formed at the interface of the oil droplets, since the generated peptides strongly affected the stability of the emulsions dictating the resulting size of lipid droplets (Iddir et al., 2019; Qazi et al., 2021). The lower level of free amino acids for all samples containing lutein, may suggest that interaction with the hydrophobic moieties of the proteins affects the amino acid release.

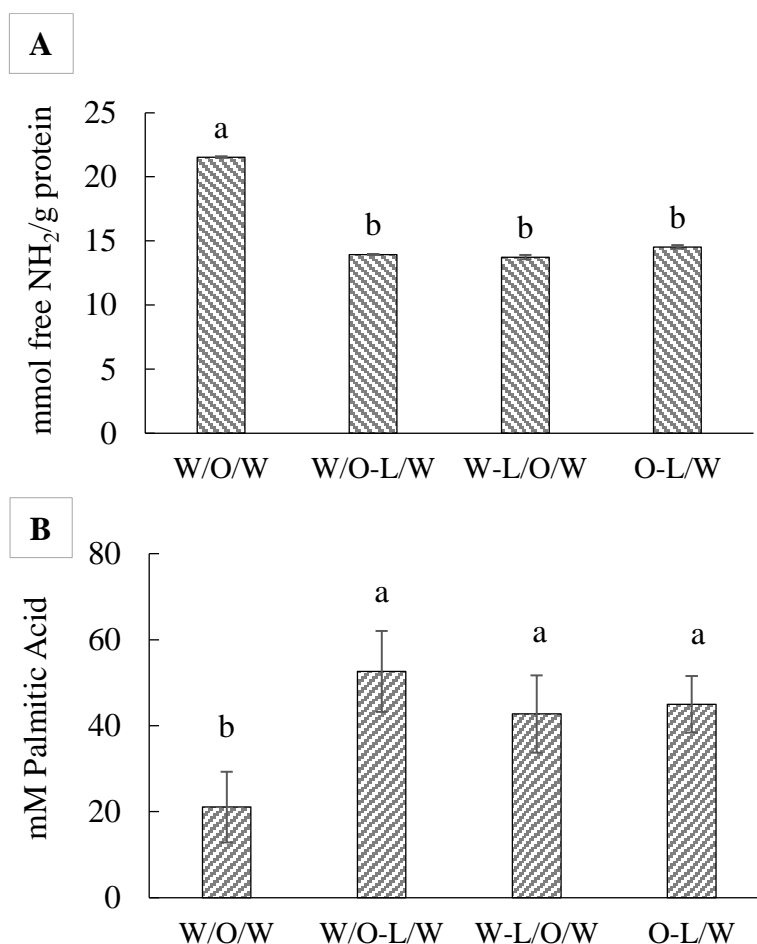


Figure 4.5- A) Free amino acids released after *in vitro* intestinal digestion expressed as L-glutamine equivalents (mM) per g of protein and B) Free fatty acids of emulsions after digestion expressed as palmitic acid equivalents (mM). The values with the same letter did not differ significantly ($p < 0.05$). W/O/W emulsion control; W/O-L/W emulsion with lutein in the oil phase and WPI nanoparticles in the water phase of the primary emulsion; W-L/O/W emulsions with lutein-loaded WPI nanoparticles in the water phase of the primary emulsion; O-L/W simple emulsion system control containing lutein in the oil phase.

The amount of lutein recovered and its bioaccessibility after *in vitro* digestion are shown in Table 4.3. No differences in lutein recovery were noticed between the double

emulsions (W/O-L/W and W-L/O/W), which displayed values close to 99 % after digestion. On the other hand, O-L/W displayed a slight loss after *in vitro* digestion of the fresh emulsion, showing a recovery of around 90 %. These results demonstrated that lutein was more prone to degradation during gastrointestinal transit when incorporated into simple O-L/W emulsions compared with double emulsions, regardless of its location. These values of lutein recovery are significantly higher than those reported in the literature, and could be attributed to the high oil fraction used in this study, which may have had a protective effect against lutein degradation during the *in vitro* digestion (Mantovani et al., 2022).

Table 4.3- Recovery and bioaccessibility after *in vitro* digestion. Different letters indicate statistically significant differences ($p < 0.05$) within a row. W/O-L/W emulsion with lutein in the oil phase and WPI nanoparticles in the water phase of the primary emulsion; W-L/O/W emulsions with lutein-loaded WPI nanoparticles in the water phase of the primary emulsion; O-L/W simple emulsion system control containing lutein in the oil phase.

	Analysis	W/O-L/W	W-L/O/W	O-L/W
After <i>in vitro</i> digestion	Recovery (%)	99.9 ± 0.1 ^a	98.7 ± 1.5 ^a	90.3 ± 4.5 ^b
	Bioaccessibility (%)	20.8 ± 1.1 ^b	28.2 ± 0.2 ^a	< 10 ^c

In addition to the recovery of lutein in the digesta, the bioaccessibility of this component was assessed in the digested samples. The bioaccessibility was defined as the amount of lutein recovered in the digesta supernatants, in other words, how much lutein was incorporated into mixed micelles. The results clearly showed that a higher bioaccessibility was observed for the double emulsions (W/O-L/W and W-L/O/W) compared to simple emulsion, with the highest in the case of the lutein incorporated in the water phase with the WPI nanoparticles (W-L/O/W). In line with the low lutein recovery in the digesta, around 10 % of lutein bioaccessibility was observed for O-L/W sample. It is important to note that despite the lower lutein stability against light exposure observed during storage for W-L/O/W (Table 4.2), this sample displayed the highest lutein bioaccessibility after *in vitro* digestion. The increased bioaccessibility may be due to the presence of complex mixed micelles also containing breakdown products interacting with lutein molecules (peptides/lutein and lutein/PGPR).

The lutein bioaccessibility after *in vitro* digestion reported in our study is lower than that reported earlier by Mantovani et al., (2022) for casein-stabilized simple emulsions. The authors reported lutein bioaccessibilities close to 40 % when lutein was incorporated into the

emulsions on its free form (non-esterified). A reason for the discrepancy could be the low oil fraction of the emulsions produced by Mantovani et al., (2022) (2 % w.w⁻¹) compared to the higher level used in the present study. It is essential to highlight that lutein was still recovered in the digesta and may contribute to a slower release of the carotenoid over time. Indeed, as seen in the confocal microscopy images (Figure 4.4), after *in vitro* digestion, still some undigested oil was present, which may have decreased the extent of incorporation of lutein into the mixed micelles and consequently reduce the lutein bioaccessibility (Mantovani et al., 2022), but may not necessarily decrease total absorption, only delay it.

4.4. Conclusions

The different ways of preparing the emulsions and the location of the lutein in the emulsified systems significantly impacted both lutein chemical stability and bioaccessibility. The double emulsions had higher encapsulation efficiency compared to the simple emulsion. The W-L/O/W sample displayed the lower lutein stability against light exposure during storage, but the higher lutein bioaccessibility after *in vitro* digestion of fresh produced samples. The incorporation of lutein, a highly hydrophobic molecule, into the oil phase of the prepared double emulsion or simple emulsion, contributed to the chemical stability of the carotenoid. The results clearly show that all samples had a high residual lutein in the digesta after *in vitro* intestinal stage, and it is important to evaluate the potential slower release of the material in the micellar phase. Indeed, due to the high oil fraction used in this study, some undigested oil was still present at the end of the digestion, especially for the double emulsion samples. There was a clear difference in the incorporation of lutein in the micellar phase depending on the structural characteristics of the emulsions. It can be suggested that interactions between the various components may form during the production, storage and digestion of the emulsions that may affect the kinetics of bioaccessibility.

Conflicts of interest

The authors state no conflicts to declare.

Acknowledgements

We are grateful for the financial support from the CAPES (Coordination for the Improvement of Higher Education Personnel, grant 88887.573461/2020-00), São Paulo Research Foundation (FAPESP, grant 2017/09214-4), Aarhus University, including 480 FOODHAY (Food and Health Open Innovation Laboratory, Danish Roadmap for Research

Infrastructure) where data were generated through accessing research infrastructure, thanks to Carl-Otto Ottosen for setting up the light chamber for the incubation experiments, and also to Hanne Søndergaard Møller for helping with protein and lipid hydrolysis analyses.

4.5. References

- Boonlao, N., Shrestha, S., Sadiq, M. B., & Anal, A. K. (2020). Influence of whey protein-xanthan gum stabilized emulsion on stability and in vitro digestibility of encapsulated astaxanthin. *Journal of Food Engineering*, 272, 109859. <https://doi.org/10.1016/j.jfoodeng.2019.109859>
- Brodkorb, A., Egger, L., Alming, M., Alvito, P., Assunção, R., Ballance, S., Bohn, T., Bourlieu-Lacanal, C., Boutrou, R., Carrière, F., Clemente, A., Corredig, M., Dupont, D., Dufour, C., Edwards, C., Golding, M., Karakaya, S., Kirkhus, B., Le Feunteun, S., ... Recio, I. (2019). INFOGEST static in vitro simulation of gastrointestinal food digestion. *Nature Protocols*, 14(4), 991–1014. <https://doi.org/10.1038/s41596-018-0119-1>
- Chen, W., Ju, X., Aluko, R. E., Zou, Y., Wang, Z., Liu, M., & He, R. (2020). Rice bran protein-based nanoemulsion carrier for improving stability and bioavailability of quercetin. *Food Hydrocolloids*, 108, 106042. <https://doi.org/10.1016/j.foodhyd.2020.106042>
- Craft, N. E., & Soares, J. H. (1992). Relative Solubility, Stability, and Absorptivity of Lutein and β -Carotene In Organic Solvents. *Journal of Agricultural and Food Chemistry*, 40(3), 431–434. <https://doi.org/10.1021/jf00015a013>
- Eisinaite, V., Duque Estrada, P., Schroën, K., Berton-Carabin, C., & Leskauskaite, D. (2018). Tailoring W/O/W emulsion composition for effective encapsulation: The role of PGPR in water transfer-induced swelling. *Food Research International*, 106, 722–728. <https://doi.org/10.1016/j.foodres.2018.01.042>
- Gasa-Falcon, A., Odriozola-Serrano, I., Oms-Oliu, G., & Martín-Belloso, O. (2017). Influence of mandarin fiber addition on physico-chemical properties of nanoemulsions containing β -carotene under simulated gastrointestinal digestion conditions. *Lwt- Food Science and Technology*, 84, 331–337. <https://doi.org/10.1016/j.lwt.2017.05.070>
- Grasberger, K. F., Gregersen, S. B., Jensen, H. B., Sanggaard, K. W., & Corredig, M. (2021). Plant-dairy protein blends: gelation behaviour in a filled particle matrix. *Food Structure*, 29, 100198. <https://doi.org/10.1016/j.foostr.2021.100198>
- Gülseren, I., Fang, Y., & Corredig, M. (2012). Whey protein nanoparticles prepared with desolvation with ethanol: Characterization, thermal stability and interfacial behavior.

- Food Hydrocolloids*, 29(2), 258–264. <https://doi.org/10.1016/j.foodhyd.2012.03.015>
- Gumus, C. E., Decker, E. A., & McClements, D. J. (2017). Gastrointestinal fate of emulsion-based ω -3 oil delivery systems stabilized by plant proteins: Lentil, pea, and faba bean proteins. *Journal of Food Engineering*, 207, 90–98. <https://doi.org/10.1016/j.jfoodeng.2017.03.019>
- Iddir, M., Degerli, C., Dingo, G., Desmarchelier, C., Schlee, T., Borel, P., Larondelle, Y., & Bohn, T. (2019). Whey protein isolate modulates beta-carotene bioaccessibility depending on gastro-intestinal digestion conditions. *Food Chemistry*, 291, 157–166. <https://doi.org/10.1016/j.foodchem.2019.04.003>
- Iddir, M., Dingo, G., Yaruro, J. F. P., Hammaz, F., Borel, P., Schlee, T., Desmarchelier, C., Larondelle, Y., & Bohn, T. (2020). Influence of soy and whey protein, gelatin and sodium caseinate on carotenoid bioaccessibility. *Food & Function*, 11, 5446–5459. <https://doi.org/10.1039/d0fo00888e>
- Jain, A., Sharma, G., Ghoshal, G., Kesharwani, P., Singh, B., Shivhare, U. S., & Katare, O. P. (2018). Lycopene loaded whey protein isolate nanoparticles: An innovative endeavor for enhanced bioavailability of lycopene and anti-cancer activity. *International Journal of Pharmaceutics*, 546, 97–105. <https://doi.org/10.1016/j.ijpharm.2018.04.061>
- Mantovani, Raphaela A., Rasesa, M. L., Vidotto, D. C., Mercadante, A. Z., & Tavares, G. M. (2021). Binding of carotenoids to milk proteins: Why and how. *Trends in Food Science and Technology*, 110, 280–290. <https://doi.org/10.1016/j.tifs.2021.01.088>
- Mantovani, Raphaela A., Xavier, A. A. O., Tavares, G. M., & Mercadante, A. Z. (2022). Lutein bioaccessibility in casein-stabilized emulsions is influenced by the free to acylated carotenoid ratio, but not by the casein aggregation state. *Food Research International*, 161, 111778. <https://doi.org/10.1016/j.foodres.2022.111778>
- Mantovani, Raphaela Araujo, Hamon, P., Rousseau, F., Tavares, G. M., Mercadante, A. Z., Croguennec, T., & Bouhallab, S. (2020). Unraveling the molecular mechanisms underlying interactions between caseins and lutein. *Food Research International*, 138, 109781. <https://doi.org/10.1016/j.foodres.2020.109781>
- Marefati, A., Sjö, M., Timgren, A., Dejme, P., & Rayner, M. (2015). Fabrication of encapsulated oil powders from starch granule stabilized W/O/W Pickering emulsions by freeze-drying. *Food Hydrocolloids*, 51, 261–271. <https://doi.org/10.1016/j.foodhyd.2015.04.022>
- McClements, D. J., & Li, Y. (2010). Structured emulsion-based delivery systems: Controlling the digestion and release of lipophilic food components. *Advances in Colloid and*

- Interface Science*, 159(2), 213–228. <https://doi.org/10.1016/j.cis.2010.06.010>
- Minekus, M., Alming, M., Alvito, P., Ballance, S., Bohn, T., Bourlieu, C., Carrière, F., Boutrou, R., Corredig, M., Dupont, D., Dufour, C., Egger, L., Golding, M., Karakaya, S., Kirkhus, B., Le Feunteun, S., Lesmes, U., MacIerzanka, A., MacKie, A., ... Brodkorb, A. (2014). A standardised static in vitro digestion method suitable for food-an international consensus. *Food and Function*, 5(6), 1113–1124. <https://doi.org/10.1039/c3fo60702j>
- Mora-Gutierrez, A., Attaie, R., Núñez de González, M. T., Jung, Y., Woldesenbet, S., & Marquez, S. A. (2018). Complexes of lutein with bovine and caprine caseins and their impact on lutein chemical stability in emulsion systems: Effect of arabinogalactan. *Journal of Dairy Science*, 101(1), 18–27. <https://doi.org/10.3168/jds.2017-13105>
- Mulet-Cabero, A. I., Rigby, N. M., Brodkorb, A., & Mackie, A. R. (2017). Dairy food structures influence the rates of nutrient digestion through different in vitro gastric behaviour. *Food Hydrocolloids*, 67, 63–73. <https://doi.org/10.1016/j.foodhyd.2016.12.039>
- Oppermann, A. K. L., Noppers, J. M. E., Stieger, M., & Scholten, E. (2018). Effect of outer water phase composition on oil droplet size and yield of (w1/o/w2) double emulsions. *Food Research International*, 107, 148–157. <https://doi.org/10.1016/j.foodres.2018.02.021>
- Qazi, H. J., Ye, A., Acevedo-Fani, A., & Singh, H. (2021). In vitro digestion of curcumin-nanoemulsion-enriched dairy protein matrices: Impact of the type of gel structure on the bioaccessibility of curcumin. *Food Hydrocolloids*, 117, 106692. <https://doi.org/10.1016/j.foodhyd.2021.106692>
- Rehman, A. U., Akram, S., Seralin, A., Vandamme, T., & Anton, N. (2020). Lipid nanocarriers: Formulation, properties, and applications. In *Smart Nanocontainers: Micro and Nano Technologies*. Elsevier Inc. <https://doi.org/10.1016/B978-0-12-816770-0.00021-6>
- Rodrigues, D. B., Mariutti, L. R. B., & Mercadante, A. Z. (2016). An in vitro digestion method adapted for carotenoids and carotenoid esters: Moving forward towards standardization. *Food and Function*, 7(12), 4992–5001. <https://doi.org/10.1039/c6fo01293k>
- Sadeghi, R., Moosavi-Movahedi, A. A., Emam-Jomeh, Z., Kalbasi, A., Razavi, S. H., Karimi, M., & Kokini, J. (2014). The effect of different desolvating agents on BSA nanoparticle properties and encapsulation of curcumin. *Journal of Nanoparticle Research*, 16(9),

2565. <https://doi.org/10.1007/s11051-014-2565-1>

- Schex, R., Bonrath, W., Schäfer, C., & Schweiggert, R. (2020). The impact of (E/Z)-isomerization and aggregation on the color of rhodoxanthin formulations for food and beverages. *Food Chemistry*, 332, 127370. <https://doi.org/10.1016/j.foodchem.2020.127370>
- Shen, X., Zhao, C., Lu, J., & Guo, M. (2018). Physicochemical Properties of Whey-Protein-Stabilized Astaxanthin Nanodispersion and Its Transport via a Caco-2 Monolayer. *Journal of Agricultural and Food Chemistry*, 66, 1472–1478. <https://doi.org/10.1021/acs.jafc.7b05284>
- Teo, A., Lee, S. J., Goh, K. K. T., & Wolber, F. M. (2017). Kinetic stability and cellular uptake of lutein in WPI-stabilised nanoemulsions and emulsions prepared by emulsification and solvent evaporation method. *Food Chemistry*, 221, 1269–1276. <https://doi.org/10.1016/j.foodchem.2016.11.030>
- Xavier, A. A. O., Mercadante, A. Z., Domingos, L. D., & Viotto, W. H. (2012). Desenvolvimento e validação de método espectrofotométrico para determinação de corante à base de luteína adicionado em iogurte desnatado. *Química Nova*, 35(10), 2057–2062. <https://doi.org/10.1590/S0100-40422012001000028>
- Xu, D., Qi, Y., Wang, X., Li, X., Wang, S., Cao, Y., Wang, C., Sun, B., Decker, E., & Panya, A. (2017). The influence of flaxseed gum on the microrheological properties and physicochemical stability of whey protein stabilized β -carotene emulsions. *Food and Function*, 8(1), 415–423. <https://doi.org/10.1039/c6fo01357k>
- Zhang, R., Zhang, Z., Zhang, H., Decker, E. A., & McClements, D. J. (2015). Influence of lipid type on gastrointestinal fate of oil-in-water emulsions: In vitro digestion study. *Food Research International*, 75, 71–78. <https://doi.org/10.1016/j.foodres.2015.05.014>
- Zhao, C., Wei, L., Yin, B., Liu, F., Li, J., Liu, X., Wang, J., & Wang, Y. (2020). Encapsulation of lycopene within oil-in-water nanoemulsions using lactoferrin: Impact of carrier oils on physicochemical stability and bioaccessibility. *International Journal of Biological Macromolecules*, 153, 912–920. <https://doi.org/10.1016/j.ijbiomac.2020.03.063>

CHAPTER 5 - RESEARCH ARTICLE 3

Title: Aging of infant formulas containing proteins from different sources.

Authorship: Lauane Nunes, Igor Lima de Paula, Marcelo Cristianini, Rodrigo Stephani, Guilherme M. Tavares.

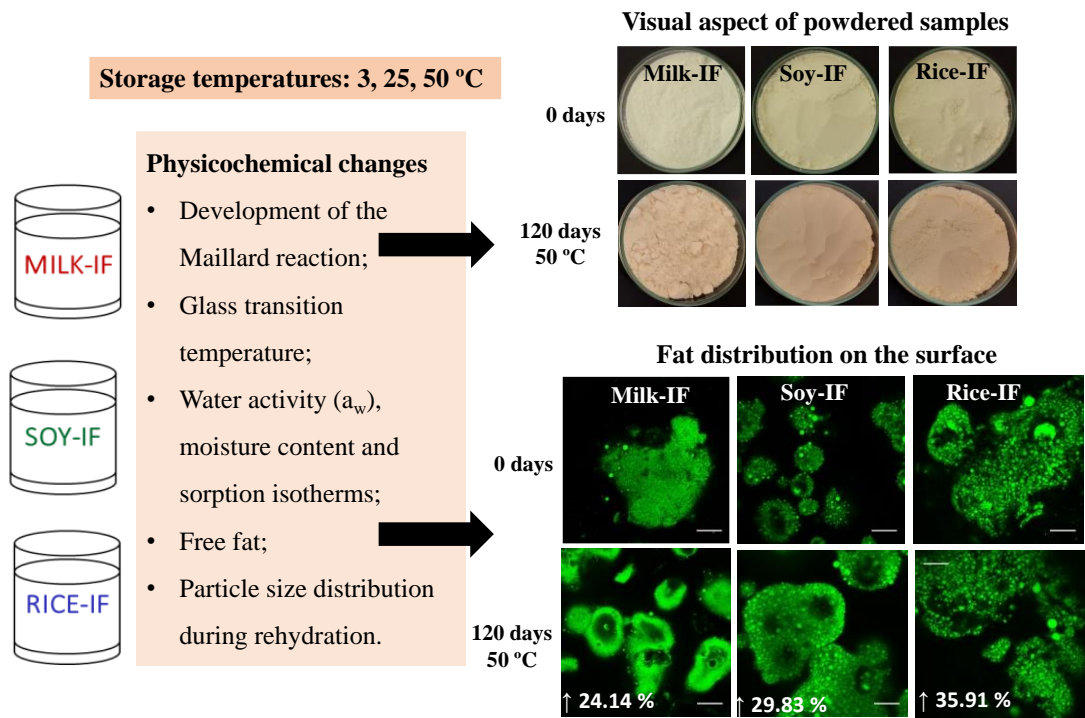
Article published in the LWT - Food Science and Technology (IF 2023: 6.056).

The license to reuse this content in the thesis is in Annex 2.

Link for the publication: <https://doi.org/10.1016/j.lwt.2021.112299>

Infant formulas have a complex composition. These are emulsified formulated systems which may be supplemented with several different bioactive compounds. In this chapter the influence of the different composition in between commercial infant formulas regarding some macro constituents was studied concerning their influence in the aging of the formulas. Critical storage temperatures should be avoided as they lead to a series of physical and chemical changes, such as the faster development of the Maillard reaction and favored the increase in the free fat content.

Graphical abstract



Abstract

Most infant formulas (IFs) use cow's milk-based ingredients as raw material. Nevertheless, to produce IFs for special needs, these raw materials may be replaced by other ones from different protein sources such as soy and rice. During transport and storage, IFs can be subjected to high temperatures, then, several physicochemical alterations may be accelerated. Even so, little is known about how the composition of IFs containing different protein sources may modulate their aging. Therefore, the objective of this work was to compare how different physicochemical parameters of IFs containing cow's milk, soy, or rice as major protein sources evolved during aging under different temperatures. Mild storage temperatures (3 °C and 25 °C) promoted little changes in the evaluated parameters. However, critical storage temperature (50 °C) (i) favored the faster development of the Maillard reaction in milk-IF and soy-IF; (ii) impaired their rehydration ability and (iii) favored the increase in the free fat content of rice-IF and soy-IF. This work is relevant in establishing parallels between different infant formulas that aim to meet the same nutritional demands of infants.

Keywords: cow's milk; soy; rice; aging; physicochemical properties

5.1.Introduction

Infant formulas (IFs) have the main purpose of replacing or complementing breast milk for infant nutrition (Blanchard et al., 2013). Thus, such products are formulated with adequate amounts of proteins, fats, carbohydrates, minerals, and vitamins to mimic as much as possible the composition of breast milk, and therefore, allowing the same growth and development observed for an infant exclusively breastfed (McCarthy et al., 2013; Tham, Yeoh, et al., 2017). Traditional IFs available on the market are formulated using cow's milk and cow's milk-based ingredients as the main protein source. However, the replacement of dairy raw materials by plant protein-based ones are recommended in formulating IFs for infants with cow's milk protein allergy (Bocquet et al., 2019). In this context, soy protein isolate or hydrolyzed rice protein is often used as preferable alternative protein sources. Nevertheless, such replacement implies other adjustments on the formulation of the IFs to ensure nutritional and functional properties close to those of breast milk and traditional IFs (Le Roux, Mejean, et al., 2020; Masum et al., 2020). Cow's milk-based IFs are enriched in lactose to mimic breast milk composition, nevertheless, this carbohydrate is usually replaced by maltodextrins, glucose syrup, sucrose, and/or starches in IFs containing alternative protein sources (Bocquet et al., 2019; Saxena et al., 2019). The fat content of IFs comes from a blend of different vegetable oils such as palm, coconut, soy, and sunflower to provide a fatty acid profile similar to the one of breast milk, thus slight differences can also be seen comparing the fat-rich ingredients used to produce IFs containing different protein sources (Tham, Yeoh, et al., 2017). The same logic may be observed for their composition of vitamins and minerals (Blanchard et al., 2013).

The IFs have a long shelf life (12 - 24 months), however, their stability during storage is highly dependent on factors such as composition and storage conditions (e.g. temperature, relative humidity, time) (Drapala et al., 2017; McCarthy et al., 2013; X. Wang et al., 2018). It is reported in the literature that these products may be subjected to temperatures above 45 °C, reaching 57 °C inside containers, over periods of 3 months during continental or intercontinental transport (Leinberger, 2006; Norwood et al., 2016). If these critical conditions are reached, several physical and chemical changes may be accelerated, such as lactose crystallization, lipid oxidation, and Maillard reaction, leading to particle collapse and caking, loss of essential nutrients, protein aggregation, and generation of oxidative products, for instance (Cheng et al., 2019; Wang et al., 2018; Zouari et al., 2020). All these aforementioned changes contribute to the deterioration of functional, sensory, and nutritional properties of IFs, which consequently compromise the absorption of nutrients by infants (Tham et al., 2016).

Considering that most of the nutrition of infants fed with IFs, in the first months of life, is obtained from the reconstituted powder formula, minimizing all these physicochemical changes during storage becomes crucial (Sabater et al., 2018).

Several processing and storage parameters applied to IFs containing alternative protein sources derive from those consolidated for cow's milk-based IFs since published scientific reports appear to be limited for the former. Most of the available reports on the use of plant proteins in IFs focus on their encapsulation capacity, digestibility, and/or allergenicity (Le Roux, Chacon, et al., 2020). However, the replacement of dairy proteins by plant proteins, even partially, has a great impact on IFs properties, which means that process parameters should be adapted for each formulation to provide satisfactory quality for the obtained IFs (Le Roux, Mejean, et al., 2020).

To understand the relationship between aging conditions and the physicochemical changes of IFs, it is important to identify their critical storage conditions, which will be highly influenced by their composition (Masum et al., 2020; Saxena et al., 2019; Tham, Yeoh, et al., 2017). Therefore, the objective of this work was to evaluate three different commercial IFs, each one formulated with one protein source (cow's milk, soy, and rice), during storage at different temperatures for up to 120 days, to identify their critical physicochemical indicators during aging. To the best of our knowledge, this is the first time that the physicochemical properties of IFs containing plant proteins have been evaluated during aging.

5.2. Material and methods

5.2.1. Material

IFs indicated for infants in the same stage, formulated with proteins from different sources, were purchased from the local market. For this study, IF formulated with cow's milk (milk-IF), soy protein (soy-IF), and rice protein (rice-IF) from two different batches were used. All IFs were recently produced and packed in metal cans for consumption. Their compositions according to the information provided by the manufacturer are summarized in Table 5.1.

Sodium acetate was purchased from Synth (São Paulo, Brazil) and the other reagents were purchased from Sigma-Aldrich (St. Louis, Missouri, USA). All were of analytical grade.

Table 5.1- Composition of the different IFs according to the information provided by the manufacturer.

Formulas	Composition (g.100g ⁻¹)			
	Carbohydrates	Fats	Proteins	Ashes
Milk-IF	55 (lactose)	24 (palm, sunflower, canola, fish, <i>Mortierella alpina</i> oil)	8.5 (cow's milk and whey protein)	2.09
Soy-IF	55 (maltodextrin)	26 (palm olein, soy, coconut, safflower, <i>Cryptocodinium cohnii</i> , <i>Mortierella alpina</i> , sunflower oil)	14 (hydrolyzed soy protein)	2.44
Rice-IF	55 (maltodextrin and corn starch)	25 (palm, canola, sunflower, coconut oil)	13 (extensively hydrolyzed rice protein)	2.07

5.2.2. Storage conditions

The IFs were divided into batches of 250 grams in aluminum coated plastic bags (composed of 5 layers of low-density polyethylene and nylon interspersed), vacuum-sealed, stored in separate environments with specific temperature conditions: refrigeration (3.30 ± 1.34 °C), ambient (24.87 ± 1.12 °C), and critical (50.44 ± 2.06 °C), respectively, for 120 days of storage. These temperatures were set to cover the temperature range potentially occurring during the transportation of powdered products.

5.2.3. Determination of glass–rubber transition temperature (T_{gr}) by rheological method

The critical temperature at which structural changes in IFs begin to occur was determined by applying the methodology described by Hogan et al. (2010). Briefly, the powder samples (~ 2 g) were compressed (30 N) between a 40 mm steel parallel plate and a Peltier plate of an AR2000-ex rheometer (TA Instruments, New Castle, Delaware, USA), then heated from 20 °C to 100 °C at a constant rate (2 °C.min⁻¹). T_{gr} was determined as the inflection point of the normal force versus temperature curve and expressed as the average of three measurements for IFs before storage (0 days).

5.2.4. Analysis of moisture content, water activity, and sorption isotherms

The moisture content of the powders was determined using an MB45 halogen infrared moisture analyzer (Ohaus, Parsippany, New Jersey, USA). Samples were dried at 105 °C with a ramp profile until a constant weight was obtained (< 1 mg change over 140 s) (Kelly et al., 2016; Murphy et al., 2015).

Water activity (a_w) was determined in AquaLab CX-2 (BrasEq, São Paulo, Brazil). Sorption isotherms were generated using AquaLab VSA (METER Food, Pullman, Washington, USA) by the Dynamic Dewpoint Isotherm (DDI) method (Schmidt & Lee, 2012). Moisture content and a_w were measured every 15 days during storage in triplicate, while sorption isotherms were generated before storage (0 days) and after 120 days of storage.

5.2.5. Advanced Maillard Products (AMP) fluorescence and Browning Index

AMP fluorescence was measured by mixing 500 μL of 5 % (w.w⁻¹) reconstituted formula with 4.5 mL of sodium acetate buffer (0.1 M; pH 4.6) followed by centrifugation at 4000 g for 10 min at room temperature (Allegra 64R Centrifuge, Beckman Coulter, Fullerton, USA), then the supernatant was filtered through a 0.45 μm nylon filter (Analítica, São Paulo, Brazil). Fluorescence measurements were performed at excitation and emission wavelength of 330 and 410 nm on Synergy MX equipment (Biotek Instruments, Winooski, Vermont, USA) (Birlouez-Aragon et al., 1998). The results were expressed as a percentage of increment from the initial measure obtained before storage.

The browning index (BI) of the powders was calculated from Equations 5.1 and 5.2, which combines the L^* , a^* and b^* values, measured using ColorQuest XE (HunterLab, Reston, Virginia, USA) (Buera et al., 1987; Norwood et al., 2016). These analyzes were performed every 15 days, in triplicate and the results were also expressed as a percentage of increment compared to the sample before storage (0 days).

$$BI = \frac{100(x-0.31)}{0,17} \quad \text{Eq. 5.1}$$

$$\text{With } x = \frac{a^* + 1,750 \times L^*}{5,645 \times L^* + a^* - 3,012 \times b^*} \quad \text{Eq. 5.2}$$

5.2.6. Free fat content

About 5 g of powder was mixed with 30 mL of petroleum ether, stirred for 15 min and filtered (n° 4, Whatman, Maidstone, UK). The filtrate was collected, placed in a fume hood to

evaporate the petroleum ether, afterwards, the samples were placed in an oven at 105 °C for 1 h, cooled and the free fat content was expressed as a percentage of powder weight (Drapala et al., 2017; McCarthy et al., 2013). This analysis was performed at 0, 60, and 120 days of storage in triplicate.

5.2.7. Confocal Laser Scanning Microscopy (CLSM)

The analysis was performed using a Zeiss LSM510 inverted confocal microscope (Carl Zeiss AG, Germany) with a 63x oil immersion objective. Lipids were marked with the 0.02 % (w.v⁻¹) Nile Red dye in 1,2-propanediol. A drop of the dye solution was added to the approximately 1 mg sample, then an argon laser was operated at an excitation wavelength of 488 nm, and emission was detected between 500 and 530 nm (McCarthy et al., 2013; Toikkanen et al., 2018). At least three specimens of each sample were observed to obtain representative micrographs of samples. This analysis was performed at 0, 60, and 120 days of storage.

5.2.8. Particle size distribution

The size distribution of the particles of rehydrated IFs was obtained using a Beckman Coulter LS 13 320 laser diffraction analyzer (Beckman Coulter, Miami, FL, USA) coupled to an aqueous liquid module (Beckman Coulter, Miami, FL, USA). Solutions of 5 % (w.w⁻¹) of the powder samples were prepared by adding the powder into distilled water at room temperature (25 °C) and then stirring the mixture for 30 min at 700 rpm using a magnetic bar. The size of the vessel and the stirring device used to prepare the solutions were standardized to subject all samples to the same rehydration protocol. A sufficient amount of rehydrated sample to generate turbidity readings was added to the liquid analysis module tank with water at room temperature (25 °C). Data were collected in the particle size range of 0.04 to 2000 µm, with an acquisition time of 90 s (Mimouni et al., 2009; Torres et al., 2017). The results were obtained using 1.332 as the refractive index for the dispersing medium (water), and 1.6 as a refractive index for IFs (Fraunhofer theory) (Mimouni et al., 2009; Murphy et al., 2015). The results were represented as the volume (%) occupied by the particles in relation to their size and the value of D₉₀ (i.e., the diameter in which 90 % of the particles have smaller sizes) of two measurements. The analysis was performed at 0, 60, and 120 days of storage.

5.2.9. Statistical data analysis

The results were evaluated by analysis of variance (ANOVA) and Tukey's test to observe significant differences between the mean values ($p < 0.05$), using the statistical program R version 3.5.3 (R Foundation for Statistical Computing, Vienna, Austria).

5.3. Results and discussion

5.3.1. Glass–rubber transition temperature (T_{gr}) determined by rheological method

When powdered products are subjected to temperatures above the T_{gr} , the increase of the molecular mobility associated with the transition from the metastable glassy state to the rubbery (fluid) one, accelerates structural changes in powders (Shrestha et al., 2007; Tham, Yeoh, et al., 2017; Zhou & Roos, 2011). Representative T_{gr} curves for each one of the analyzed IFs are shown in Figure 5.1. The T_{gr} of 32.6 ± 2.1 °C, 81.1 ± 1.2 °C, and > 100 °C were found for milk-IF, soy-IF, and rice-IF respectively. These results suggest that milk-IF stored at critical temperature (50.44 ± 2.06 °C) will be more susceptible to structural changes compared to soy-IF and rice-IF. On the other hand, minimal effects are expected for all three IFs stored at refrigeration (3.30 ± 1.34 °C) and ambient (24.87 ± 1.12 °C) temperatures.

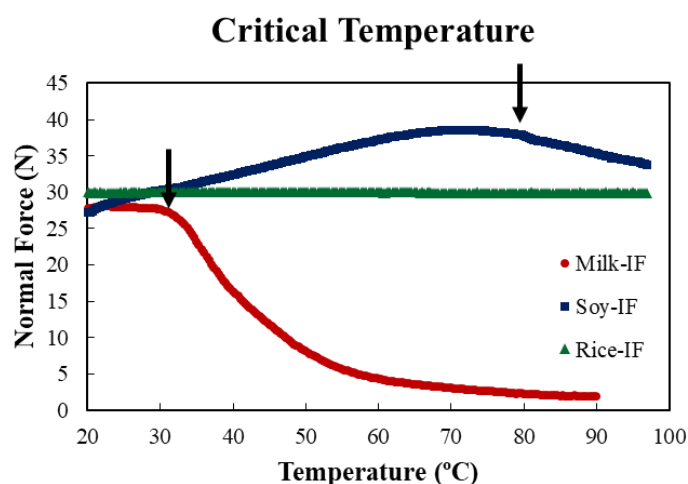


Figure 5.1- Representative T_{gr} curves for each one of the analyzed IFs. Arrows indicate the position of T_{gr} .

The T_{gr} found for milk-IF is lower than data reported in the literature for model IFs based on cow's milk, which describe glass transition temperatures varying between 40 °C and 60 °C (Cheng et al., 2019; Kelly et al., 2016; Le Roux, Mejean, et al., 2020; McCarthy et al.,

2013; Sun et al., 2018; Zhu et al., 2018). The aforementioned difference is in part related to the applied method since all cited papers applied differential scanning calorimetry while in this work the method of mechanical compression was used, also, determinations made on commercial products can be affected by the other components of the infant formula when compared to model products. In this way, Hogan et al. (2010) also applied the mechanical compression method to determine the T_{gr} of fat-enriched micellar casein powders and obtained values of $29 \pm 2 \text{ }^\circ\text{C} - a_w 0.28$, $34 \pm 1 \text{ }^\circ\text{C} - a_w 0.32$, in the same magnitude order of the one reported in this work for milk-IF. The profile of the T_{gr} curves obtained for milk-IF (Figure 5.1) was compatible with those reported in the literature for milk-based powders (Hogan et al., 2010). Although no reports were found in the literature describing the T_{gr} for IFs containing only proteins from plant sources, the T_{gr} found for soy-IF and rice-IF were in accordance with those reported for their major carbohydrates (Roos & Karel, 1991). Even if soy-IF and rice-IF contain hydrolyzed proteins which could lead to a decrease of their T_{gr} , the major carbohydrates in each one of the IFs seemed to play a more important role in such parameter (Kelly et al., 2016; Murphy et al., 2015). Since soy-IF contains maltodextrin and rice-IF contains maltodextrin and corn starch, a higher T_{gr} of the second ($> 100 \text{ }^\circ\text{C}$) could be expected due to the higher degree of polymerization of the carbohydrates in this product (Gutierrez et al., 2016).

5.3.2. Water activity (a_w), moisture content and sorption isotherms of IFs during aging

The a_w and moisture content of the IFs during aging was measured and the obtained values at 0 and 120 days of storage are shown in Table 5.2. Before aging, the values found for both parameters were consistent with those reported for powdered food products and close to optimal values allowing to minimize the occurrence of chemical reactions in the product (Kelly et al., 2014, 2016; Le Roux, Chacon, et al., 2020; Le Roux, Mejean, et al., 2020). After 120 days of aging a slight trend of a_w increase could be observed for milk-IF (2.7 %), soy-IF (6.9 %) and rice-IF (60.6 %) at $50 \text{ }^\circ\text{C}$. After 120 days of aging, the a_w and moisture content, for all samples, remained in the usual range of powdered food products.

Table 5.2- Water activity (a_w) and moisture content and free-fat content of milk-IF, soy-IF and rice-IF at 0 and 120 days of storage in different temperatures. The values for a given analysis and formula with the same lowercase superscript did not differ significantly ($p < 0.05$). The values for a given analysis, temperature and time with the same uppercase superscript did not differ significantly ($p < 0.05$).

Analysis	Time / Storage temperature	a_w		Moisture content (% w.w ⁻¹)		Free fat (% w.w ⁻¹)	
		0 days	120 days	0 days	120 days	0 days	120 days
Milk-IF	3 °C		0.294 ±		2.367 ±		0.768 ±
				0.009 ^{bA}		0.090 ^{bC}	
	25 °C	0.208 ±	0.314 ±	2.363 ±	3.337 ±	0.619 ±	0.711 ±
		0.006 ^{cA}	0.002 ^{aA}	0.067 ^{bB}	0.076 ^{aC}	0.058 ^{bC}	0.041 ^{abC}
	50 °C		0.214 ±		1.950 ±		0.768 ±
				0.007 ^{cA}		0.040 ^{cC}	
Soy-IF	3 °C		0.204 ±		2.987 ±		1.611 ±
				0.003 ^{bB}		0.015 ^{bA}	
	25 °C	0.160 ±	0.318 ±	2.980 ±	3.853 ±	1.357 ±	1.505 ±
		0.006 ^{cB}	0.005 ^{aA}	0.035 ^{bA}	0.015 ^{aA}	0.029 ^{dB}	0.024 ^{cB}
	50 °C		0.171 ±		2.510 ±		1.762 ±
				0.006 ^{cB}		0.020 ^{cB}	
Rice-IF	3 °C		0.132 ±		2.627 ±		2.630 ±
				0.003 ^{cC}		0.064 ^{cB}	
	25 °C	0.098 ±	0.231 ±	2.467 ±	3.483 ±	1.901 ±	2.350 ±
		0.005 ^{dC}	0.005 ^{aB}	0.035 ^{dB}	0.035 ^{aB}	0.035 ^{cA}	0.045 ^{bA}
	50 °C		0.158 ±		2.767 ±		2.583 ±
				0.005 ^{bB}		0.051 ^{bA}	

Figure 5.2 shows the water sorption behavior of all IFs before aging and after 120 days of storage at 50 °C. The sorption isotherms obtained after 120 days of storage at 3 °C and 25 °C displayed a behavior very close to the one observed before aging, therefore such data are not shown. The sorption isotherms of milk-IF (Figure 5.2-A) had a profile similar to the one usually observed for spray dried milk powder (Carter & Schmidt, 2012). After the critical a_w (around 0.4) an increase in the moisture sorption rate is observed as a consequence of water moving easily from the surface into the bulk of the powder due to the increase of

molecular mobility promoted by the glass transition (Carter & Schmidt, 2012). Afterward, during lactose crystallization, sorbed water is expelled, which leads to a sharp decrease in the moisture sorption rate (referred to as inflection point) (Kelly et al., 2016; Queiroz et al., 2021). Therefore, the typical shoulder observed in the sorption isotherm of milk-IF was not reproduced in the other samples since they do not contain lactose in their composition, and they are less susceptible to glass transition during moisture sorption compared to milk-IF. On the other hand, soy-IF (Figure 5.2-B) and rice IF (Figure 5.2-C) had sorption isotherms of type III which were similar to the one obtained for soy protein isolate as described by Schmidt & Lee, (2012). This kind of sorption isotherms is associated with materials that may have fairly low adsorption of water until the a_w becomes sufficient for dissolution to begin, thereby increasing molecular mobility, and water sorption increases (Roos & Drusch, 2015). Rice-IF had greater moisture sorption than soy-IF during the initial stages of the sorption isotherm which may be related to the extensively hydrolyzed rice protein contained in the former. It has been reported that by increasing the degree of hydrolysis of proteins in IFs, their moisture sorption also increased due to the rising number of available hydrophilic sites (Kelly et al., 2016). The final moisture content at a_w 0.9 was much higher for soy-IF and rice-IF compared to milk-IF, which was probably related to the lactose crystallization in milk-IF during moisture sorption, since crystalline lactose sorbs very little moisture compared to amorphous maltodextrin contained in soy-IF and rice-IF for instance (Tham et al., 2016).

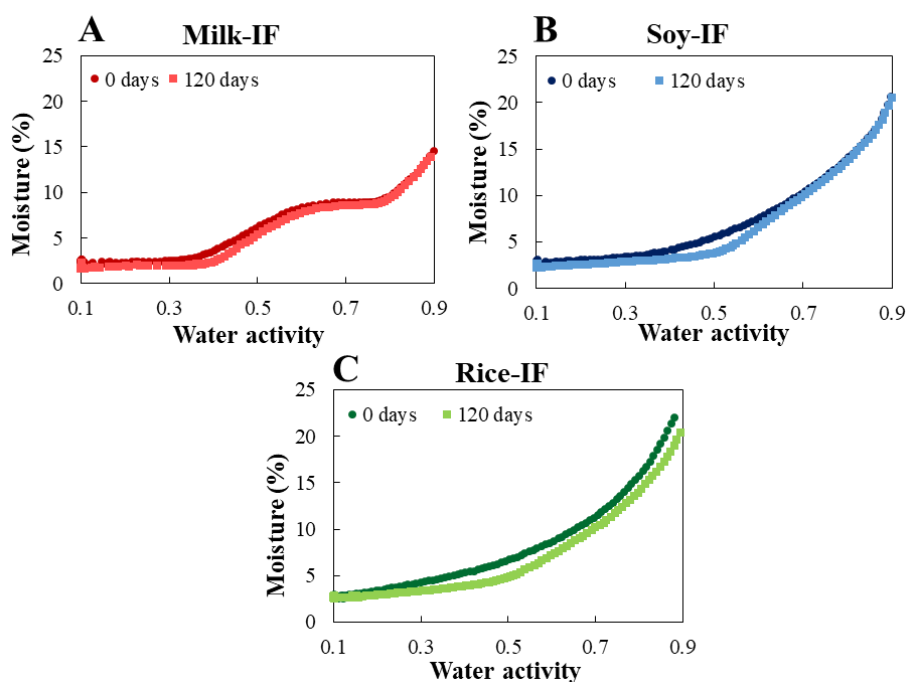


Figure 5.2- Sorption isotherms of (A) milk-IF, (B) soy-IF, (C) rice-IF at 0 and 120 days of storage at 50 °C. Isotherms were generated at 25 °C.

After 120 days of aging at 50 °C, the overall profile of the isotherms remained unchanged compared to the one before aging, but a decrease in the moisture sorption capacity at low a_w was observed for all three IFs, although it is more flagrant for soy-IF and also for rice-IF (Figure 5.2). Such phenomenon occurs due to the carbohydrates crystallization (in the case of milk-IF), Maillard reaction occurrence during aging and decrease of available sites for interacting with water molecules as a consequence of protein polymerization (Tham, Yeoh, et al., 2017). As these last two phenomena intensely occurred in soy-IF during aging, this may explain the greater change in the moisture sorption isotherm profile observed before and after aging for this IF compared with rice-IF.

5.3.3. Development of the Maillard reaction

The development of Maillard reaction in the different IFs during aging was monitored by determining the fluorescence associated with advanced Maillard products (AMP) (Birlouez-Aragon et al., 1998; Wang et al., 2018) and by calculating their browning index (Buera et al., 1987; Norwood et al., 2016). Independently of the protein source contained in the IFs, no significant changes in the fluorescence of AMP could be noticeable during the 120 days of storage at temperatures of 3 °C and 25 °C. The same behavior was observed for the browning index of these samples. These results are in accordance with those reported by Zhu et al. (2018), in which powders stored in milder temperatures did not show significant development of the Maillard reaction. On the other hand, great evolution of both parameters was observed during aging of samples stored at 50 °C, since the kinetics of the Maillard reaction is potentiated at high temperatures (Damodaran et al., 2008), which goes along with the observed for whey protein isolate powders during aging at temperatures between 40 °C and 60 °C (Norwood et al., 2016; Vidotto & Tavares, 2020), as well as in IFs stored at temperatures of 55 °C and 70 °C (Cheng et al., 2017).

Figure 5.3-A shows the relative increment of AMP fluorescence of the different IFs stored at 50 °C during 120 days of aging. The relative increase of the AMP fluorescence during storage displayed an exponential profile, which evolved faster for milk-IF and soy-IF compared with rice-IF. After 120 days of aging, the AMP fluorescence increased 241 % and 335 % for milk-IF and soy-IF respectively, while for rice-IF the observed increment was only about 88 %. According to Figure 5.3-A, it can be inferred that AMP were formed with greater significance after 45 days of storage for milk-IF and soy-IF, and after around 60 days of storage for rice-IF. In its turn, Figure 5.3-B displays the relative increment of the BI of samples during storage at 50 °C, as well as their visual aspect before and after 120 days of

storage at this temperature. The evolution of the BI of the different samples overtime at 50 °C also displayed an exponential profile. Until 90 days of storage, the evolution of the BI for all three different samples was in the same magnitude order and increased progressively to around 20 % compared with the BI before aging. From 90 to 120 days of storage, the BI drastically increased up to 82.5 %, 66.9 % and 54.1 % for milk-IF, soy-IF and rice-IF respectively. The time shift observed for the exponential increase of the BI compared with the one of AMP fluorescence is related to the extra time needed to reach the final stages of the Maillard reaction with the consequent color change, therefore, the determination of the AMP fluorescence could help on identifying critical Maillard reaction progress before noticeable changes in the color of the products. The increase in brown color of the powder after 120 days of aging at 50 °C is so clear that it is detectable even with the naked eye, as shown by the visual aspect of the samples in Figure 5.3-B.

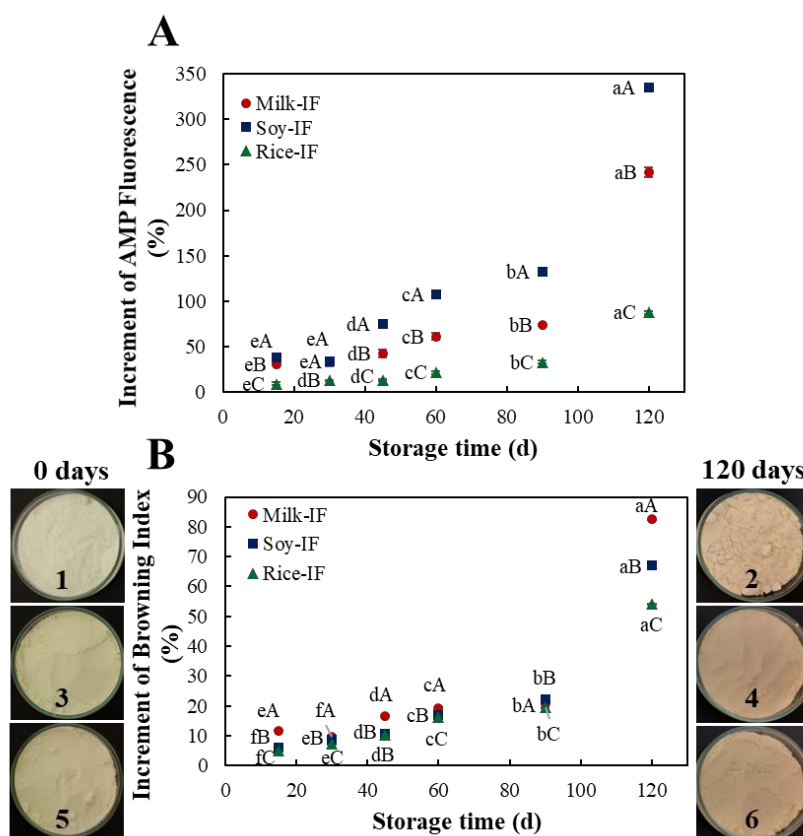


Figure 5.3- Increment of AMP (A) and Browning Index (B) of the different IFs during aging at 50 °C. (B) The visual aspect of powdered samples at 0 and 120 days of storage at 50 °C of the milk-IF (1-2), soy-IF (3-4), rice-IF (5-6). The values for a given IF with the same lowercase letter did not differ significantly ($p < 0.05$). The values for a given time with the same uppercase letter did not differ significantly ($p < 0.05$).

Milk-IF suffered the greater browning during aging at 50 °C compared with soy-IF and rice-IF. The achievement of the final stages of the Maillard reaction occurrence during the aging of milk-IF at 50 °C was favored compared with soy-IF and rice-IF stored at the same temperature due to the low T_{gr} of the former, which contributes to increasing molecular mobility and also due to the presence of lactose, which is more reactive compared to carbohydrates contained in other samples (O'Mahony et al., 2017; Tham, Xu, et al., 2017). Although the enrichment of soy-IF and rice-IF with peptides and some free amino acids such as lysine and methionine which are more prone to participate in the Maillard reaction than complex proteins, the weak reactivity of maltodextrin and corn starch compared to lactose seemed to counterbalance such effect. Comparing the browning of soy-IF with the one of rice-IF after aging at 50 °C, once more, the nature of the carbohydrates contained in each one of the IF helps to explain the less intense browning of the last (Bocquet et al., 2019; Gutierrez et al., 2016; O'Mahony et al., 2017). In addition to the occurrence of the Maillard reaction, it is important to state that the browning of the samples during aging may also be promoted by the increase of free fat on the surface of the powder particles (Ho et al., 2019), which will be discussed below.

5.3.4. Free fat

Free fat in food powders correspond to the non-emulsified lipids located on the surface, pores and capillaries of powder particle (Vignolles et al., 2007; Wang et al., 2018). Table 5.2 displays the content of free fat of all three different samples determined before and after 120 days of storage at different temperatures. Figure 5.4, on the other hand, shows the confocal microscopy images of the samples before and after 120 days of aging at 50 °C, where the highly fluorescent spots indicate free fat droplets on the surface of powder particles. Before storage, rice-IF had the highest content of free fat, followed by soy-IF and finally, by milk-IF. Certainly, differences in fat composition and processing conditions between the different IFs may contribute to explain the observed differences. For IFs production, a mixture of vegetable oils is optimized to achieve fatty acid profiles similar to breast milk, and fat with a lower melting point can be released on the powder surface more easily, on the other hand, increased homogenization pressure during processing may create smaller fat globules, resulting in smaller content of free fat (Kelly et al., 2014; Vignolles et al., 2007). Even so, the nature of the proteins in IFs plays a crucial role in the stabilization of the oil-in-water emulsion (Masum et al., 2020). The emulsifying properties of plant proteins are generally reported to be inferior compared with those of milk proteins, as observed by Le Roux,

Chacon, et al. (2020). Rice-IF displayed the highest value of free fat, as their emulsifying capacity was not optimal under the conditions of production of IFs. In addition, emulsifying properties of hydrolyzed protein may decrease because small peptides usually have reduced steric stabilizing properties compared with intact proteins (Drapala et al., 2017; Murphy et al., 2015; O'Mahony et al., 2017). Moreover, the free fat content found in all three samples before aging was smaller than those reported in the literature for spray dried dairy powders (1.76 - 3.36 % w.w⁻¹) and for IFs with plant proteins partially replacing milk proteins (2.2 ± 0.3 % w.w⁻¹) (Kelly et al., 2014; Le Roux, Mejean, et al., 2020).

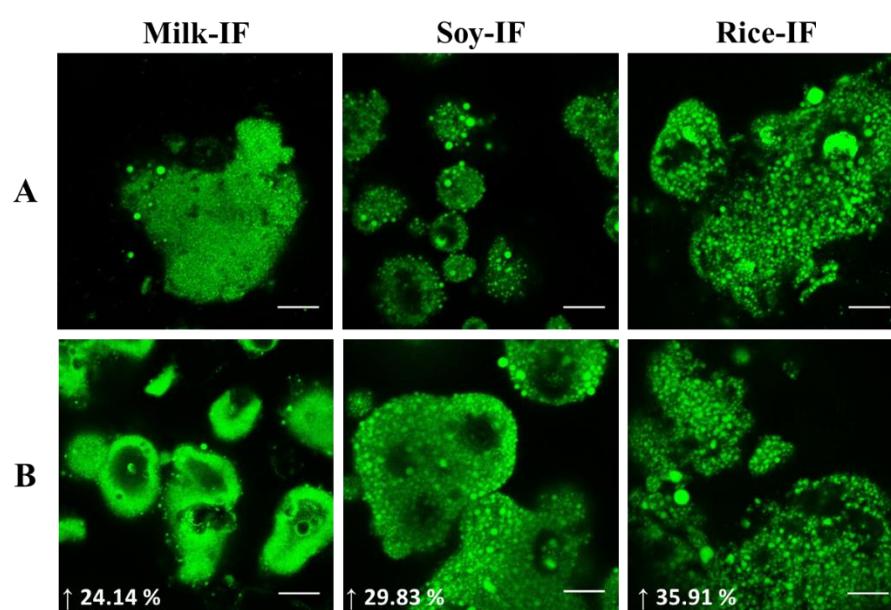


Figure 5.4- Confocal microscopy images of the different IFs at (A) 0 and (B) after 120 days of storage at 50 °C with the percentage of increase of the free fat content. Scale bars represent 22 μm .

An increase in the free fat content was observed with the advance in storage for all three samples independently of the aging temperatures. The increases observed in free fat at temperatures of 3 °C and 25 °C can be justified because the fat phase is partially crystallized at temperatures below 41 °C, also, infant formulas are subject to temperature variations during storage, which may favor the crystallization of fat and consequently the formation of free fat (Lopez et al., 2006; Vignolles et al., 2007). The free fat content after 120 days of aging at 50 °C compared to the one before aging was about 24 %, 30 %, and 36 % higher for milk-IF, soy-IF, and rice-IF respectively. The observed behaviour followed the logic of inferior emulsifying properties of plant proteins discussed above. However, despite the increase in

free fat with storage, all IF had less than 5 % free fat, which is considered satisfactory for such products, indicating a good fat encapsulation efficiency during production (Vignolles et al., 2007). The micrographs of Figure 5.4 allow observing the increase of the number and size of fat droplets on the surface of the powder particles of the different IFs after 120 days of aging at 50 °C. For rice-IF, particularly, it is easy to note spots of aggregated fat on the surface of the particles even before storage. The increase of free fat content in IFs transported or stored in elevated temperatures is critical because surface free fat can form liquid bridges between powder particles that become stronger bonds when the temperature is subsequently reduced and solid fat bridges are formed, in addition, it can impair the rehydration properties of the IFs and also favor the lipid oxidation (Sabater et al., 2018; Tham, Xu, et al., 2017; Thomas et al., 2004; Toikkanen et al., 2018).

5.3.5. Particle size distribution during rehydration

The particle size distribution after rehydration of the different IFs before and after aging at different temperatures was characterized by the distribution of the percentage of the volume occupied by the particles according to their hydrodynamic diameter, as shown in Figure 5.5 (Mimouni et al., 2009). Comparing all three IFs before aging, milk-IF displayed the smaller particle size distribution followed by rice-IF and then by soy-IF, with D_{90} of around 3.3 μm , 57.0 μm and 89.8 μm respectively. Two main particle populations could be observed for rehydrated milk-IF, the first one probably corresponds to the casein micelles (centered at approximately 0.2 μm), while the second should correspond to the fat droplets (centered at approximately 0.76 μm) (Toikkanen et al., 2018; Torres et al., 2017). Such particle size profile was in agreement with the one reported by Le Roux, Mejean, et al. (2020) also for milk-IF. On the other hand, the particle size profile observed for soy-IF and rice-IF was characteristic of agglomerated powder displaying inefficient rehydration ability (Torres et al., 2017). In addition, the higher initial free fat content of soy-IF and rice-IF may also play a role in their inefficient rehydration (Toikkanen et al., 2018). Le Roux, Mejean, et al. (2020) also reported a high particle size profile for rehydrated IFs containing milk and plant proteins (pea and faba), although the mechanism behind such phenomenon is not completely elucidated.

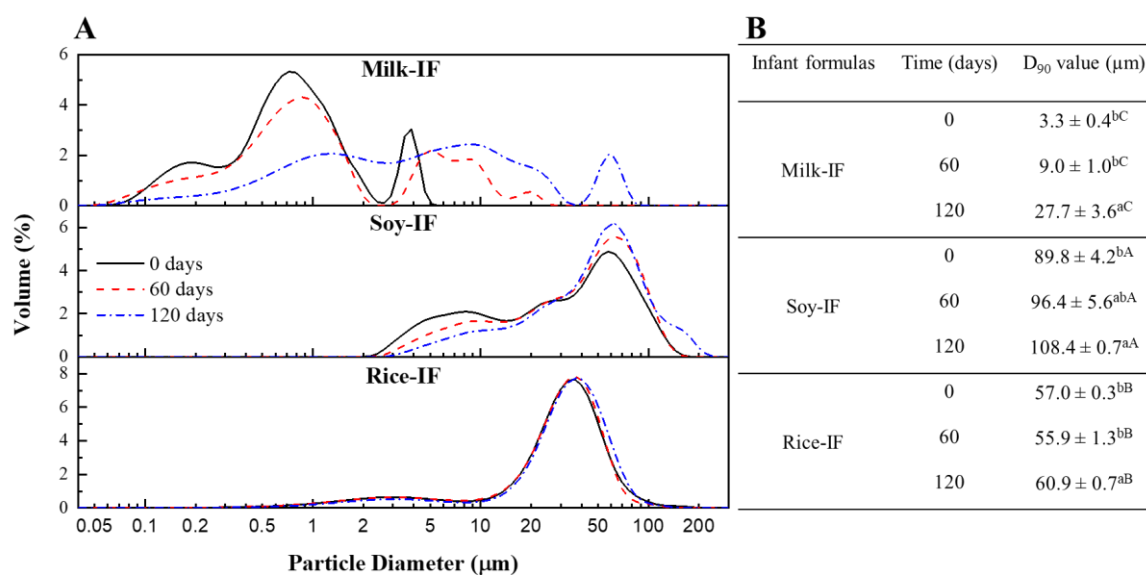


Figure 5.5- Particle size distribution characterized by the volume (%) occupied by the particles in relation to their size (A) and the cumulative volume diameters D₉₀ (B) after rehydration of the different IFs before and after 60 and 120 days of aging at 50 °C. The values for a given IF with the same lowercase superscript did not significantly differ ($p < 0.05$). The values for a given time with the same uppercase superscript did not differ significantly ($p < 0.05$).

Little or no change in the particle size distribution after rehydration was noticeable for samples stored at 3 °C and 25 °C compared with the profile obtained before aging (data not shown). Therefore, for these samples, the increase of the free fat content during aging seemed to have little impact on prejudicing powder rehydration. In the same way, little impact on the particle size distribution after rehydration was observed for rice-IF during aging at 50 °C, which evolved from a D₉₀ of about 57.0 μm to around 60.9 μm, representing an increase of 6.8%, conserving the overall profile of particle size distribution. On the other hand, milk-IF and soy-IF stored at 50 °C displayed a progressive increase in the size of the particles after rehydration. After 120 days of aging at 50 °C, the D₉₀ of milk-IF and soy-IF increased around 736.7 % and 20.7 %. The progress of the Maillard reaction during the storage of protein-rich powder is reported to be correlated to the formation of covalent cross-links between proteins, which negatively affects their rehydration ability (Le et al., 2013; Norwood et al., 2016; O'Mahony et al., 2017). Therefore, in addition to the increase of the free fat content during aging at 50 °C, the intense Maillard reaction occurrence seemed to promote the increase of the particle size distribution during the rehydration of the samples. Despite the greater increase of

the D_{90} of milk-IF during aging at 50 °C, it is worth noting that this sample still had a smaller particle size distribution after rehydration compared with the other IFs.

5.4. Conclusions

The stability of IFs depends on many factors, including composition, such as the nature and content of proteins and carbohydrates. During the aging of IFs, it was observed that mild temperatures, such as refrigeration and environment, promoted little or no change in the evaluated IFs. In contrast, critical storage temperatures should be avoided as they lead to a series of physical and chemical changes, which varied according to the evaluated IF. The increase of the Maillard reaction rate in milk-IF during aging seemed to be triggered by its lactose content and low T_{gr} . On the other hand, the presence of hydrolyzed proteins and the enrichment with reactive amino acids may be inferred as the main factors for increasing the Maillard reaction rate in soy-IF. While the weak reactivity of maltodextrin and corn starch compared to lactose seemed to counterbalance the effect of the presence of peptides and some free amino acids on the progress of the Maillard reaction in the rice-IF. Conversely, aging promoted the increase of the particle size distribution during the rehydration of milk-IF and soy-IF and an increase of the free fat amount in soy-IF and rice-IF.

Despite the physicochemical changes observed in infant formulas, the replacement of dairy raw materials by plant protein-based ones is still promising, since the analyzed parameters remained in the usual range of powdered dairy products. However, as the formulas are different, it is not possible to use the same well-established processing and storage parameters of cow's milk-based IFs for alternative protein sources, as is normally done. All these mentioned changes are important as they can influence the functional, sensory, and nutritional properties of IFs and consequently compromise the absorption of nutrients. In addition, this work is also relevant in establishing parallels between different IFs that aim to meet the same nutritional demands of infants. To elucidate how each one of the different compositional parameters, such as the nature and content of proteins and carbohydrates of the IFs dictates their aging, further studies are needed using well-controlled model matrices.

Acknowledgements

The Brazilian funding agency CNPq (National Council for Scientific and Technological Development, grant 141708/2018-2) is acknowledged. We are grateful to the access to equipment and assistance provided by the National Institute of Science and

Technology on Photonics Applied to Cell Biology (INFABIC) at the State University of Campinas.

5.5. References

- Birlouez-Aragon, I., Nicolas, M., Metais, A., Marchond, N., Grenier, J., & Calvo, D. (1998). A rapid fluorimetric method to estimate the heat treatment of liquid milk. *International Dairy Journal*, 8, 771–777. [https://doi.org/10.1016/S0958-6946\(98\)00119-8](https://doi.org/10.1016/S0958-6946(98)00119-8)
- Blanchard, E., Zhu, P., & Schuck, P. (2013). Infant formula powders. In B. Bhandari, N. Bansal, M. Zhang, & P. Schuck (Eds.), *Handbook of Food Powders: Processes and properties* (1st ed., pp. 465–483). Woodhead Publishing Limited. <https://doi.org/10.1533/9780857098672.3.465>
- Bocquet, A., Dupont, C., Chouraqui, J. P., Darmaun, D., Feillet, F., Frelut, M. L., Girardet, J. P., Hankard, R., Lapillonne, A., Rozé, J. C., Simeoni, U., Turck, D., & Briend, A. (2019). Efficacy and safety of hydrolyzed rice-protein formulas for the treatment of cow's milk protein allergy. *Archives de Pédiatrie*, 26(4), 238–246. <https://doi.org/10.1016/j.arcped.2019.03.001>
- Buera, M. D. P., Chirife, J., Resnik, S. L., & Wetzler, G. (1987). Nonenzymatic browning in liquid model systems of high water activity: kinetics of color changes due to Maillard's reaction between different single sugars and glycine and comparison with caramelization browning. *Journal of Food Science*, 52(4), 1063–1067.
- Carter, B. P., & Schmidt, S. J. (2012). Developments in glass transition determination in foods using moisture sorption isotherms. *Food Chemistry*, 132, 1693–1698. <https://doi.org/10.1016/j.foodchem.2011.06.022>
- Cheng, H., Erichsen, H., Soerensen, J., Petersen, M. A., & Skibsted, L. H. (2019). Optimising water activity for storage of high lipid and high protein infant formula milk powder using multivariate analysis. *International Dairy Journal*, 93, 92–98. <https://doi.org/10.1016/j.idairyj.2019.02.008>
- Cheng, H., Zhu, R.-G., Erichsen, H., Soerensen, J., Petersen, M. A., & Skibsted, L. H. (2017). High temperature storage of infant formula milk powder for prediction of storage stability at ambient conditions. *International Dairy Journal*, 73, 166–174.
- Damodaran, S., Parkin, K. L., & Fennema, O. R. (2008). *Fennema's Food Chemistry* (S. Damodaran, K. L. Parkin, & O. R. Fennema (eds.); 4th ed.). CRC Press.
- Drapala, K. P., Auty, M. A. E., Mulvihill, D. M., & O'Mahony, J. A. (2017). Influence of

- emulsifier type on the spray-drying properties of model infant formula emulsions. *Food Hydrocolloids*, *69*, 56–66. <https://doi.org/10.1016/j.foodhyd.2016.12.024>
- Gutierrez, N. C., Durrieu, V., Raynaud, C., & Rouilly, A. (2016). Influence of DE-value on the physicochemical properties of maltodextrin for melt extrusion processes. *Carbohydrate Polymers*, *144*, 464–473.
- Ho, T. M., Chan, S., Yago, A. J. E., Shrivaya, R., Bhandari, B. R., & Bansal, N. (2019). Changes in physicochemical properties of spray-dried camel milk powder over accelerated storage. *Food Chemistry*, *295*, 224–233. <https://doi.org/10.1016/j.foodchem.2019.05.122>
- Hogan, S. A., Famelart, M. H., O’Callaghan, D. J., & Schuck, P. (2010). A novel technique for determining glass-rubber transition in dairy powders. *Journal of Food Engineering*, *99*, 76–82. <https://doi.org/10.1016/j.jfoodeng.2010.01.040>
- Kelly, G. M., O’Mahony, J. A., Kelly, A. L., & O’Callaghan, D. J. (2014). Physical characteristics of spray-dried dairy powders containing different vegetable oils. *Journal of Food Engineering*, *122*, 122–129. <https://doi.org/10.1016/j.jfoodeng.2013.08.028>
- Kelly, G. M., O’Mahony, J. A., Kelly, A. L., & O’Callaghan, D. J. (2016). Effect of hydrolyzed whey protein on surface morphology, water sorption, and glass transition temperature of a model infant formula. *Journal of Dairy Science*, *99*(9), 6961–6972. <https://doi.org/10.3168/jds.2015-10447>
- Le Roux, L., Chacon, R., Dupont, D., Jeantet, R., Deglaire, A., & Nau, F. (2020). In vitro static digestion reveals how plant proteins modulate model infant formula digestibility. *Food Research International*, *130*, 108917.
- Le Roux, L., Mejean, S., Chacon, R., Lopez, C., Dupont, D., Deglaire, A., Nau, F., & Jeantet, R. (2020). Plant proteins partially replacing dairy proteins greatly influence infant formula functionalities. *LWT - Food Science and Technology*, *120*, 108891. <https://doi.org/10.1016/j.lwt.2019.108891>
- Le, T. T., Holland, J. W., Bhandari, B., Alewood, P. F., & Deeth, H. C. (2013). Direct evidence for the role of Maillard reaction products in protein cross-linking in milk powder during storage. *International Dairy Journal*, *31*(2), 83–91. <https://doi.org/10.1016/j.idairyj.2013.02.013>
- Leinberger, D. (2006). Temperature and humidity in ocean containers. In *Proceedings of Dimensions*. International Safe Transit Association.
- Lopez, C., Briard-Bion, V., Camier, B., & Gassi, J. Y. (2006). Milk Fat Thermal Properties and Solid Fat Content in Emmental Cheese: A Differential Scanning Calorimetry Study.

- Journal of Dairy Science*, 89(8), 2894–2910. [https://doi.org/10.3168/jds.S0022-0302\(06\)72562-0](https://doi.org/10.3168/jds.S0022-0302(06)72562-0)
- Masum, A. K. M., Huppertz, T., Chandrapala, J., Adhikari, B., & Zisu, B. (2020). Physicochemical properties of spray-dried model infant milk formula powders: Influence of whey protein-to-casein ratio. *International Dairy Journal*, 100, 104565. <https://doi.org/10.1016/j.idairyj.2019.104565>
- McCarthy, N. A., Gee, V. L., Hickey, D. K., Kelly, A. L., O'Mahony, J. A., & Fenelon, M. A. (2013). Effect of protein content on the physical stability and microstructure of a model infant formula. *International Dairy Journal*, 29, 53–59. <https://doi.org/10.1016/j.idairyj.2012.10.004>
- Mimouni, A., Deeth, H. C., Whittaker, A. K., Gidley, M. J., & Bhandari, B. R. (2009). Rehydration process of milk protein concentrate powder monitored by static light scattering. *Food Hydrocolloids*, 23, 1958–1965. <https://doi.org/10.1016/j.foodhyd.2009.01.010>
- Murphy, E. G., Roos, Y. H., Hogan, S. A., Maher, P. G., Flynn, C. G., & Fenelon, M. A. (2015). Physical stability of infant milk formula made with selectively hydrolysed whey proteins. *International Dairy Journal*, 40, 39–46. <https://doi.org/10.1016/j.idairyj.2014.08.012>
- Norwood, E.-A., Chevallier, M., Le Floch-Fouéré, C., Schuck, P., Jeantet, R., & Croguennec, T. (2016). Heat-Induced Aggregation Properties of Whey Proteins as Affected by Storage Conditions of Whey Protein Isolate Powders. *Food and Bioprocess Technology*, 9, 993–1001. <https://doi.org/10.1007/s11947-016-1686-1>
- O'Mahony, J. A., Drapala, K. P., Mulcahy, E. M., & Mulvihill, D. M. (2017). Controlled glycation of milk proteins and peptides: Functional properties. *International Dairy Journal*, 67, 16–34. <https://doi.org/10.1016/j.idairyj.2016.09.012>
- Queiroz, E. S., Rezende, A. L. L., Perrone, Í. T., Francisquini, J. d'Almeida, Carvalho, A. F. de, Alves, N. M. G., Oliveira, L. F. C. de, & Stephani, R. (2021). Spray drying and characterization of lactose-free goat milk. *LWT - Food Science and Technology*, 147, 111516. <https://doi.org/10.1016/j.lwt.2021.111516>
- Roos, Y. H., & Drusch, S. (2015). *Phase Transitions in Foods* (Steve Taylor (ed.); 2nd ed.). Academic Press.
- Roos, Y., & Karel, M. (1991). Phase Transitions of Mixtures of Amorphous Polysaccharides and Sugars. *Biotechnology Progress*, 7(1), 49–53.
- Sabater, C., Montilla, A., Ovejero, A., Prodanov, M., Olano, A., & Corzo, N. (2018). Furosine

- and HMF determination in prebiotic-supplemented infant formula from Spanish market. *Journal of Food Composition and Analysis*, 66, 65–73. <https://doi.org/10.1016/j.jfca.2017.12.004>
- Saxena, J., Adhikari, B., Brkljaca, R., Huppertz, T., Chandrapala, J., & Zisu, B. (2019). Physicochemical properties and surface composition of infant formula powders. *Food Chemistry*, 297, 124967. <https://doi.org/10.1016/j.foodchem.2019.124967>
- Schmidt, S. J., & Lee, J. W. (2012). Comparison between water vapor sorption isotherms obtained using the new dynamic dewpoint isotherm method and those obtained using the standard saturated salt slurry method. *International Journal of Food Properties*, 15(2), 236–248. <https://doi.org/10.1080/10942911003778014>
- Shrestha, A. K., Howes, T., Adhikari, B. P., & Bhandari, B. R. (2007). Water sorption and glass transition properties of spray dried lactose hydrolysed skim milk powder. *LWT - Food Science and Technology*, 40(9), 1593–1600. <https://doi.org/10.1016/j.lwt.2006.11.003>
- Sun, X., Wang, C., Wang, H., & Guo, M. (2018). Effects of Processing on Structure and Thermal Properties of Powdered Preterm Infant Formula. *Journal of Food Science*, 83(6), 1685–1694. <https://doi.org/10.1111/1750-3841.14162>
- Tham, T. W. I., Wang, C., Yeoh, A. T. H., & Zhou, W. (2016). Moisture sorption isotherm and caking properties of infant formulas. *Journal of Food Engineering*, 175, 117–126. <https://doi.org/10.1016/j.jfoodeng.2015.12.014>
- Tham, T. W. Y., Xu, X., Yeoh, A. T. H., & Zhou, W. (2017). Investigation of caking by fat bridging in aged infant formula. *Food Chemistry*, 218, 30–39. <https://doi.org/10.1016/j.foodchem.2016.09.043>
- Tham, T. W. Y., Yeoh, A. T. H., & Zhou, W. (2017). Characterisation of aged infant formulas and physicochemical changes. *Food Chemistry*, 219, 117–125. <https://doi.org/10.1016/j.foodchem.2016.09.107>
- Thomas, M. E. C., Scher, J., Desobry-Banon, S., & Desobry, S. (2004). Milk powders ageing: Effect on physical and functional properties. *Critical Reviews in Food Science and Nutrition*, 44(5), 297–322. <https://doi.org/10.1080/10408690490464041>
- Toikkanen, O., Outinen, M., Malafronte, L., & Rojas, O. J. (2018). Formation and structure of insoluble particles in reconstituted model infant formula powders. *International Dairy Journal*, 82, 19–27. <https://doi.org/10.1016/j.idairyj.2018.03.001>
- Torres, J. K. F., Stephani, R., Tavares, G. M., Carvalho, A. F. de, Costa, R. G. B., de Almeida, C. E. R., Almeida, M. R., Oliveira, L. F. C. de, Schuck, P., & Perrone, Í. T.

- (2017). Technological aspects of lactose-hydrolyzed milk powder. *Food Research International*, *101*, 45–53. <https://doi.org/10.1016/j.foodres.2017.08.043>
- Vidotto, D. C., & Tavares, G. M. (2020). Impact of Dry Heating in an Alkaline Environment on the Structure and Foaming Properties of Whey Proteins. *Food and Bioprocess Technology*. <https://doi.org/10.1007/s11947-020-02519-5>
- Vignolles, M.-L., Jeantet, R., Lopez, C., & Schuck, P. (2007). Free fat, surface fat and dairy powders: interactions between process and product. A review. *Le Lait*, *87*(3), 187–236.
- Wang, X., Esquerre, C., Downey, G., Henihan, L., O’Callaghan, D., & O’Donnell, C. (2018). Assessment of infant formula quality and composition using Vis-NIR, MIR and Raman process analytical technologies. *Talanta*, *183*, 320–328. <https://doi.org/10.1016/j.talanta.2018.02.080>
- Zhou, Y., & Roos, Y. H. (2011). Characterization of Carbohydrate – Protein Matrices for Nutrient Delivery. *Journal of Food Science*, *76*(4), 368–376. <https://doi.org/10.1111/j.1750-3841.2011.02126.x>
- Zhu, R.-G., Cheng, H., Li, L., Erichsen, H. R., Petersen, M. A., Soerensen, J., & Skibsted, L. H. (2018). Temperature effect on formation of advanced glycation end products in infant formula milk powder. *International Dairy Journal*, *77*, 1–9.
- Zouari, A., Briard-Bion, V., Schuck, P., Gaucheron, F., Delaplace, G., Attia, H., & Ayadi, M. A. (2020). Changes in physical and biochemical properties of spray dried camel and bovine milk powders. *LWT - Food Science and Technology*, *128*, 109437. <https://doi.org/10.1016/j.lwt.2020.109437>

CHAPTER 6 - GENERAL DISCUSSION

The demand for natural and functional ingredients has been on the rise in recent years. Carotenoids are one such group of natural compounds that have attracted significant attention due to their various putative benefits (Mantovani et al., 2021; Paiva et al., 2020). The design of delivery systems based on emulsions shows great potential for improving carotenoids stability and bioaccessibility with reduced adverse effects on the food sensory properties (McClements & Li, 2010). The choice of the method of delivery is an important point to be considered, being milk proteins indicated as preferable for binding carotenoids due to a series of advantages (Mantovani et al., 2021; Stephenson et al., 2021; Tavares et al., 2014). Considering the diversity of emulsified delivery systems that may be used, they should be evaluated to understand the effects on physicochemical properties and possible applications.

In Chapter 3, an understanding of the influence of the steps for the incorporation of lutein, a bioactive carotenoid, into oil/water emulsions stabilized by whey proteins was discussed. To understand this, different systems were produced. Ethanolic lutein solution was added to the oil phase of the emulsion, which was removed by rotary evaporation before (O-L/W) or after (O+E-L/W) the emulsification step. Another system was produced by adding the ethanolic lutein solution into the aqueous dispersion of whey proteins, then the ethanol was eliminated by rotary evaporation and the emulsification step was performed (O/W-L). The small droplet size observed in the O/W-L emulsion promoted good stability against phase separation. Regarding the lutein photo-stability, the O+E-L/W emulsion displayed a significantly greater yellow color (higher b^* value) compared to the others. It may be linked to the largest hydrodynamic diameter of particles in this sample and potential differences in the aggregation state of lutein. The carotenoid in this was subjected to high shear stress in the presence of large amounts of ethanol which could promote better lutein dispersion before solvent elimination, increasing the yellow character of this sample. Despite the high lutein degradation during storage observed when it was found in the continuous aqueous phase for the O/W-L sample, the overall lutein degradation of O-L/W and O/W-L emulsions was not significantly different, but smaller compared with O+E-L/W samples. The results indicate that the method used to produce the O/W-L emulsion may positively contribute to extending the chemical and physical stability of products.

In Chapter 4, it was discussed other types of delivery systems in which lutein was incorporated into simple and double emulsions containing protein nanoparticles, to evaluate the effects on the stability and bioaccessibility of lutein. Due to the advantages of using

desolvation, this method was also incorporated into the production of the different samples. The inner aqueous phase, which contained whey protein isolate (WPI) nanoparticles obtained by desolvation, was emulsified in sunflower oil stabilized by polyglycerol polyricinoleate (PGPR). The primary emulsion was then emulsified in a continuous aqueous phase containing whey protein isolate (WPI) and xanthan gum. Lutein was incorporated using different strategies: 1) lutein entrapped by WPI nanoparticles obtained by desolvation within the inner water phase of a double emulsion (W-L/O/W); 2) lutein incorporated into the oil phase of the double emulsion (W/O-L/W); 3) lutein incorporated in the oil phase of a single emulsion (O-L/W).

The different ways of preparing the emulsions and the location of the lutein in the emulsified systems significantly impacted both lutein chemical stability and bioaccessibility. The lowest values of lutein degradation were observed for the emulsions prepared by dispersing lutein into the oil phase (W/O-L/W and O-L/W), with the greatest degradation of lutein observed for W-L/O/W (43 %). This could be related to a protective effect of the oil and/or PGPR for the chemical stability of lutein, and when dispersed in water, carotenoids tend to form aggregates due to their high hydrophobicity.

Samples before digestion showed large droplets and it was possible to still detect the presence of oil droplets after digestion, but much less in number and only very few could be seen in the intestinal stage, suggesting extensive digestion for all treatments. Besides that, a higher bioaccessibility was observed for the double emulsions (W/O-L/W and W-L/O/W) compared to the simple emulsion, with the highest in the case of the lutein incorporated in the water phase with the WPI nanoparticles (W-L/O/W). It is important to note that despite the lower lutein stability against light exposure observed during storage for W-L/O/W, this sample displayed the highest lutein bioaccessibility after *in vitro* digestion, showing that interactions between the various components may form during the production, storage, and digestion of the emulsions that may affect the kinetics of bioaccessibility.

The development of functional products often involves the design of blends that attempt to mimic the composition and properties of natural foods, such as infant formulas. The case study of Chapter 5, it was evaluated critical physicochemical indicators of three different commercial IFs containing cow's milk, soy, or rice as major protein sources during storage at different temperatures for up to 120 days. Mild storage temperatures (3 °C and 25 °C) promoted little changes in the evaluated parameters. However, critical storage temperature (50 °C) led to a series of physical and chemical changes, which varied according to the evaluated IF. The increase of the Maillard reaction rate in milk-IF during aging seemed

to be triggered by its lactose content and low T_{gr} . On the other hand, the presence of hydrolyzed proteins and the enrichment with reactive amino acids may be inferred as the main factors for increasing the Maillard reaction rate in soy-IF. The increase in the brown color of the powder, resulting from the final stages of the Maillard reaction, after 120 days of aging at 50 °C was so clear that it was detectable even with the naked eye.

Conversely, aging promoted the increase of the particle size distribution during the rehydration of milk-IF and soy-IF and an increase of the number and size of free-fat droplets (non-emulsified) on the surface of the powder particles in soy-IF and rice-IF.

As the composition of formulas is different, it is not possible to use the same well-established processing and storage parameters of cow's milk-based IFs for those produced with alternative protein sources, as is normally done. All these mentioned changes are important as they can influence the functional, sensory, and nutritional properties of IFs and consequently compromise the absorption of nutrients, such as carotenoids, and also distance themselves from the composition of breast milk, considered the optimal source of nutrition for infants.

CHAPTER 7 - GENERAL CONCLUSION AND PERSPECTIVES

Overall, this study discusses useful insights for using WPI-lutein complexes to produce lutein-enriched emulsions and highlights the importance of the steps in which lutein is incorporated dictating the behavior of the obtained systems. The use of desolvation to incorporate lutein into simple emulsions may contribute to extending the chemical and physical stability of the emulsified systems. In addition, in the case of double emulsions, it may promote an increase in lutein bioaccessibility after *in vitro* digestion. Besides that, it is reasonable to infer that interactions between the various components during the production, storage, and digestion of the emulsions will affect their bioaccessibility.

In the case of complex formulated food products, it is crucial to understand these interactions between the different components to guide their development and ensure the delivery of all nutrients. This is particularly relevant in the case of infant formulas, considering that most of the nutrition of infants fed with IFs, in the first months of life, is obtained from the reconstituted powder formula.

The results compiled in this thesis reinforce the importance of designing appropriate structures for delivering bioactive compounds displaying improved physicochemical stability and being able to improve the bioaccessibility of the targeted molecules. In this scenario, a direct perspective of this thesis is the development of model infant formulas with varying compositions that contain lutein incorporated into simple or double emulsions using the desolvation method. The aim of this approach is to assess how well these formulas protect and deliver the carotenoid. To enable this research, it is crucial to ensure the complete removal of ethanol from emulsified systems.

CHAPTER 8 - REFERENCES

- Blanchard, E., Zhu, P., & Schuck, P. (2013). Infant formula powders. In B. Bhandari, N. Bansal, M. Zhang, & P. Schuck (Eds.), *Handbook of Food Powders: Processes and properties* (1st ed., pp. 465–483). Woodhead Publishing Limited. <https://doi.org/10.1533/9780857098672.3.465>
- Borad, S. G., Kumar, A., & Singh, A. K. (2017). Effect of processing on nutritive values of milk protein. *Critical Reviews in Food Science and Nutrition*, 57(17), 3690–3702. <https://doi.org/10.1080/10408398.2016.1160361>
- Bocquet, A., Dupont, C., Chouraqui, J. P., Darmaun, D., Feillet, F., Frelut, M. L., Girardet, J. P., Hankard, R., Lapillonne, A., Rozé, J. C., Simeoni, U., Turck, D., & Briend, A. (2019). Efficacy and safety of hydrolyzed rice-protein formulas for the treatment of cow's milk protein allergy. *Archives de Pédiatrie*, 26(4), 238–246. <https://doi.org/10.1016/j.arcped.2019.03.001>
- Le Roux, L., Chacon, R., Dupont, D., Jeantet, R., Deglaire, A., & Nau, F. (2020). In vitro static digestion reveals how plant proteins modulate model infant formula digestibility. *Food Research International*, 130, 108917.
- Le Roux, L., Mejean, S., Chacon, R., Lopez, C., Dupont, D., Deglaire, A., Nau, F., & Jeantet, R. (2020). Plant proteins partially replacing dairy proteins greatly influence infant formula functionalities. *LWT - Food Science and Technology*, 120, 108891. <https://doi.org/10.1016/j.lwt.2019.108891>
- Mantovani, R. A., Rasera, M. L., Vidotto, D. C., Mercadante, A. Z., & Tavares, G. M. (2021). Binding of carotenoids to milk proteins: Why and how. *Trends in Food Science and Technology*, 110, 280–290. <https://doi.org/10.1016/j.tifs.2021.01.088>
- Masum, A. K. M., Huppertz, T., Chandrapala, J., Adhikari, B., & Zisu, B. (2020). Physicochemical properties of spray-dried model infant milk formula powders: Influence of whey protein-to-casein ratio. *International Dairy Journal*, 100, 104565. <https://doi.org/10.1016/j.idairyj.2019.104565>
- McClements, D. J., & Li, Y. (2010). Structured emulsion-based delivery systems: Controlling the digestion and release of lipophilic food components. *Advances in Colloid and Interface Science*, 159(2), 213–228. <https://doi.org/10.1016/j.cis.2010.06.010>
- Miranda-Dominguez, O., Ramirez, J. S. B., Mitchell, A. J., Perrone, A., Earl, E., Carpenter, S., Feczko, E., Graham, A., Jeon, S., Cohen, N. J., Renner, L., Neuringer, M., Kuchan, M. J., Erdman, J. W., & Fair, D. (2022). Carotenoids improve the development of

- cerebral cortical networks in formula-fed infant macaques. *Scientific Reports*, *12*(1), 1–13. <https://doi.org/10.1038/s41598-022-19279-1>
- Mirmoghtadaie, L., Aliabadi, S. S., & Hosseini, S. M. (2016). Recent approaches in physical modification of protein functionality. *Food Chemistry*, *199*, 619–627. <https://doi.org/10.1016/j.foodchem.2015.12.067>
- Paiva, P. H. C., Coelho, Y. L., da Silva, L. H. M., Pinto, M. S., Vidigal, M. C. T. R., & Pires, A. C. dos S. (2020). Influence of protein conformation and selected Hofmeister salts on bovine serum albumin/lutein complex formation. *Food Chemistry*, *305*, 125463. <https://doi.org/10.1016/j.foodchem.2019.125463>
- Saxena, J., Adhikari, B., Brkljaca, R., Huppertz, T., Chandrapala, J., & Zisu, B. (2019). Physicochemical properties and surface composition of infant formula powders. *Food Chemistry*, *297*, 124967. <https://doi.org/10.1016/j.foodchem.2019.124967>
- Stephenson, R. C., Ross, R. P., & Stanton, C. (2021). Carotenoids in Milk and the Potential for Dairy Based Functional Foods. *Foods*, *10*, 1263. <https://doi.org/10.1016/B978-0-12-384731-7.00172-0>
- Tavares, G. M., Croguennec, T., Carvalho, A. F., & Bouhallab, S. (2014). Milk proteins as encapsulation devices and delivery vehicles: Applications and trends. *Trends in Food Science and Technology*, *37*, 5–20. <https://doi.org/10.1016/j.tifs.2014.02.008>
- Teo, A., Lee, S. J., Goh, K. K. T., & Wolber, F. M. (2017). Kinetic stability and cellular uptake of lutein in WPI-stabilised nanoemulsions and emulsions prepared by emulsification and solvent evaporation method. *Food Chemistry*, *221*, 1269–1276. <https://doi.org/10.1016/j.foodchem.2016.11.030>
- Tham, T. W. Y., Xu, X., Yeoh, A. T. H., & Zhou, W. (2017). Investigation of caking by fat bridging in aged infant formula. *Food Chemistry*, *218*, 30–39. <https://doi.org/10.1016/j.foodchem.2016.09.043>
- Zhao, C., Shen, X., & Guo, M. (2018). Stability of lutein encapsulated whey protein nanoemulsion during storage. *PLoS ONE*, *13*(2), 1–10. <https://doi.org/10.1371/journal.pone.0192511>

CHAPTER 9 - ANNEXES

Annex 1. License to reuse the review article (Chapter 2).



Thermal treatments and emerging technologies: Impacts on the structure and techno-functional properties of milk proteins

Author: Lauane Nunes, Guilherme M. Tavares

Publication: Trends in Food Science & Technology

Publisher: Elsevier

Date: August 2019

© 2019 Elsevier Ltd. All rights reserved.

Journal Author Rights

Please note that, as the author of this Elsevier article, you retain the right to include it in a thesis or dissertation, provided it is not published commercially. Permission is not required, but please ensure that you reference the journal as the original source. For more information on this and on your other retained rights, please visit: <https://www.elsevier.com/about/our-business/policies/copyright#Author-rights>

BACK

CLOSE WINDOW

Annex 2. License to reuse the research article (Chapter 4).

[Sign in/Register](#)**Compartmentalization of lutein in simple and double emulsions containing protein nanoparticles: Effects on stability and bioaccessibility****Author:** Lauane Nunes, Negin Hashemi, Sandra Beyer Gregersen, Guilherme M. Tavares, Milena Corredig**Publication:** Food Research International**Publisher:** Elsevier**Date:** November 2023

© 2023 Elsevier Ltd. All rights reserved.

Journal Author Rights

Please note that, as the author of this Elsevier article, you retain the right to include it in a thesis or dissertation, provided it is not published commercially. Permission is not required, but please ensure that you reference the journal as the original source. For more information on this and on your other retained rights, please visit: <https://www.elsevier.com/about/our-business/policies/copyright#Author-rights>

[BACK](#)[CLOSE WINDOW](#)

Annex 3. License to reuse the research article (Chapter 5).

Home | Help ▾ | Live Chat | Sign in | Create Account



Aging of infant formulas containing proteins from different sources

Author: Lauane Nunes,Igor Lima de Paula,Marcelo Cristianini,Rodrigo Stephani,Guilherme M. Tavares

Publication: LWT - Food Science and Technology

Publisher: Elsevier

Date: December 2021

© 2021 Elsevier Ltd.

Journal Author Rights

Please note that, as the author of this Elsevier article, you retain the right to include it in a thesis or dissertation, provided it is not published commercially. Permission is not required, but please ensure that you reference the journal as the original source. For more information on this and on your other retained rights, please visit: <https://www.elsevier.com/about/our-business/policies/copyright#Author-rights>

[BACK](#)

[CLOSE WINDOW](#)